CHAPTER 1

1 INTRODUCTION: BUILDING THERMAL ANALYSIS

Despite the fact that buildings are, in the first instance, erected to provide shelter and comfort from the outdoor climate, many designers of new buildings are often predominantly interested in the aesthetic and functional aspects of the building. The indoor environment is relegated to the consulting engineer who, supposedly, will contrive whatever is required to establish and maintain an acceptable level of indoor comfort. However, the design of the facade of the building, to a large extent, determines the economics of the air–conditioning system, which forms a significant part of both the building construction and operating cost. According to Bevington and Rosenfeld [1] the fragmentation of the building industry is a serious impediment to greater efficiency: "A commercial building project, for example, typically involves a series of handoffs: an architect designs the building but then hands it over to the engineer, who in turn specifies materials, systems and components, before passing the responsibility to a contractor. Eventually the finished building is turned over to a maintenance and operations staff, who had virtually no say in the design process but probably know most about the buildings day–to–day performance." If the thermal characteristics of the building are not given sufficient attention during the whole design process and, especially, at the very early design stages, it leads to the erection of thermally inefficient buildings. In South Africa and other countries a significant fraction of the total energy consumption is wasted on the maintenance of a comfortable indoor climate, in thermally inefficient buildings [2].

According to Carroll [2] energy consumption in buildings account for 23% of the total primary energy usage in South Africa. While this figure is reasonably low when compared to other countries – probably because of our moderate climate – it still represents a substantial national expenditure. In a recent American article it is predicted that the efficiency of buildings could double by the year 2010 [2]. German measurements in a number of energy efficient houses suggest that as much as 40% reduction in heating energy requirements can be realized [3]. Some researchers even suggest that savings as high as 75% in new buildings and 50% in existing buildings are possible [1]. Local studies [4,5] indicate, that in the moderate South African climate, it is often feasible to provide acceptable indoor comfort without any mechanical refrigeration at all, provided sufficient care is taken with the thermal design of the envelope. In [2] it is claimed that by clever exploitation of the the capacity of buildings to store heat in massive structures, air–conditioning costs can be reduced by from 30 to 70 percent.

1.1 Historical Perspective

In the first six decades of this century, energy costs were insignificant and played virtually no role in the design of buildings and air–conditioning systems. With the oil–crisis in the seventies, and the subsequent escalations in the cost of energy, a very heavy emphasis was placed on energy efficiency measures. This emphasis on reducing energy consumption sometimes lead to the installation of inadequate conditioning systems. According to Sun [6] many buildings erected in the seventies and eighties were equipped with under–designed air–conditioning systems which have resulted in many complaints and the prevalent investigations in the literature of the so–called *sick building syndrome*. Thornley [7] states: "Of course the HVAC industry isn't blameless either; often we haven't understood the complicated interaction of system performance. Often our very resolve to save space, to save energy, and to save cost, has resulted in systems which fail to satisfy."

The continuing increase in the cost of energy will doubtless increase the pressure on the building industry to design energy efficient buildings. Thornley [7]: "The catch 'Can we afford to save energy?' has a peculiar connotation for air conditioned buildings, for although the cost of energy in recent years has outstripped the general rate of inflation, the cost of operating an air conditioning installation can still be a small proportion of the total owning and operating cost of the building. It is therefore still argued that there is little inducement to refine designs and install additional energy saving equipment. I prefer the contrary argument that energy saved is money saved, although I recognize that we cannot rely wholly upon conscience and that some form of cost effectiveness must prevail." A new approach in building design is called for. Building and air-conditioning system must be designed together, as a complete indoor climate conditioning unit. Increasing the efficiency of buildings requires extensive co-operation between architect, engineer and developer. The air-conditioning system and passive thermal response of the building must match the local climate to ensure adequate comfort. The architect must carefully consider the thermal implications of his design, the engineer must optimize the design of the air-conditioning system but without sacrificing comfort. Building developers and owners must be provided with the means to enforce comfort prescriptions. Thornley [7] states the situation in the United Kingdom: "A great deal has been said and written in the last quarter-century on multidisciplinary co-ordination and the integration of buildings and their services; this is never more important than when a building is to be air-conditioned. While much has been achieved in this area, honestly successful solutions will depend on an even finer understanding between building owners, architects, and engineers than seems to exist at this time."

1.2 A Design Tool for Building Thermal Performance

It is clear that in future the thermal aspects of a particular design should be high on the priority list of designers of new buildings. To aid them, A friendly and easy to use computer program is required which will facilitate evaluation of the thermal response of a building, without the need for detailed technical knowledge of thermo-flow. The program must cater for analysis of the passive response of the building, the air-conditioning system, comfort criteria and total design evaluation. Such a program, commercially known as QUICK, was developed by the Centre for Experimental and Numerical Thermo-flow (CENT) at the Department of

Mechanical Engineering, University of Pretoria, under the leadership of Prof. E.H. Mathews. The project received support from the Department of Public Works and Land Affairs, Department of Finance, Laboratory for Advanced Engineering, University of Pretoria as well as the National Energy Council. Although this program was developed for South African conditions, it also generated a fair amount of overseas interest and won a prize at the International Congress on Building Energy Management (ICBM) at Laussane Switzerland in 1987 [8].

The program was designed to run on an inexpensive personal computer and to facilitate rapid and accurate evaluation of building thermal characteristics at sketch design stage. The user interface is extremely friendly, consisting of a pull down menu structure with many help screens, while a database of building materials is available on–line. The program, which has now gone through it's third revision, succeeds admirably in relieving all the tedium of performing a thermal analysis and is suitable for use both by engineers and architects. It provides for the determination of the passive response of a building i.e. interior temperature as well as load estimation. In the latest version it is also possible to obtain comfort criteria [9].

The thermal model on which the program is based was developed by Mathews and co–workers [10,11] with the philosophy that a design tool should place greater emphasis on ease of use than absolute accuracy and detailed thermal modelling. The program is capable of predicting the hourly indoor temperature as well as the energy load required to maintain a comfortable indoor climate; for given meteorological conditions. The method caters for multi–layered constructions, shaded windows and solar penetration, interior heat generation and extraction and natural and mechanical ventilation [9].

However, like all other thermal prediction programs, the method also has limitations [10]. It is a highly simplified method which essentially estimates the heat conductance of the building shell and the total amount of stored heat in the massive structures. Since these limitations are the main topics of this thesis we state them explicitly:

a) The most important limitation, from a theoretical point of view, is probably the restriction to single zones. This means the program can not handle heat flow between adjacent rooms at different interior temperatures. This assumption implies that all internal zones in a buildings are assumed to be at more or less the same temperature, or alternatively, that the partitions between zones do not allow heat transfer between the zones. This limitation is in practice seldom a big constraint. Conditioned buildings normally have all zones controlled at nearly the same temperature, and in passive buildings it is the heat flow through the shell which is the most important.

b) It is also assumed that the thermal response of the building can be characterized with a single pole thermo–flow network. This approach employs a single heat storage capacitor to account for all the storage in the massive elements of the building. The method leads to a highly simplified model which is easily understood and can be solved quickly. It's use is justified by the very reasonable comparison of the predictions with measured results [10]. Obviously, with such a simplified method, the accuracy depends largely on the methodology for estimating the *active thermal capacitance of the building*, or rather, the instantaneous quantity of stored heat.

c) Another assumption is that the interior air is well mixed and at a uniform temperature. Also the interior surfaces of the walls are assumed to be at the same temperature; so that radiative exchange between the walls can be ignored. This last assumption is closely coupled to the previous assumption of well mixed interior air. When the indoor air is agitated, temperature differences between the surfaces of the walls are reduced by convection as well as radiation.

Note that the assumption is not that radiation plays no part, rather, it is assumed that interior conditions are such that radiation and convective heat transfer are highly efficient in reducing temperature differences between interior surfaces.

d) A further limitation is the restriction to fixed ventilation rates. In many naturally ventilated buildings the ventilation rate varies considerably due to diurnal and seasonal wind patterns. In buildings with mechanical ventilation, the ventilation rates may also vary: a high ventilation rate may be used during the night to cool the building in summer and a low ventilation rate during the day for comfort. This restriction to constant ventilation rates is different to the other limitations, in that it is not an inherent limitation of the mathematical model of the thermo–flow, but is simply an assumption to expedite the numerical solution of the model. In the second part of this thesis a method is described whereby this restriction is circumvented with no sacrifice in computation speed.

The indoor temperature prediction of the method was extensively evaluated by Mathews and Richards [10] by comparing predicted indoor temperatures with measured temperatures in more than 60 existing buildings of various types. These included office blocks, shops, schools, residential buildings, town houses, medium and high mass experimental buildings, low mass well insulated structures with ground contact such as factories and low mass poorly insulated structures e.g. agricultural buildings. For details of the validation see [10]. The accuracy proved to be satisfactory for the stated objective, i.e. to be a thermal analysis tool at sketch design stage of buildings, when many of the details are still unavailable and rapid results and ease of use, rather than absolute accuracy, is important. The program was also instrumental in establishing thermal design norms for the Department of Finance [12].

One of the objectives of this thesis is to determine the theoretical validity of the method from first principles. In chapter 2 the method of Mathews and Richards [10] is thoroughly investigated from a theoretical point of view. It is shown that the simple thermo–flow network they use (see figure 2.1) can be approximately derived from a more comprehensive model, by appropriate assumptions and reductions. From this analysis, a discussion of the theoretical validity of the original assumptions of Mathews and Richards[1] is possible. In the process, a somewhat more refined model, which incorporates the basic simplicity of the original model but which is more attractive from a theoretical point of view, is also presented. In later chapters some possible extensions of the method are investigated, and a new method of solution, which incorporates time variable parameters, is given.

1.3 The Objectives and Scope of this Study

The objective of this study is fourfold:

- A To investigate the theoretical underpinnings of the method of Mathews and Richards with emphasis on the active thermal storage capacitance of buildings.
- B To extend the method to buildings incorporating structural storage systems.
- C To extend the model to also cater for inter–zone heat flow in a convenient manner.
- D To obtain an efficient solution for the model when the parameters are time variable.

It is not in the scope of this study to substitute for the method of Mathews and Richards, a new method, although a new method with certain advantages is presented in chapter 2. A substitute method will require

[1]We shall from now on frequently refer to the method of [10] and [11] as the method of Mathews and Richards without further reference.

implementation in a computer program and extensive validation studies; tasks which were not attempted. We are also not so much concerned with the accuracy of the method *per se* as with the assumptions which are required by the method. This study is mainly concerned with theoretical considerations, and the implementation of solutions.

1.4 The Contributions of this Study

This study contributed to building thermo–flow research the following original results:

It is shown that the method of Mathews and Richards can indeed be derived from first principles with certain assumptions. The nature of these assumptions are illuminated and their validity is discussed. In particular, it is shown that the basic assumption required to derive the model of Mathews and Richards is; that the bulk temperatures of all the massive elements of the zone must be approximately equal. This is a more accurate formulation of the basic assumption, it replaces the assumption of equal interior surface temperatures as given by Mathews and Richards.

The simplification of interior thermo–flow networks is discussed in some depth. It is indicated that various assumptions about interior temperatures will lead to different definitions of interior surface heat transfer coefficients. Although effective film–coefficients are often discussed in the literature, the author could find no coherent and reasonably complete treatment of their definition and validity.

The lumping of distributed elements is treated from first principles. Many others have discussed this aspect, and methods for obtaining lumped representations, as well as criteria for accurate lumping, are well known. However, no complete study of the applicability of lumped representations to common building elements could be found. By calculating the accuracy of the lumped representation of more than 100 existing building elements, it is shown that the lumping of distributed thermal elements can often be justified. Formulae for determining lumped parameters from the physical properties of the materials are obtained from first principles. It is shown that the pre–condition for accurate lumping of building elements is, in the first place, on the thickness of the walls with respect to the wavelength of the thermal wave propagating through the wall. These results are known in the literature but their physical interpretation, as stated above, is often misunderstood and obscured by statements about the thermal conductivity of the material.

The concepts of active stored heat and active thermal capacitance are clarified.

The definition of the mean external forcing function (mean sol–air temperature), as used by Mathews and Richards, is clarified.

In the method of Mathews and Richards it is necessary to apply an empirical correction to the phase shift of the interior temperature. It is shown that this phase shift can be attributed to two sources: the lumping of thick walls and the definition of the mean sol–air temperature.

It is shown that the technique of combining the heat storage capacitance of interior massive elements with those of the shell, as given by Mathews and Richards, can not be justified. It requires the assumption that the mean temperature of the interior mass is equal to the mean temperature of the massive parts of the shell. This can not be since the interior mass is driven by the interior temperature, and the shell mass by the difference between interior and exterior temperatures.

A revised simple thermo–flow model is presented. The method requires further investigation, implementation and also verification. The method is conceptually very similar to the method of Mathews and Richards but is theoretically better founded and has certain other advantages.

The method of Mathews and Richards is extended to cater for thermal control systems which utilize heat storage in the structure of the building directly.

The method is extended to allow effective multi–zone thermal performance predictions. It is shown that the proposed multi–zone method is a natural extension of the existing single–zone method.

A new numerical method for the solution of the thermo–flow network is proposed which allows efficient predictions with cyclic, time–variable parameters. An explicit formulation for the initial value, which is required to obtain periodic solutions, is derived. The new method allows the prediction of variable parameter thermal response, without the need for Fourier analysis or a long initial integration period to get rid of transients. It is applicable to any system of discrete cyclic equations with cyclic forcing functions. Besides this numerical method, an alternative approximate method is demonstrated which is based on a complex Fourier series representation with time dependent coefficients.

These contributions are not all original to the same extend. The method for numerical solution of time dependent heat flow is, to the authors knowledge, completely original. In other contributions the work of others have been either applied to the thermo–flow model of Mathews and Richards, or it was attempted to find a clearer or more comprehensive description and understanding, or the results were interpreted in a different way.

We have endeavoured to indicate, by way of reference, all authors which we feel directly influenced this study. There are also many others who have indirectly contributed; by enhancing our understanding and moulding our perception.

1.5 The Contents of this Thesis

Besides the objectives mentioned in §1.3, this study is also an attempt to unify the theory and techniques useful for constructing simple thermo–flow networks for buildings. In this thesis, we have accordingly not strictly confined ourselves to the above stated contributions and objectives, but we also discuss other well known relevant matters, such as the method for linearizing the radiation heat transfer coefficient, the solution of periodic thermoflow problems through walls with the aid of matrices, the definition of the sol–air temperature, the definition of the ventilation resistance etc. We hope in this way to make this thesis useful for those encountering these matters for the first time.

In addition we have gone to some pains in chapter 5 to describe the literature on time variable systems, since this literature is not widely known and often somewhat obscure. In this regard it is also important that the techniques we investigated, but found lacking, be documented.

The presentation of this thesis closely follows objectives A to D in §1.3 above, with each chapter (chapters 2 to 5) devoted to a theme. References, symbols and short appendices are given after each chapter. The final chapter is a summary of all the results, conclusions and recommendations of chapters 2 to 5.

Computer programs and other calculations are not given in full detail in the thesis and appendices. Programs are written in FORTRAN 77, Turbo C, Turbo C++ and MATHCAD. Instead, a floppy–disk (MS–DOS formatted) is attached to the backcover which contains all the programs, input data and detailed results. In case further analyses are required for future investigations, the files on the floppy–disk contain sufficient descriptive comments that they can be used and modified[2].

[2]This thesis was compiled with the T^3 Scientific Wordprocessor and printed on a HP Laserjet. Figures were drawn with HP Drawing Gallery on the Laserjet, most graphs were compiled with Quattro Professional.

REFERENCES Chapter 1

[1] **D. Carrol**, Energy Consumption and Conservation in Buildings An International Comparison, *Proc. 3rd Int. Symp. Energy Conservation in the Built Environment*, Vol. 1A, CIB/An Foras Forbartha, Dublin, 1982, pp. 190 –203.

[2] **R. Bevington, A.H. Rosenfeld**, Energy for Buildings and Homes, *Scientific American*, Sept. 1990, pp. 39 – 45.

[3] **H. Erhorn**, Solarenergiehäuser in der Praxis Welche Energie–einsparergebnisse erbringen sie wirklich? *Bauphysik 11(1989), H, 1,* pp. 70 –73.

[4] **G. van Aarle, T Herman**, Potential for the air–conditioning of office buildings without mechanical refrigeration, *The South African Mechanical Engineer*, Vol. 36, June 1986, pp. 192 – 197.

[5] **W. Kruger, M. Kleingeld**, Design Guidelines and Norms for Evaporative Cooling, Ventilation, Daylighting, *Final Report, CENT*, Dept. of Mech. Eng., UP, Oct 1990.

[6] **T.–S. Sun**, A reflection on 30 years in air–conditioning design and energy conservation, *Plenary Paper, ASHRAE–FRIGAIR 90*, 23 – 25 April 1990, Pretoria, Vol 1.

[7] **D. L. Thornley**, The Case for Air Conditioning–a Keynote Discourse, *Air Conditioning System Design for Buildings,* Editor A.F.C. Sherrat, McGraw–Hill, pp. 1 – 16.

[8] **Proc. 3rd Int. Congress on Building Energy Managment**, Lausanne, 1987, *Presses Polytechniques Romandes*, Lausanne

[9] **QUICK user's and reference manual**, Release 3 of 1990, *CENT, Department of Mechanical Engineering, University of Pretoria.*

[10] **E. H. Mathews, P.G. Richards**, A Tool for Predicting Hourly Air Temperatures and Sensible Energy Loads in Buildings at Sketch Design Stage, *Energy and Buildings*, 14(1989), pp.61 – 80.

[11] **E. H. Mathews, P.G. Rousseau, P.G. Richards, C. Lombard**, A Procedure to Estimate the Effective Heat Storage Capability of a Building, *Energy and Buildings*, accepted for publication, 1990.

[12] **W. Kruger**, Thermal Norms for Buildings on South Africa, *Master of Engineering Thesis, Dept. of Mech. Eng., University of Pretoria.*

CHAPTER 2

2 A THEORETICAL FOUNDATION FOR THE THERMAL ANALYSIS METHOD OF MATHEWS AND RICHARDS

2.1 Background and Objective of this Chapter

In this chapter we aim to examine the theoretical underpinnings of the highly simplified thermal model of Mathews and Richards [10]. Before we do so, we first motivate why we chose this method, from many others, for further investigation.

2.1.1 The Variety of Available Methods for Building Thermal Analysis

A large variety of computer programs and methods for building thermal analysis are available today. Most popular (in English speaking countries) are certainly the *response factor* [1] method promulgated by ASHRAE in Northern America and the *admittance* [2] method of CIBS in the United Kingdom. Other prominent methods are the method of Muncey [3] as extended by Walsh and Delsante [4] in Australia, the *Total Thermal Time–Constant* method of Givoni and Hoffman [5], and in South Africa, the *CR* method of Wentzel, Page–Shipp and Venter [6]. Some of these methods are discussed and compared by Tuddenham [7], Walsh and Delsante [4], Athienitis [8,9] and Mathews and Richards [10]. According to Tuddenham [7]:

"1. There is a wide range of theories and program types in use.
2. The degree of variation in results between various programs is high – the degree of accuracy is largely unknown.
3. There is strong evidence that the largest factor in the difference between program results is engineering interpretation.
4. There is no evidence that more complex engineering models give more accurate results."

Tuddenham also remarks that: "The most remarkable feature of computer load estimation work today is the continuing paucity of supporting work to validate the calculation theories, although some work is now being undertaken, notably in the USA."

The method of Mathews and Richards[1] has the considerable advantage of using an extremely simple thermo–flow network with a clear interpretation in terms of the main thermal components of the building. Furthermore, the lumping of shell conductance and heat capacitance effectively circumvents the need for solving partial differential equations. Despite this simplicity of the network – or perhaps on account of this simplicity – extensive validation measurements in existing buildings indicate that all the essentials are adequately represented [10,11] and the observed error against measurements is below 2 ^{o}C in more than 80% of the cases. The simplicity of the method allows very efficient numerical solution, and the clear physical interpretation enables ready extension of the method. Recently the method has been extended to include simulation of active systems of various complexity and such exotic systems as evaporative cooling, structural cooling and night cooling [12].

But whatever the merits of a new method may be, general acceptance by the building industry is not something which will come about automatically. The old methods are well–known and consultants have learned their quirks, they are firmly established. Tuddenham observes [7]: "In more recent years, programs in the commercial field have tended to adopt a theory which is underwritten by the UK or American establishment, notably the CIBS 'admittance' method or the ASHRAE 'response factor' method. However, it may be that this trend is based more on their apparent respectability than on their proven excellence."

A large number of computer programs for building thermal analysis is available. According to Tuddenham [7] there are more than one hundred in the United Kingdom and many hundreds more elsewhere. Most of

[1]See footnote page 7.

these methods are based on the above mentioned admittance method of the CIBS [2], or the response factor method of ASHRAE [1]. The CIBS method was originally developed for manual calculations [13]. It employs pre–calculated tables of decrement– and other factors for building materials. The response factor method was originally developed for computer implementation [14] although it also employs pre–calculated 'response factors'. It does seem, however, that the method was severely influenced by the very crude computer hardware and software available at the time and the central theme of the method appears to be an attempt to alleviate the problem of evaluating the convolution integral, as required to obtain the forced response [15]. In view of the undreamt of growth in computer technology and numerical techniques in the last 30 years, both these methods appear outdated. The Fast Fourier Transform has made the evaluation of convolution integrals a very simple and computationally efficient exercise [16]. Consequently, frequency domain techniques are now predominant in numerical implementations in diverse scientific disciplines.

Both the CIBS and the ASHRAE method (and others e.g. [3,4]) employ the exact analytical solution of the diffusion equation in the form of matrices [15]. These matrices are then used to obtain the response\decrement factors from which the thermal response is obtained. In the admittance procedure the factors are used to obtain amplitude and phase–shift values for the internal temperature. The response factor method obtains the solution by superimposing the response to a series of triangular pulses. Strictly speaking, both methods are only applicable to linear time–invariant thermal systems. (Note, in [17] invariability is erroneously stated as a requirement for using the method of superposition; linearity is sufficient. Invariability is only required for the Laplace transform method to be tractable [18].)

Since the exact matrix solution for heat conduction is simple and amendable to computer implementation, and standard two port theory can be used to combine the matrices of various elements, it is unnecessary that computer programs still employ response factors which have to be pre–calculated. Certainly, the matrices are more suited to time invariant systems, but so are the response factors, since they are derived from the matrices. For the time invariant case, it seems that a modern comprehensive method would compute the matrices for the various elements at a number of frequencies, combine the matrices with two port theory, and compute the exact solution via the super–positioning of the responses to the various frequencies (See chapter 5) as suggested by Athienitis [9]. Computationally this is certainly feasible and practical on modern desktop computers. The method can be used to obtain both transient and steady state solutions by employing either the Laplace or the Fourier domain; although the availability of the Fast Fourier Transform considerably increases the computational speed in the Fourier domain. Later in this chapter we use this comprehensive matrix method to derive a simple model for thermo–flow in buildings.

In [14] some emphasis is placed on the response factor method being applicable to non–steady state conditions. To simulate non–steady conditions one would have to specify initial conditions which can only be guessed or become known by measurements. Therefore, simulation of non–steady conditions seems rather academic. In practice one is confronted with continuous variables which can be described as quasi–periodic; there is no clearly defined initial state. One should therefore rather attempt to find the quasi–periodic solutions which are often sufficiently accurately represented by periodic solutions [9]. This is especially true if the principle of a design day is adhered to, where a single day is specifically chosen, and used to evaluate the building under the further assumption that all other days are similar. If results are required for e.g. one extraordinary day in a series of ordinary days, the periodicity can be assumed to extend to a number of days, e.g. 7 days or a design week. Computationally this approach is probably at least just as efficient as a time–domain non–steady analysis, where integration would have to extend over at least 5 thermal time–constants to get rid of the initial transient.

In view of the availability of the practical, exact matrix solution to the heat conduction equation with steady excitation, it is also surprising to find many programs employing finite difference or finite element techniques. It is often stated that these numerical methods facilitate solution of a time variable, fully non–linear model [8]. In fact the powerful but often tedious numerical techniques are essentially employed to solve the time invariant, linear, heat conduction equation. The time variability and non–linearities in thermal models of buildings do not arise from heat conduction but from other heat transfer modes. The advantage of the finite difference\element techniques is rather that they allow a unified treatment of all aspects of thermo–flow in buildings. However, they are not the most efficient techniques, they are also quite remote from the physical structure, and, they often require careful fine–tuning to ensure convergence, accuracy etc.

One could use the matrix solution for the conduction equation and combine it with time variable non–linear two ports. The complete solution is then obtained from non–linear network methods which were extensively developed in recent years [19]. Athienitis in an important contribution [9] remarks that "Discrete frequency analysis, although virtually ignored in passive solar design, is computationally efficient and easy to program."

A central theme in the above discussion and in the literature is the use of matrices to obtain exact solutions for heat transmission through walls with sinusoidal boundary conditions. Matrices were first applied to heat transfer problems by Pipes [20], but many others, *viz.* [21–23,3,4,13,17], have also used the matrix solutions. For a description of the method refer to §2.5.3, see also Givoni [5] and Kimura [15]. This method has the clear distinction – from the many numerical methods – in that it is an exact solution of the heat diffusion equation. However, it is based on Fourier analysis and therefore awkward when extended to time variable systems. Nevertheless, in many programs based on the matrix method, one disconcertingly finds that the extreme power of the matrix (two–port) theory for combining various elements is not appreciated. This is inexplicable, especially since these methods are ideally suited for computer implementation. For example, in the program described by Walsh and Delsante [4], which is based on the work of Muncey [3], one finds that the final result is evaluated, not from a final matrix description of the the total system, but rather, in terms of the response of the various elements of the building to certain types of input functions.

The modelling of thermal response with two–ports was extensively developed by Athienitis [8]. He has shown that the frequency domain matrix techniques can be extended to include time–varying parameters such as night insulation and variable ventilation. In this thesis, use is made of this fairly exact method to illuminate the assumptions and limitations of the simplified method of Mathews and Richards.

An important point we wish to clear–up at this stage, is that some present thermal analysis methods attempt to be extremely accurate, with emphasis on exact simulation, e.g. [24]. Highly refined numerical analysis techniques are used. The result is that these techniques need large mainframe computers and detailed specification of the construction, consequently, they are mostly of academic value. The established simplified methods of ASHRAE and CIBS on the other hand, are outdated. A design tool for use at sketch design stage should be sufficiently accurate with a design philosophy (e.g. design day) in mind – and practical. In this thesis we are interested in design tools and it is evident that there is scope for new methods and further developments in this regard [10]. For such a new method to be acceptable, the following points warrant consideration:

a) A complete description of the thermo–flow in real buildings requires many details, some of which (e.g. ventilation rates) are wholly unknown or only partly known. This is even more true if the objective is a design tool, since the thermal properties of a building are largely determined in the very early design stages when no details at all are available.

b) Many studies and empirical models [25,26] indicate that a few essential parameters of buildings, such as heat storage capacity and shell admittance, are crucial and should be emphasized rather than details. It is also crucial that the assumptions underlying the model be clear, easy to explain and to understand. The model must have a very clear physical connection.

c) A successful computer design tool must employ a very simple model with a straightforward physical explanation to allow the designer's good judgment and experience to play its essential part. Highly refined models and exact solutions are better employed in research laboratories for verification purposes and the extension of knowledge and understanding.

d) For a design tool, extreme numerical accuracy – at the cost of computing time – is detrimental. Certain essential parameters of thermo–flow in buildings, such as ventilation rates, are largely unknown. The emphasis should be on establishing the relative merit of various designs, rather than absolute predictive accuracy. It must be remembered that the probability that the weather conditions, used for the simulation, will actually occur in practice, is small. The tool must endeavour to be indicative of the response of the building, rather than predictive.

e) A design tool should allow innovation and easy extension to cater for creative ideas and new techniques.

f) A computer procedure should not be based on 'established' techniques which were developed for hand calculations and which are overly simplified or unnecessarily rigid.

g) A design tool should follow a total approach. Both the passive response of the building and the HVAC system must receive due attention, but of the two, the passive response is probably the more important factor, since it essentially determines the required HVAC system and therefore the installation and running costs.

The method of Mathews and Richards was initially developed with these considerations in mind [10] and is therefore an excellent vehicle for further study and improvement.

2.1.2 The Objective of this Chapter

In the next sections of this chapter a theoretical foundation for the simple model of Mathews and Richards for thermo–flow in buildings is derived. This further establishes the validity of the method and will promote it's general acceptance. The point is exemplified by other methods, which appear theoretically unsound, although they may have empirical merit, e.g. the TTTC method [27] where time–constants are averaged[2].

Here we endeavour to illuminate the method of Mathews and Richards. The procedure we follow is to model a simple building, consisting of only two surfaces, comprehensively, and to deduce from this comprehensive model the parameters of the simplified model. The comprehensive model is constructed in terms of the exact frequency domain matrix method discussed above. This procedure enables investigation of the effect and validity of each simplifying assumption in

[2]See discussion of TTTC method in §2.5.3 e.

turn. The simple two surface building we use is approximated by a large flat building where one surface may be the roof and the other the floor. Although the quantitative results are limited to this theoretical building, the procedure we follow is applicable to any building. The building merely serves to provide quantitative results for evaluating the thermal response of typical building structures. The advantage of using only two surfaces is that the complexity of the comprehensive model is greatly reduced, so that the essential physical mechanisms of heat transfer are not obscured by detail. We begin the discussion by first introducing the simple thermal model of Mathews and Richards.

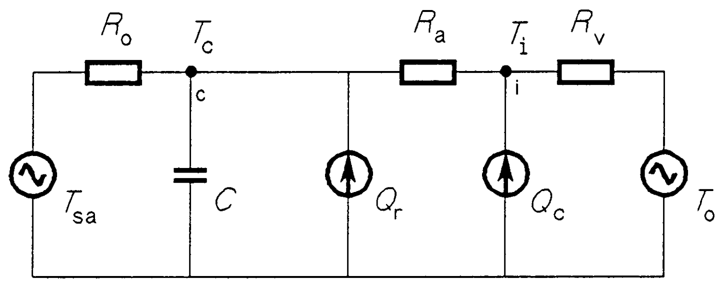

FIGURE 2.1 The simple electrical analog of Mathews and Richards for thermo–flow in buildings. Symbols are defined above. From [10].

2.2 The Method of Mathews and Richards

In figure 2.1 the electrical network equivalent of Mathews and Richards for the heat flow problem in buildings is shown [10]. In this figure T_{sa} is the averaged sol–air temperature (for definition see §2.4.4 a), T_o is the outside air temperature, T_i is the indoor air temperature, Q_r is the radiative heat source and Q_c is the convective heat source. The shell resistance and thermal capacity of the building is represented by R_o and C respectively, R_a is the heat transfer coefficient of the internal surfaces and R_V is the ventilation resistance. The most notable aspect of the circuit is the extreme simplicity, a single capacitor is used to represent all the mass available for heat storage. The conductance through the shell is modelled with a single resistance R_0, and a single exterior forcing function, T_{sa}, is used.

2.3 Assumptions, Limitations and Possible Extensions of the Method

In the development of the thermal model of Mathews and Richards they found it expedient to simplify the network to a single zone thermal system. It is assumed that the temperatures in adjacent rooms are equal, so that no exchange of heat occurs between them [10]. A more important assumption is that the interior surfaces are at the same temperature. Radiation between interior surfaces can therefore be completely ignored. It is also assumed that the surface heat transfer coefficients can be fixed. In the development of the model, a higher priority was assigned to speed of calculation and ease of use, than absolute accuracy. These assumptions will be discussed shortly.

Mathews and Richards stress that it is important to bear in mind that some important contributions to the heat flow, such as ventilation rates, are highly uncertain. These parameters can only be guessed so that there is a definite upper limit to the theoretical achievable accuracy for any thermal response model. In practice, it turns out that useful answers can be obtained with the single zone and other assumptions, and that a significant improvement in thermal performance of new buildings, designed with this model, is obtained. These conclusions of are fully in accordance with points a) to g) of §2.1. The successful verification of the method [10], and the ready acceptance by some consultants, fully justifies further investment in the improvement- and promotion of the method.

Further enhancement will be beneficial since the simplified model was originally conceived as a design tool for architects, but lately, the engineering fraternity has also shown considerable interest. Their objective is rather different; primarily, they desire to use the program to determine the required capacity of new air conditioning installations, and, to optimize these systems. The program is helpful for estimating the future running costs of a proposed new building. There exists a further possibility that, by improving the control systems used for maintaining the indoor climate at prescribed settings, the program may significantly decrease the running costs of existing buildings. For these engineering applications the accuracy obtained via the single zone approach and the other assumptions may sometimes be insufficient and a more refined model is called for. The logical approach to an extension of the applicability of the method is to remove the limitation to single zone analysis, fixed ventilation rates and to provide for active systems. These extensions must be incorporated without sacrificing the extensive base of understanding, knowledge and technique that has been proved in practice. The extension of the model of Mathews and Richards to include multi–zone thermal response, structural storage systems and variable parameters is treated in later chapters.

This chapter of the thesis is, in the first instance, an attempt to investigate theoretically the validity of the assumptions. Besides that, this thesis is also concerned with refining the model if the validity of some of the assumptions can not be substantiated. A theoretical study will in this way enhance the understanding of the implications of the assumptions and the behaviour of the method under various conditions.

A very important assumption of Mathews and Richards, which leads to great simplification, is the assumption that the essentially distributed massive elements comprising the walls, floors and interior masses, can be adequately represented with a single lumped capacitor. This is a very fundamental assumption, it enables the analysis method to obtain predictions for room thermal response without the need for obtaining first solutions to the heat diffusion equation. The validity of this assumption (and the others) must be based on measurements in actual buildings. Many such verification experiments have been carried out [11], and the results indicate that adequate accuracy is obtained with the indoor temperature predictions. It does appear, however, that the correct time delay between peak exterior forcing temperature and peak interior temperature is not always obtained [11].

In the next two sections an attempt is made to elucidate these assumptions of Mathews and Richards by examining their validity in the light of a more refined model. As stated already, a very simple building structure, consisting of two infinite walls, often serves as butt of the discussion.

2.4 A More Comprehensive Theoretical Model

We model the thermal attributes of buildings along the same lines as Athienitis [8]. The model of Walsh and Delsante [4] also has close parallels, as well as the model presented by ASHRAE [28]. This comprehensive model we present here, is a refinement of the model of Mathews and Richards particularly in the following aspects:

1. The assumption that the internal air is well mixed is retained but the assumption that the interior wall surfaces are at the same temperature is dropped. In this model, heat transfer between the surfaces via both convection and radiation is incorporated. The objective of this part of the study is to determine the difference in temperature between the various internal surfaces and the accuracy of the assumption of isothermal interior surfaces.
2. The lumping of conductance and heat storage of the building shell in a single resistor and single capacitor network is avoided. Instead, the exact matrix solution of the diffusion equation is employed. The accuracy of the lumped model can be investigated in this way. In addition, the method of lumping, especially for laminated surfaces, as well as the

combination of the surfaces in a single RC network, is investigated.

3. Besides the lumping of the shell capacitance, the model of Mathews and Richards also combines the storage capability of internal masses with those of the shell in a single capacitor. In the refined model these internal masses are treated separately.
4. The external surfaces are treated individually. Mathews and Richards assume that it is possible to obtain a mean sol–air temperature which applies to all external surfaces. In the comprehensive model external surfaces are given individual boundary conditions.

2.4.1 The Building Shell

The walls forming the enclosure, as well as the roof, are modelled as laminae of various materials. The heat flow through these laminae are adequately described by the one–dimensional diffusion equation, with radiative and convective boundary conditions. This approach ignores two dimensional edge effects at the corners. It is easily shown, in the steady state case, that the effects of the edges are negligible[3]; solutions for steady state heat conduction are tabulated in Holman [29] for various geometries in the form of:

$$q = k \cdot S \cdot \nabla T$$

with q heat flow [W], k conductivity in [W/m$^2\cdot$K], S the *shape factor* in [m] and ∇T the temperature difference forcing the heat flow in [K]. The shape factor for a wall is [29]: $S_w = A/\ell$, with A the area of the wall in [m^2] and ℓ the thickness of the wall in [m]. The shape factor for the edge between two walls is: $S_e = 0.54 \cdot D$ where D is the length of the edge. For the corners where three surfaces meet the shape factor is $S_c = 0.15 \cdot \ell$ with ℓ the thickness of the surfaces. For a simple

[3]These results are well known. We include it for the sake of completeness and to aid newcomers to the science of building thermal response.

cubicle of 3 x 3 x 2.75 m^3 with wall thickness 250 mm these factors factors are: S_w = 33 m, S_e = 1.62 m and S_c = 0.0375 m. For steady state conditions the contribution of the heat heat flow though the edges is clearly negligible and the one dimensional approach is very accurate. This conclusion is valid for all thin walled buildings. Only when the thickness of the wall is a sizable fraction of the cubic root of the internal volume will the assumption be erroneous.

The roof can be treated as just another surface. The presence of air–space between ceiling and roof must be accounted for by assigning an effective conduction coefficient to account for the radiative and convective heat exchange, which is in general dependent on the temperatures of the surfaces in contact with the air. It is not really necessary to resort to effective conductances to model ceiling space; the air gap can be treated from first principles. This will entail using a multi–zone approach to model the roof where one zone is the ceiling space and the other the interior space [28]. For the purposes of this study this is not necessary. The principle of an effective conductance is quite adequately established experimentally [5] and the extra detail will obscure more important aspects.

The solution of the heat diffusion equation for each surface must be determined with the appropriate boundary conditions for each surface. This will normally mean the sol–air temperature and the associated film coefficient must be determined for each external surface. The internal surfaces are coupled to each other via radiative exchange and to the internal air node via internal film coefficients. The solution of the diffusion equation is determined for steady periodic conditions in the form of a transmission matrix (two port) as set out in §2.5.3. We therefore have for each surface of the shell a two port and the two ports are driven from the outside by the sol–air temperatures. Internally, the two–ports are connected with a radiative exchange network between the internal surfaces and convection coefficients to the internal air. The model is shown schematically in figure 2.2.

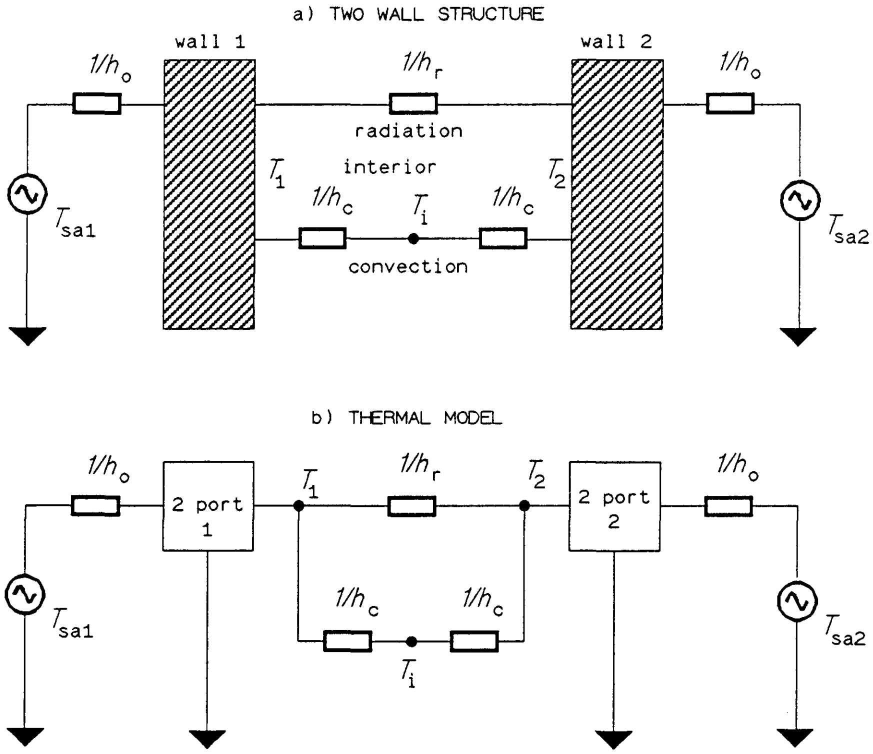

FIGURE 2.2 Model of simple two wall structure with sol–air forcing function on external surfaces, internally interconnected via a radiation coefficient h_r and via the the convective coefficient h_c to the interior air–node. The walls are represented by two–port networks. The outside surface coefficient h_o is the effective film coefficient to the sol–air which includes convection to the outside air, shortwave radiation from the sun as well as long wave radiation to the sky.

Ventilation (see §2.4.4) can be included by simply adding another forcing function T_o to the internal air node, via the ventilation resistance R_v as in figure 2.1. Ventilation is further discussed in §2.4.4 b.

2.4.2 The Floor

The model of the floor of a building presents no additional complication if the floor is a suspended floor of a multi-storey building. However, if the floor is in contact with the ground, as is frequently the case, considerable complication arises. The ground underneath the building is not insulated from the floor slab and heat will be exchanged between the soil and the interior air through the slab. This exchange is essentially three dimensional in nature [3]. The problem of ground contact receives considerable attention in the literature. According to [11], the soil can be introduced as another layer underneath the concrete slab up to a depth of 75 mm, at which point the temperature is essentially the (seasonally) mean outdoor air temperature. Delsante [30] recently published an analytical solution for the heat flow in the soil underneath the building. He indicates that a considerable heat flow exists between interior air and exterior air along a path through the soil underneath the foundations. The model of the floor is of minor importance for this study, since we are mainly concerned with the lumped representation of the walls.

2.4.3 Heat Exchange Between Internal Surfaces

One of the most important simplifying assumptions inherent in the model of Mathews and Richards, is the assumption of isothermal interior surfaces. In effect, this assumption ignores all heat exchange between the interior surfaces. This does not mean that the method assumes no heat exchange takes place, but rather, that it is very effective so that dynamic equilibrium is soon attained and little temperature differences will be observed. Two modes of heat exchange between interior surfaces evidently occur; direct radiation between the surfaces and indirect convection with internal air. A temperature difference between two walls will cause radiative transfer of heat directly from the hot to the cold surface. In addition, if the interior surface temperatures differ, they can not all be equal to the interior air temperature. Consequently, a natural convection current will be set up so that heat will be transferred from the hot surfaces to the air and then from the air to the cold surfaces.

Indoor comfort are dependent on both the air temperature and the temperature of the interior surfaces [1]. Muncey [3] indicates that the interior heat flow network may be simplified from delta to star (∇ to Y) form. It is then possible to find a single node representation of the interior temperature, although it is difficult to give a physical interpretation of this, so called, effective– or environment temperature. In the absence of ventilation and infiltration, the temperature of the interior air must equal the mean temperature of the internal surfaces, provided the air is well mixed and the convection coefficients of all the internal surfaces are the same. In this section we examine the radiative and convective exchange of heat between interior surfaces in some detail.

a) Radiative Heat Exchange

Radiative heat exchange between interior surfaces is intrinsically a non–linear phenomenon. The basic law of heat exchange via radiation is the Stefan–Boltzman law [1,5,8,15,29,31], which can be put in the following form [15] for two parallel surfaces of area A:

$$q = F_{12} \cdot A_1 \cdot \epsilon_1 \cdot \epsilon_2 \cdot \sigma \cdot (T_1^4 - T_2^4) \qquad (2.1)$$

with q the radiative heat flux [W]
F_{12} a geometric form factor
A_1 the area of surface 1 [m^2]
σ Boltzman's constant = $5.669 \cdot 10^{-8}$ W/m$^2 \cdot$K^4
ϵ_1 and ϵ_2 the emissivities of the respective surfaces and
T_1 and T_2 are the absolute temperatures of the respective surfaces in Kelvin.

If it is assumed that the temperature difference between the surfaces are small compared to the mean absolute temperature, the equation can be linearized. It is a well known procedure [15] but for completeness it is again included here. Write (2.1) in the form[4]:

$$q = F_{12} \cdot A_1 \cdot \epsilon_1 \cdot \epsilon_2 \cdot \sigma \cdot (T_1^2 + T_2^2) \cdot (T_1 + T_2) \cdot (T_1 - T_2), \quad (2.2)$$

and define a radiative coefficient:

$$h_r = F_{12} \cdot A_1 \cdot \epsilon_1 \cdot \epsilon_2 \cdot \sigma \cdot (T_1^2 + T_2^2) \cdot (T_1 + T_2). \quad (2.3)$$

With $\Delta T = (T_1 - T_2)$ and $(T_1 + T_2)/2 = T_m$ (2.3) becomes:

$$\begin{aligned} h_r &= F_{12} \cdot A_1 \cdot \epsilon_1 \cdot \epsilon_2 \cdot \sigma \cdot (4 \cdot T_m^3 + \Delta T^2 \cdot T_m)) \\ &= F_{12} \cdot A_1 \cdot \epsilon_1 \cdot \epsilon_2 \cdot \sigma \cdot T_m^3 \cdot (4 + [\Delta T/T_m]^2). \quad (2.4) \end{aligned}$$

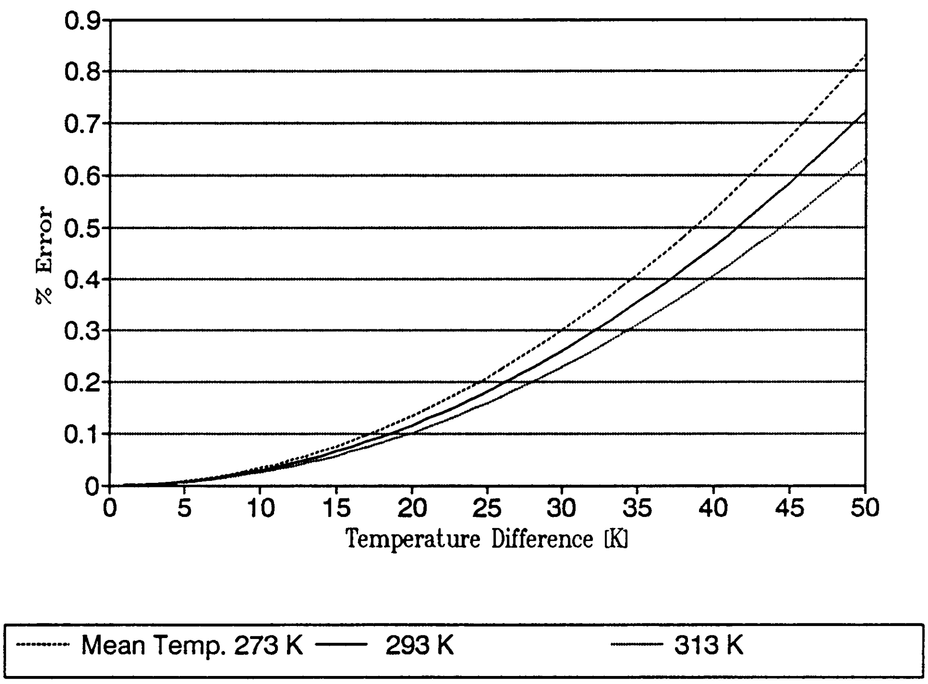

FIGURE 2.3 Percentage error of linearized h_r, as a function of temperature difference of the radiating surfaces at a mean temperature of 20°C.

[4]These results are well known. We include it for the sake of completeness and to aid newcomers to the science of building thermal response.

In buildings, conditions are such that $\Delta T/T_m$ is a very small fraction. (With $T_m = 20^oC$ and $\Delta T = 20^oC$, $\Delta T/Tm = 20/(293) = 0.068$.) Consequently, the second term in (2.4) is very much smaller than 4 and we find approximately:

$$h_r \approx 4 \cdot F_{12} \cdot A_1 \cdot \epsilon_1 \cdot \epsilon_2 \cdot \sigma \cdot T_m{}^3. \tag{2.5}$$

We see that with this definition of h_r, radiant heat transfer can be written in the same form as convective heat transfer:

$$q = h_r \cdot A \cdot (T_1 - T_2)$$

One can also define a radiant heat transfer resistance:

$$R_r = \frac{T_1 - T_2}{q} = 1/h_r A.$$

The error in using (2.5) instead of (2.4) is shown in figure 2.3 where the percentage error is given as a function of ΔT with $Tm = 20$ °C. Even at $\Delta T = 50$ °C the error is below 1 %. Linearizing the radiative coefficient is seen to be extremely accurate for building thermal applications.

In the thermal model of the building each interior surface must be connected to every other interior surface with a radiation coefficient as in figure 2.2 [8,1,28]. For more than just two surfaces, a very complicated thermo–flow network is obtained[5].

b) Convective Heat Exchange

Convective heat exchange on interior surfaces have been the subject of many papers and is discussed in [1,3,5,15] and elsewhere. Convection is usually treated by defining a mean convection coefficient h_c as in

[5]For examples of realistic interior heat transfer networks see [8] and [28 p101].

Newton's law of cooling[6]:

$$q = h_c \cdot A \cdot (T_w - T_\infty)$$

with q the convective heat flux [W]

h_c the convection (film) coefficient [W/m^2·K]

A the area of the surface [m^2]

T_w the temperature of the surface [^{o}C]

T_∞ the free temperature of the air [^{o}C].

Although it is possible to derive theoretical values for convection coefficients from boundary layer theory[7], in practice, convection coefficients are usually based on empirical correlations between non–dimensional groups [29]. Various authorities have published indoor convection coefficients for buildings [1,5,31].

In the model of thermo–flow in buildings each interior surface surface must be connected to the interior air–node with a convective resistance given by $R_c = 1/h_c$ (for surfaces of unit area), as in figure 2.2.

c) Combined Film Coefficient for Interior Surfaces

The combined radiative and convective heat exchange network for an enclosure consisting of only two surfaces is given in figure 2.4a. In general, buildings will consist of more than just two surfaces. If all these surfaces are connected to each other via radiation resistances, and to the interior air via convection resistances, a very complicated circuit arises [8,28 p101]. Athienitis [8] has shown that these complicated networks can be solved efficiently.

It is possible to simplify the internal heat flow network by introducing the concept of a combined film coefficient, h_i, which incorporates both

[6]These results are well known. We include it for the sake of completeness and to aid newcomers to the science of building thermal response.

[7]See appendix C of chapter 4 for an example of a theoretical calculation of the interior convection coefficient.

convective and radiative heat exchange. The definition of the combined coefficient is not unique and depends on certain simplifying assumptions. The procedure will be demonstrated for four distinct assumptions with the aid of the simple two surface structure of figure 2.2.

Method 1: Airtight Enclosure

In the circuit of figure 2.2 the interior air node T_i is not connected to the exterior air which would be the case if infiltration or ventilation is included. In this case it is possible to determine a unique and accurate definition of the combined coefficient. First apply a ∇ to Y transform to the interior heat transfer network which translates the interior network of figure 2.2, reproduced as figure 2.4a, to the equivalent network of figure 2.4b. (It was assumed that convection from both interior surfaces are equal.)

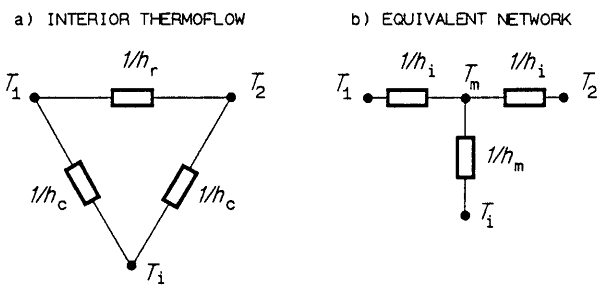

FIGURE 2.4 Simplification of interior heat exchange for two wall structure via ∇ to Y transform of interior network.

The result is that the surfaces are inter–connected with conductances $h_i = h_c + 2 \cdot h_r$ and via conductance $h_m = h_c/h_r \cdot h_i$ to the interior air, for surfaces of unit area. The artificial node, T_m , which results from the transformation is non–physical. It represents an *environment temperature.* In the absence of ventilation and infiltration, no heat flows through h_m and the temperatures on both sides of h_m are the same, i.e.

the air–temperature is equal to the environment temperature. In this case, we see that the surfaces are effectively connected via h_i to the air temperature node T_i, and an equivalent film coefficient which incorporates both convection and radiation is:

$$h_i = h_c + 2 \cdot h_r. \tag{2.6}$$

For three surfaces one finds from figure 2.5:

$$h_i = h_c + 3 \cdot h_r. \tag{2.7}$$

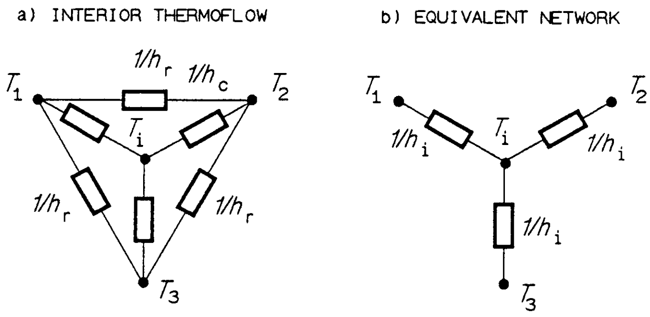

FIGURE 2.5 Interior thermo–flow network for a 3 wall structure.

For n surfaces accordingly[8]:

$$h_i = h_c + n \cdot h_r \tag{2.8}$$

It is seen that each additional surface increases the effective coefficient to the interior air for all other surfaces, since it provides additional area for convection via the radiation. Note that (2.8) assumes the radiation resistances and convection resistances are equal for all the surfaces. Obviously this will not be so in practice. Besides differences in area the

[8]Equation (2.8) is only valid when the concevtion coefficients of all the surfaces are equal. If the convection coefficients differ, one can follow a similar procedure but it is a little more involved. E.g. in figure 2.5 the coefficients h_c are first converted to ∇ format, which places them in parallel to h_r. The combined coefficients are then obtained by transforming once more, this time from ∇ to Y. For more surfaces the procedure is obviously complicated and requires the simultaneous solution of a set of equations.

orientations of the surfaces and emissivities will affect the radiative exchange. Furthermore, we have neglected the resistance h_m in figure 2.4. Actual buildings are also very seldom airtight, in which case the effect of h_m on the interior air temperature will not be negligible and this definition of h_i can not be sustained.

Method 2: Adiabatic surfaces

If it is assumed that the second surface is an interior partition, that is, when there is no net flow of heat through it, the interior effective convection coefficient for two walls can be defined as:

$$h_i^a = h_c/(h_c + h_r)\cdot h_i \tag{2.9}$$

from figure 2.4b with no net flow of heat through the conductance h_i connected to T_2. For multiple surfaces, it is clear that in the adiabatic case (all other walls regarded as partitions), the combined coefficient must represent the total coefficient for transportation of heat from the relevant surface, directly to the interior air, and via radiation to the other surfaces, and then by convection from the other surfaces indirectly to the interior air. Therefore, if the enclosure is made up of many surfaces the combined coefficient of each surface includes the following heat flows: a) convection from surface to air, b) radiation from the surface to every other surface, and from that surface, via convection, to the air. Heat flow a) for the surface is given by h_c, and heat flow b) from surface n to m by $h_c\cdot h_{rnm}/(h_c + h_{rnm})$, where h_c is the convective coefficient from the surface, and h_{rnm} the radiative coefficient from surface n to surface m. The combined adiabatic coefficient for the surface is thus given by:

$$h_i^a = h_c + \sum_j h_{cj}\cdot h_{rj}/(h_{cj} + h_{rj}) \tag{2.10}$$

where the summation extends over all surfaces, except the current surface for which the combined coefficient is being defined.

Method 3: Surface temperatures equal to air–temperature

Kimura [15] gives typical values for a combined coefficient h_i under the assumption that "all inside surfaces of the room enclosure elements, other than that of the exterior wall concerned, stay at the same temperature as the room air". In this case the convection from the other surfaces are neglected and the combined coefficient is found to be the sum of the convective and radiative coefficients, which follows immediately from figure 2.4a if $T_2 = T_i$:

$$h_i{}^i = h_c + h_r. \tag{2.11}$$

For n surfaces, each of unit area, one correspondingly finds:

$$h_i{}^i = h_c + (n-1)\cdot h_r. \tag{2.12}$$

These results are clearly similar to that of method 1 given by (2.8).

Method 4: Isothermal surfaces

Another assumption which yields a combined coefficient is the assumption that all the interior surfaces are at the same temperature. This assumption will be realized in the circuit of figure 2.4a when the radiative coefficient is very large compared to the convective coefficient.

Condition	Combined Coefficients [W/m²K]		
Number of surfaces	2	4	6
1) Airtight enclosure	11.5	19.5	27.5
2) Adiabatic surfaces	5.4	9.1	12.8
3) Surfaces equal to air	7.5	15.5	23.5
4) Isothermal surfaces	7.0	14.0	21.0

TABLE 2.1 Numerical values for various definitions of the combined heat transfer coefficient, with h_c assumed 3.5 W/m²·K, and h_r 4 W/m²·K.

In this case, radiation is so effective that heat conducted from an exterior surface, and arriving at an interior surface, is radiated immediately to all other interior surfaces, and then convected from all surfaces to the interior air. The combined coefficient for n surfaces of unit area is in this case:

$$h_i^c = n \cdot h_c \tag{2.13}$$

In table 2.1 we show the combined interior coefficients for 2 and 6 surfaces of unit area, as obtained from the various definitions. A typical value for h_c is 3.5 W/m^2·K, and for h_r, 4 W/m^2·K. The table was constructed with these values and under the assumption all areas are 1 m^2.

At this stage it is clear that the concept of a combined heat transfer coefficient is highly dependent on certain assumptions and that various assumptions lead to different definitions of the combined coefficient. Mitalas [32] has assessed the influence of the convection coefficient and the combined coefficient by extensive simulation on an analog computer. He comes to these conclusions: "...the cooling load required to maintain the room air temperature constant is quite insensitive to changes in the inside surface convection coefficients." On the combined coefficient he remarks: "The results show that it is not possible to select a particular value of the combined heat coefficient (h_i) which would approximate the radiant heat interchange by the inside room surfaces equally well in al situations." He also remarks: "The other disadvantage of the combined coefficient (h_i) is that the value of (h_i), which gives a good approximation of the cooling load, introduces large errors in the calculation of the surface temperatures." This last remark is of great importance; it indicates that one should not expect a single circuit to be equally applicable to temperature predictions and load estimation.

Mathews and Richards [10] state that they assume the interior surfaces are isothermal. Their combined coefficient should therefore correspond to $h_i^c = n \cdot h_c$ above. In practice, one can determine empirical values of interior surface coefficients for a specific thermal model by selecting values for a best fit of the predictions with measured data. The values of the internal film coefficients, as given by Mathews and Richards, were presumably determined in this manner to suit the preceding CR–method [6].

It must be borne in mind that the convection coefficient is dependent on air flow speed, and therefore, in the case of natural convection, also on the temperature differences between the surfaces which drive the convection. Obviously, it is also dependent on ventilation rates. The radiation coefficient is to the third power dependent on the mean absolute surface temperatures (2.5). The use of constant empirical film coefficients can only be justified by verification experiments. The excellent results obtained by Mathews and Richards are therefore in agreement with the above quoted statement of Mitalas that the thermal response is fairly insensitive to these coefficients.

2.4.4 The Forcing Functions

The various forcing functions which influence the indoor environment have been described by Mathews and Richards [10] and also by many others. We restate them here for sake of completeness.

a) Sol–Air Temperature

The primary thermal forcing function on earth is radiation from the sun. The exterior surfaces of the building will both receive electromagnetic energy from the sun, as well as reradiate some of this energy to deep space and other surrounding surfaces[9]. The irradiation consists of both direct radiation from the sun and indirect or *diffuse* radiation from other hot surfaces. The radiation from the sun is mostly in the spectral range with wavelength 0.1 to 3 μm while the *longwave* emissions are at wavelengths of around 10 μm [29]. The radiation exchange is in accordance with the Stefan–Boltzman law given in §2.4.3.

[9]These results are well known. We include it for the sake of completeness and to aid newcomers to the science of building thermal response.

The dominant physical features of the exterior surface which determines the radiation is the shape factor F, which in this case can be taken as a shading factor, and the emissivity ϵ_w of the surface.

Besides radiation, the temperature of the exterior surface is determined also by convective heat exchange with the surrounding air. This convective exchange is highly dependent on the movement of air over the external surfaces and the air temperature. This convection is also governed by Newton's law of cooling, see §2.4.3., with an external convection coefficient, h_{ce}.

To enable a unified treatment of radiation and convection Mackey and Wright [33] introduced the concept of sol–air temperature. The effects of convection, as well as direct and indirect radiation, are combined by defining an equivalent forcing function, the sol–air temperature T_{sa}, together with an appropriate film coefficient h_o. T_{sa} is a fictitious temperature which together with the film coefficient, will give the same rate of heat transfer to the surface, as would result from convection and radiation combined. (In electrical terminology, it represents a Thevenin equivalent source.) T_{sa} is defined by consideration of the external wall surface temperature when no heat flows through the wall (adiabatic surface). In this case a heat balance at the wall surface gives:

$$q_s = q_l + q_c \tag{2.14}$$

where $q_s = \alpha\ I_s$ is the incident radiation from the sun and other hot objects, α is the absorptivity, I_s is the irradiance on the surface, $q_l = \epsilon \cdot (T_w{}^4 - T_s{}^4)$ is longwave re–radiation to cooler objects and the sky, ϵ is the emissivity, T_w is the wall surface temperature, T_s the mean surrounding (sky) temperature, and $q_c = h_{ce} \cdot (T_w - T_o)$ is convective heat losses to the air, h_{ce} is the external convection coefficient and T_o the ambient air temperature. The longwave radiative heat transfer can be represented with an equivalent radiation coefficient h_{re} in the manner described in §2.4.3. If we define the external film coefficient $h_o = h_{ce} + h_{re}$ the sol–air temperature equals T_w as defined above:

$$T_{sa} = \frac{\alpha \cdot I_s + h_{re} \cdot T_s + h_{ce} \cdot T_o}{h_o}. \tag{2.15}$$

Some authorities which published lists of external heat transfer coefficients are [1,2,6,15,31].

The external coefficient h_o is obviously determined by exterior radiant temperatures and flow–rates. Nevertheless, many researchers [10,8 and references just cited] indicate that a constant value between 15 and 25 $W/m^2 \cdot K$ is often adequate.

The sol–air temperature will differ from one external surface element to another. (E.g. the intensity of sun light on northern and southern walls is different). In a general model, each element of the shell which is subject to a different sol–air temperature, must receive individual treatment, and be individually represented in the thermal model (see figure 2.7). The reduction of the various sol–air forcing functions of the model to one effective forcing function is discussed in §2.5.4.

b) Ventilation

The most problematic aspect of the prediction of thermal performance of buildings is natural ventilation. Ventilation will significantly affect the thermal interior temperature by direct convection of interior heat to and from the outside air. The problem is not that the physical mechanism of heat transport is unknown, but rather, the accurate prediction of ventilation rates. Ventilation is a strong function of local outdoor air flow, placing and type of windows, occupant behavior etc. Kimura [15] reviews existing models for infiltration. In [1] various procedures for the estimation of ventilation rates are given. These models can only be used if adequate meteorological data are available. Fortunately, for a design tool, the problem can be circumvented by assuming 'standard' conditions or worst case conditions. Nevertheless, it is important to have some idea of typical ventilation rates in order to be able to specify standard conditions. In this study we are interested in the mathematical modelling of heat flow in buildings and will not investigate ventilation in detail. It suffices to state that provided ventilation rates are known, ventilation is easily included in the two port model of the simple building by adding another *ventilation resistance*, and a temperature source, as in the model of Mathews and Richards (figure 2.1). The new temperature source is equal to the entry temperature of the ventilating air, which will normally be the outdoor air temperature T_0. The resistance through which T_0 acts is the ventilation resistance R_V which is determined by the rate of heat transport by ventilation, which is again directly related to the air change rate per hour *ach* via (from [10])[10]:

$$R_V = 3.6/Vol \cdot \rho \cdot c_P \cdot ach \qquad (2.16)$$

where *Vol* is the volume of the zone in [m³], *ach* the air change rate per hour [/h], ρ is the air density [kg/m³], and c_P the specific heat of the air at constant pressure [kJ/kg·K].

The main problem is clearly the determination of the air change rate as a function of the exterior wind, windows, building orientation etc. This problem is also discussed in [10]. ASHRAE [1] has published some estimates of air infiltration which take the form of power laws with respect to the pressure difference across the building, but states: "Unfortunately it is very difficult to determine accurate values of flow opening area and pressure difference for actual buildings, which consist of complex air leakage passages."

Although ventilation is a very important aspect in the thermal performance of buildings (it may constitute as much as 30% of the heating load [1, 28 p140]), it is, as we have stated, outside the scope of this thesis. More relevant here is the uncertainty which unknown

---

[10]These results are well known. We include it for the sake of completeness and to aid newcomers to the science of building thermal response.

ventilation rates enforce on thermal models of buildings. Even 'air-tight' conditioned buildings are still subject to unknown infiltration rates of outside air through the pores of the structure. It makes little sense to attempt to predict all other aspects of heat transfer in buildings with extreme accuracy, when a very basic component is largely unknown, and will in all probability never be completely known [10]. It follows that the accuracy of the simple model of Mathews and Richards should not be judged in absolute terms, but rather, in terms of the usefulness of the method as a design tool. It is, accordingly, not the objective of this thesis to express a final judgment on the accuracy of the method, but rather, to investigate the theory behind the method to gain a better understanding of the method and it's limitations.

c) Internal Loads

Besides ventilation, other internal loads may influence the interior temperature. Electrical equipment, people, air conditioning etc. adds to the internal load. The most important component is usually the rays of sunlight penetrating through windows. All these effects are easily included in the thermal model by adding the necessary sources and resistances (see [10] and figure 2.1). It is a major benefit of the simple thermal model of Mathews and Richards that it allows such easy extension. In chapter 3 of this thesis the ease with which the method is extended to include – in this case – structural storage is demonstrated.

2.4.5 A Comprehensive Model

We have modelled the walls of a rudimentary building, consisting of just two opposing walls, with two ports which are exact solutions of the diffusion equation for sinusoidal forcing functions. The only assumption for heat flow through the walls is that the one dimensional treatment is adequate. Our chief aim with this model is to investigate a) the lumping of conductance and capacitance of the massive parts of the building, and b) the temperatures of the interior surfaces. Obviously, the floor and earth underneath will contribute to the total heat storage capacitance of a building in contact with the ground, and, the roof may introduce further complications. However, these issues fall outside the scope of this study.

We use the simple structure, consisting of only two opposing surfaces, to demonstrate comprehensive modelling of thermo–flow in buildings. In figure 2.6 the complete model for the simple building structure is shown. This model is directly related to figure 2.2 but includes separate internal mass. We only include the sol–air sources since the others are not needed for this investigation. This thermo–flow model is very similar to the model of Athienitis [8] and also to the 'room' model of ASHRAE [28], but it is highly simplified and unrealistic because of the presence of only two walls. It is, however, adequate for demonstrating the general points we wish to investigate.

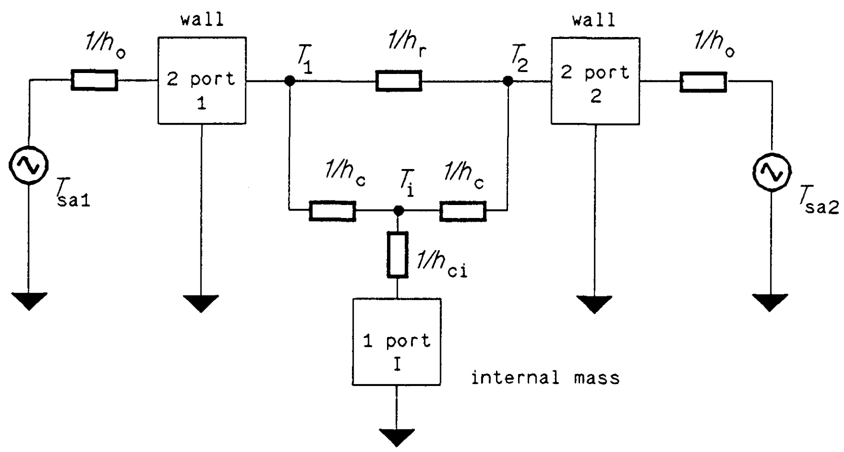

FIGURE 2.6 Comprehensive thermo–flow model for a simple single zone structure, with only two external surfaces, and no infiltration or ventilation.

The interior surfaces of the two walls in figure 2.6 are inter–connected with radiative coefficients to each other and with convective coefficient to the interior air as discussed previously in §2.4.3. The interior air and other interior massive elements are represented by the one port *I*, which can also include contributions from partitions separating neighbouring zones (see chapter 4). One conspicuous omission of the model of Mathews and Richards is the absence of an explicit capacitance for internal mass. It is an important assumption inherent in the model of figure 2.1 that interior mass can be combined with the mass of the shell, "in order to provide an economical description of empirical facts" [11]. This assumption is discussed in more detail in §2.6.1.

As said before, the only forcing functions we take into consideration are the sol–air temperatures on each external surface. We have not included the intricacies of ventilation, interior loads, floors with ground contact etc. since the objective with the comprehensive model is not accurate modelling *per se*, but rather the investigation of certain critical assumptions of the model of Mathews and Richards.

It is fairly easy to extend the comprehensive model to include interconnected zones. Normally, in the single zone approach, a fraction of the storage capacitance of the partitions between the zones is included as internal mass in each zone; since it is assumed that the temperatures in adjacent zones are approximately equal. If this is not the case, then, instead of including the partitions between the zones in the internal mass, they should be used as connections between the various zones, as described in chapter 4.

2.4.6 Solution of the Comprehensive Model

The solution of the model of figure 2.6 involves standard two port theory as discussed in §2.5.3. The two ports for laminated walls are evaluated by multiplying the individual cascade matrices of the laminae[11], and the two ports for surfaces in parallel are obtained by converting to the admittance matrix representation and adding the individual matrices of the surfaces. Surfaces with different external forcing functions are combined into an admittance matrix, which gives the interior temperature and heat–flows through the surfaces by matrix inversion. The procedure was described by Athienitis [8].

We shall not solve the model of figure 2.6 here. We are not really interested in results for this highly simplified two wall structure. Our objective is to derive the simple model of Mathews and Richards from this comprehensive thermal model.

2.5 Derivation of The Model of Mathews and Richards from the Comprehensive Model

We have described a rather comprehensive two–port model for thermo–flow in the simple building structure. In this section, it is attempted to derive the parameters of the simple model of Mathews and Richards, from this comprehensive model, by suitable assumptions and simplifications. The assumptions of Mathews and Richards were stated in §2.3. It is the objective of this section to assess the validity of these assumptions, and to present possible alternatives for determining the circuit parameters of figure 2.1.

2.5.1 Single Zone Approximation

The most basic assumption of Mathews and Richards is the single zone assumption, which enables ignoring the effect of neighbouring zones. The assumption boils down to assuming interior surface temperature differences, in– and between the zones, are far smaller than external–internal temperature differences. It is obviously not an assumption which can be substantiated by theoretical arguments or even

[11] Two–ports, cascade– and admittance matrices are defined in §2.5.3 b and e.

empirical considerations. Interior surfaces which are e.g. irradiated through windows, will obviously experience similar temperatures as external surfaces. According to [8] air temperature differences between 1 K and 3 K will exist between two rooms, even though they may be connected through an open doorway.

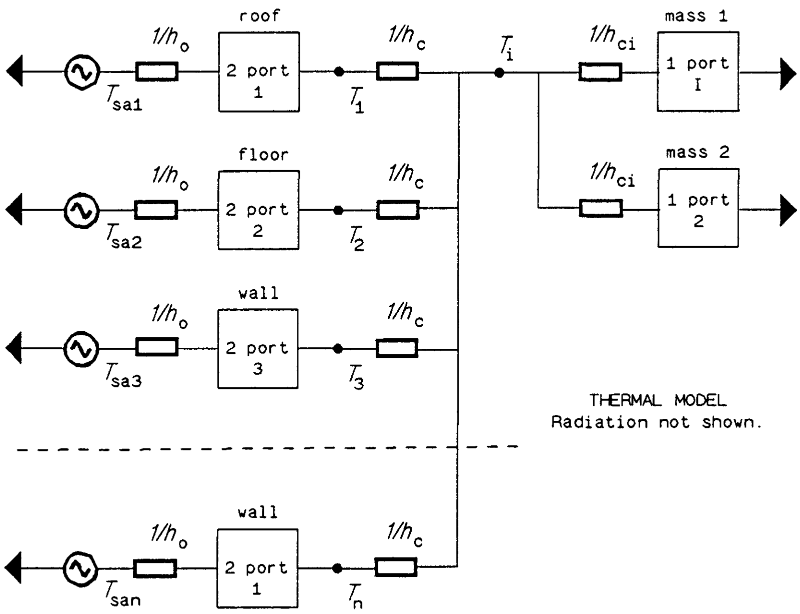

FIGURE 2.7 Two port model for enclosure with more than just two walls. The interior radiative heat flow between surfaces are not shown. It is assumed the film coefficients are equal for all the surfaces.

The single zone assumption is satisfied when all the zones are subject to active climate control, with identical set point temperatures. It is also justified when the partitions between the zones are insulators, so that no inter–zone heat flow occurs. In passive buildings, it can not be justified as an *a priori* assumption. In [10] it is indicated that the utility of the multizone approach lies in it's simplicity, and that its use is justified solely by the useful results obtained with this assumption; as testified by validation studies. In this chapter, we shall confine ourselves to a single zone treatment. Extensions to more zones are discussed in chapter 4.

2.5.2 The Effective Heat Storage Capacitance

In the comprehensive model of the two surface structure, figure 2.6, the massive walls are represented by a two port. Similarly, actual structures with more than just two walls, require a two port descriptor for each wall as in figure 2.7.

In the simple model of figure 2.1 a single capacitor with associated resistances are used to describe all the walls as well as internal mass. In the reduction of the network of figure 2.7 to that of figure 2.1, two alternative sets of assumptions can be used. They are:

i) the surfaces of the massive parts contributing to the stored heat in the building are always approximately at the same temperature,

ii) the distributed elements can be approximated with a lumped single resistance–capacitance network.

Alternatively, the following assumption can be invoked:

iii) it is possible to find a single resistance–capacitance network which will adequately describe the thermal response of the building.

These assumptions lead to considerable reduction in the complexity of the network. It enables a description of the thermo–flow with a simple, first order, ordinary differential equation instead of a system of partial differential equations.

With the first alternative of the two sets of assumptions, a simple network is derived by progressively simplifying the comprehensive model.

Assumption i) enables all the different masses to be combined in a single large mass and assumption ii) allows an RC representation. With this method one would try to couple the elements directly to certain characteristics of the physical construction, e.g. R_0 in figure 2.1 represents the shell resistance, C represents the massive elements etc. The second alternative, iii), leads to an interpretation of the model which is less physical. With this assumption, one simply assumes the network of figure 2.1 can be used as an abstract representation of the thermo–flow, and attempts to find values for the elements which yields a good fit of the network to the theoretical or empirical response of the structure. In this case one does not try to give physical substance to the elements. (This latter alternative is often employed in empirical methods where the values of the parameters are determined by regression e.g.[6,36]). Since Mathews and Richards give a physical interpretation of their parameters, and this physical interpretation is considered a decided advantage, the first method through assumptions i) and ii) will be followed.

We have indicated above how assumptions i) and ii) may be used to derive the circuit of figure 2.1. The procedure will be discussed in more detail shortly. But first, let us deal with the second alternative, assumption iii). The various film resistances in figure 2.7 can be absorbed in the two ports describing the walls. Athienitis [8] has shown that this model can be transformed into one where the various forcing functions are combined in one effective source, which together with the effective admittance matrix of all the walls, determine the interior temperature. Exactly the same procedure can then be carried out with the simple circuit of figure 2.1. The correct resistances and capacitance for the simple network can now be determined by matching the two versions of the admittance matrix, since the simple network and the comprehensive network must yield similar results. In general, it will not be possible to select values for the resistances and capacitances for an exact match. It will be necessary to determine the best values for an optimum fit [21,36]. The procedure is very similar to the method described in §2.5.3 d and will be omitted here. Suffice to say that, in principle, it is possible to obtain any sort of circuit description for the thermo–flow problem in this way. The most general method requires the analytic solution of the comprehensive thermal network, and then obtains an approximate RC network for this comprehensive network by means of network synthesis [34].

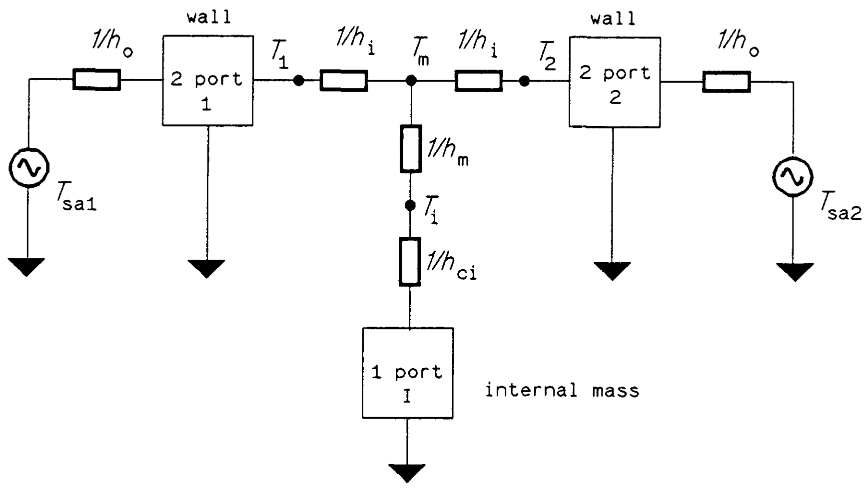

FIGURE 2.8a Model of figure 2.6 with internal heat flow simplified via ∇ – Y transform.

Assumptions i) and ii) allow the determination of an equivalent network in a less abstract manner. If the surface temperatures of the massive elements are approximately equal, the network of figure 2.6, reduces to that of figure 2.8b after first applying the ∇–Y transform, to obtain the circuit of figure 2.8a. The exact condition required is: the temperatures on both sides of the two port must be equal for all the elements, that is, all the external surfaces must be at one temperature and all the internal surfaces at another. The masses are then combined by transforming to the admittance representation and adding the matrix elements as described in §2.5.3 d. The forcing functions on the exterior walls are combined in a single effective forcing function, and the interior resistor network is simplified as in figure 2.8c. This circuit is now very close to the model of Mathews and Richards, when the internal sources and ventilation in their model (figure 2.1) is ignored. The final step is the simplification of the two port representation of the masses in figure 2.8c to the single RC representation in figure 2.1. It will be discussed later. Note that the procedure is also applicable to zones with any number of surfaces.

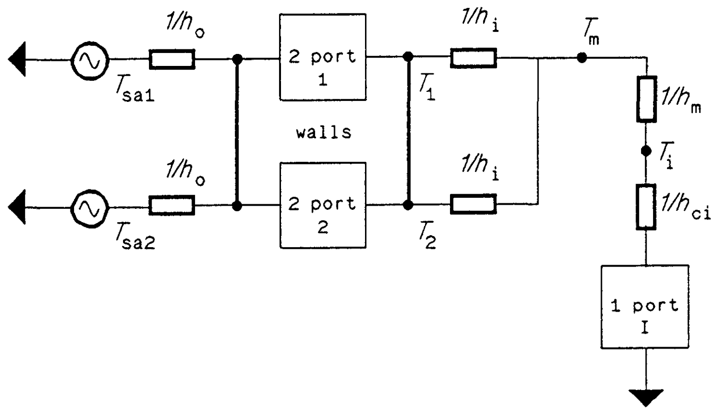

FIGURE 2.8b Circuit with surface temperatures assumed equal.

Another method of reduction, in complexity and accuracy more or less in between the exact method of Athienitis [8], and the method of the previous paragraph, is given in figures 2.9 a and b, starting again with the circuit of figure 2.8a. In this method, it is only assumed that the internal surfaces are isothermal. The only difference between this third method and the method in [8] is the treatment of interior heat flow. The combined two port for the walls, and effective exterior forcing function, is obtained by finding the equivalent Thevenin representation of all heat flows, incident from the exterior surfaces, on the – assumed isothermal – interior surfaces.

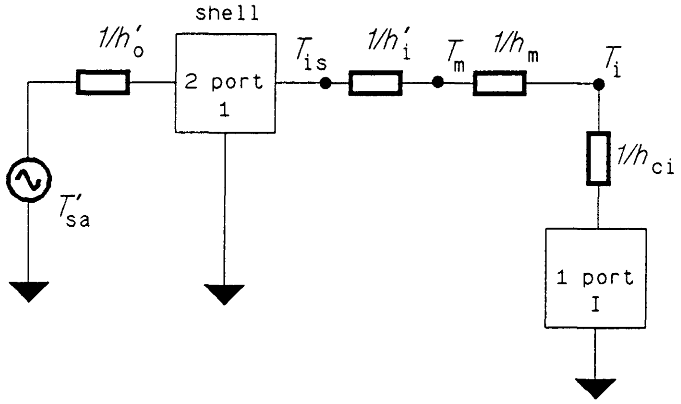

FIGURE 2.8c Final simplified circuit.

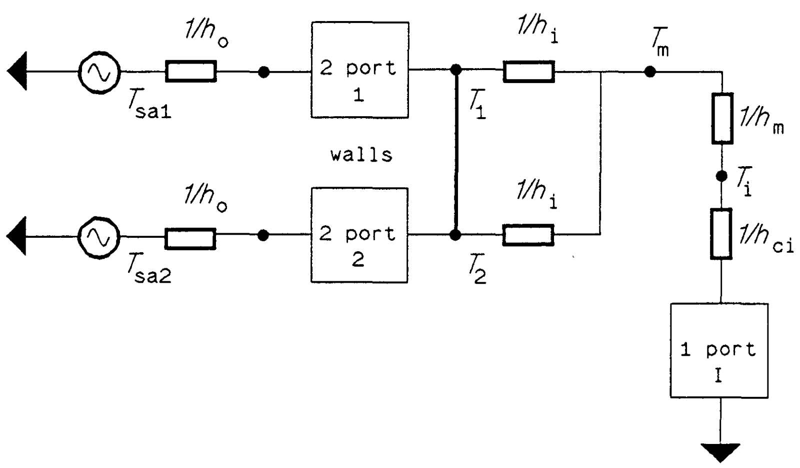

FIGURE 2.9a Reduction with isothermal interior surfaces.

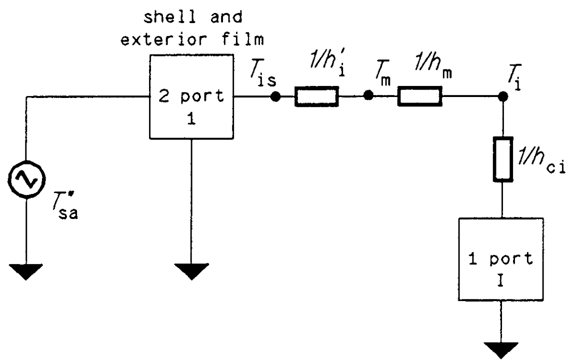

FIGURE 2.9b Final simplified circuit with isothermal interior surfaces.

Clearly all three methods yield equivalent circuit topologies. The parameters of the three methods will however be different and will reflect the different assumptions. Obviously, the first method will be the most accurate and the second the least. Mathews and Richards state that their method assumes isothermal interior surfaces and it should therefore be equivalent to the last method. In fact, it is not so easy to determine which method is actually approximated by them. The topologies are the same, so the formulas employed to obtain numerical values for the different network elements must be compared. If this is done, (see §2.5.3e) it is found that their method corresponds more to the second method than the third. This indicates that inherent in the model of figure 2.1 is also the assumption that the temperatures of the external surfaces are approximately equal. In fact, since the internal mass is also included in the single C in figure 2.1, the best expression of the basic assumption is probably: the bulk temperatures of all the massive elements of the buildings is assumed fairly equal.

In the circuits of figures 2.8 and 2.9 the massive elements are still modelled with two ports. It was indicated above, that one method for determining an RC lumped equivalent for a two port, is to assume a certain RC form, e.g. the single R and C form used by Mathews and Richards, and then to obtain the two port representation for this assumed form. The definitions of elements are then obtained by matching the two port of the assumed form with the exact two port obtained from the solution of the diffusion equation. Another alternative is to derive an RC equivalent via RC network synthesis techniques. Penman [35] shows that the values of the model parameters can also be obtained from parameter estimation techniques, through measurement of the thermal response. This empirical method has, together with other empirical methods such as [6], the drawback that they can only with confidence be applied to those buildings which were originally included in the empirical studies. It is also possible to find an equivalent lumped circuit representation under the assumption that the frequency of variation of the thermo–flow is small. This technique will be used here and is described in the next section.

In order for the lumped representation to be useful, it is required that the parameters of the circuit be determined in terms of the physical properties of the building elements. The only method which yields an obvious connection between the parameters and the physical properties is when it is assumed that all the massive elements are always at the same temperature. In this case the quantity of stored heat is given by the total available heat capacitance multiplied by the temperature of the massive elements. In other methods the capacitance is not directly related to the physical properties, but theoretically represents the *active heat* stored in the structure. The concept can be clarified by noting that heat stored in a massive wall, which is thoroughly insulated on it's interior surface, can not influence the interior temperature. In this case, although the amount of stored heat may be substantial, the active heat is small. The concept is further clarified by figures 2.10 a and b. In figure 2.10 a the total amount of stored heat in the wall is given by $Q_1 = T_w \cdot \rho \cdot c_p$ J/m^3, where T_w is the uniform temperature distribution across the wall. If, at a later instant, the temperature distribution changes to the linear profile given by figure 2.10 b, the active stored heat is the heat which took part in the change, it is thus given by the change in the amount of stored heat $Q_a = \Delta T \cdot \rho \cdot c_p / 2$ J/m^3. In the next section it is shown that the matrix solutions of the heat conduction equation provides a very useful definition of the active capacitance of a layered structure; if it is assumed that the temperature distribution in each layer remains almost uniform.

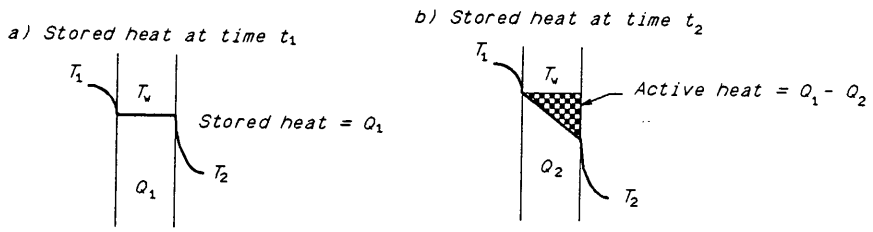

FIGURE 2.10 The active stored heat is the change in stored heat which accompanies changes in the temperature distribution across the wall.

2.5.3 Lumping the Distributed Parameter Structures

One of the most obvious simplifications of the model of Mathews and Richards, figure 2.1, from the comprehensive model of figure 2.6, is the representation of distributed parameter elements with lumped elements. It is highly desirable to obtain a lumped representation of the heat flow since the lumped circuit circumvents the problem of solving the partial differential equation for heat conduction. This allows a much simpler solution process and facilitates further extensions of the method to include more complicated active systems.

According to Muncey [3]: "The whole subject (lumping of elements) requires further study to define reasonable limitations within which lumped circuit calculations may be used confidently." In this section, the lumping of distributed parameter networks for 1 dimensional heat flow problems is discussed. The approximations and conditions for accurate lumping are derived. It is shown that the heat flow through the walls of typical building constructions can be modelled with reasonable accuracy with a lumped thermal resistance–capacitance network. Formulas to obtain the values of the lumped circuit elements, from the heat conduction and capacitance values of the materials, are derived.

The discussion is mostly concerned with the lumping of the thermal capacitance of the elements. The conductivities are also important but are less problematic. The thermal response of the building can be regarded as approximately linear, so that the mean and swing thermo–flow components can be handled separately. We assume that the swing component is sinusoidal without loss of generality since any periodic swing can be obtained from a superpositioning of sinusoidal components, according to Fourier's theorem. The total response is given by the superposition of the mean component and the sinusoidal swing. During consideration of the mean heat flow, the capacitive effects play no role and the conductances are the total heat conductance of the wall. For the sinusoidal swing, heat storage effects and capacitances are most important and the conductances should ideally be so defined, that they, together with the capacitance, yield a good approximation of the distributed response. Mathews and Richards retain the values of the conductances which are valid for the mean components also for the swing components. This is very convenient but theoretically it might be possible to obtain better lumped representations by choosing both the R's and the C's for the most accurate representation of the distributed elements [34].

One approach to lumping is to choose parameters which will accurately reflect the total available heat storage capacity of the structure. This approach is justified when the Biot number (see next section) of the structure is small. Another approach is to preserve the actual amount of heat stored in the structure. However, it is not important that the value of the lumped C reflects the total available heat capacity of the structure, or the actual amount of stored heat. It is far more important that the correct amount of active heat[12] for a specific change in temperature distribution, be reflected by the value assigned to C. This leads to the concept of *active thermal capacitance.* We shall see that this capacitance is only indirectly related to the physical capacitance of the structure.

a) <u>Lumping for walls with small Biot numbers</u>

A well known condition for lumping [29] is that the ratio of external resistance (surface resistance) to internal conduction resistance of the wall, must be much less than 1. This condition ensures that the temperature drop across the wall is small relative to the temperature drop across the surface coefficients. The condition is conveniently expressed in terms of the Biot number defined by:

$$Bi = h_c \cdot \Delta x / k \tag{2.17}$$

with h_c the convective heat transfer coefficient [W/m^2·K], Δx the thickness of the layer [m], and k the thermal conductance of the material [W/m·K]. Biot numbers are small for good thermal conductors

[12]See the last paragraph of the previous section for a discussion of the concept of active stored heat.

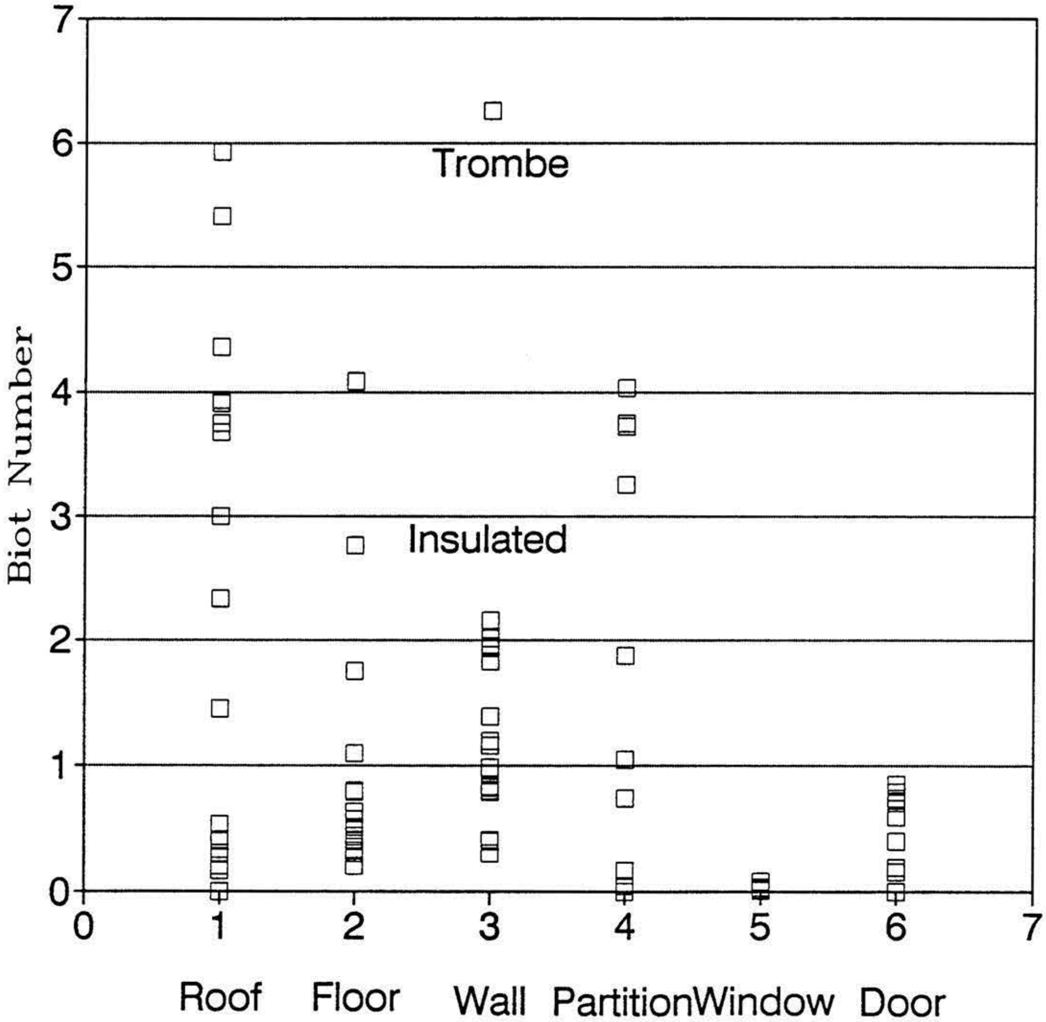

FIGURE 2.11 Biot numbers for building surfaces with respect to a film coefficient of 3 $W/m^2 \cdot K$.The walls with Bi>1 are insulated and cavity walls.

i.e. metallic elements. Most building materials are heat insulators rather than conductors. However, in buildings the surface coefficients also are often quite small and it is not at all obvious that the Biot number for walls should be large. If the Biot number of a wall (calculated from the total conduction resistance of all the layers) is small, further assumptions about the temperature distribution across the wall, for the purpose of defining the active capacitance is unnecessary. A small Biot number actually indicates that the interior temperature distribution is approximately uniform. Therefore, the distinction between active stored heat and stored heat can be dropped and all the physical available capacitance can be regarded as active. Calculation of the Biot numbers for many actual structures indicates that this assumption is often justified for uninsulated walls.

In figure 2.11 we show the Biot numbers obtained for 106 different wall structures from 20 existing buildings. These Biot numbers were calculated with reference to a film coefficient of 3 $W/m^2 \cdot K$ and from the combined resistance of all the layers of the wall. From the figure we see that for most elements the Biot number is in the numerical range 0 to 2.

Strictly speaking the lumped model is only accurate for Biot numbers below 0.1. Obviously, this condition is not satisfied by most of the elements in the figure, but nevertheless, many important wall constructions have quite small Biot numbers as set out in table 2.2. Notably, we find for brick and concrete walls of thickness up to 110 mm, Biot numbers below 0.5. For a double brick wall of 220 mm the Biot number is close to 1. Examination of these results reveal that it is mostly insulated walls or cavity walls which have Biot numbers above 0.5. In appendix 2A these results are listed. Details of the construction of the walls are available in the file 'results.txt' on the floppy diskette in the back–cover. It is seen that it is mostly the insulated walls and constructions with cavities which have large Biot numbers. These results indicate that for many uninsulated, uniform structures, one could probably take the total heat capacitance of the structure as active capacitance. However, based on the results in figure 2.11, one can come to no firm conclusion about the accuracy of lumping, except to say that the Biot numbers are not so large that the possibility of a lumped model must be totally discarded.

Wall Description	Biot number
110 mm brick	0.4
220 mm brick	0.8
330 mm brick	1.2
150 mm concrete	0.3
200 mm concrete	0.4
cavity wall	0.8
9 mm asbestos	0.04

TABLE 2.2 Biot numbers for some typical buildings walls. The total conduction resistance of the wall is compared to a surface coefficient of 3 $W/m^2 \cdot K$.

For sinusoidal heat flow, another condition which will also lead to a lumped representation, is that the wavelength of the thermal wave, as it propagates through the walls, is much longer then the thickness of the wall. While this condition is clearly also connected with the conductivity of the wall, it differs from the condition represented by a small Biot number, in that the propagation wavelength is completely determined by the material from which the wall is constructed, and the frequency of the swing. It is independent of the film coefficients. Note that a small Biot number will always ensure accurate lumping, independent of the forcing temperatures, while this condition is only applicable to sinusoidal temperature variations, i.e. to the swing component. To investigate the accuracy of this method the exact solution of the diffusion equation, for sinusoidal temperature variations, is obtained in the next section.

If the wall is very thick, a single lumped capacitor representation is not possible unless some assumption is made of the variation of the temperature distribution across the wall and the concept of active capacitance is invoked. Another approach is to use a multiple RC representation as discussed in [21 and 36]. In general, the procedure is as follows:

i) decide on the number of nodes (capacitors) which will be used to represent the distribution,

ii) choose the values of the lumped elements to minimize the difference of the RC response with the distributed response.

According to Davies [21] three capacitors are quite adequate to represent common building structures. For very thick structures 5 nodes are sometimes required. We wish to avoid using more than one capacitor to represent the walls since the simplicity of the model is largely centered in the single pole treatment of the variable flow.

b) <u>Exact Solution of the Heat Conduction Equation with Matrices</u>

It is assumed the heat flow through the wall is one dimensional (see discussion §2.4.1). The one dimensional heat conduction equation is:

$$\frac{\partial q_0}{\partial t} = \alpha \cdot \frac{\partial^2 q_0}{\partial x^2} \tag{2.18}$$

where: $$\alpha = \frac{k}{\rho \cdot c_p}$$

is the thermal diffusivity of the material. Assume a sinusoidally varying heat flow with time (more complicated forcing functions can be built up from sinusoidal functions according to Fourier's theorem) i.e.

$$q_0(t) = q(x) \cdot e^{j\omega t} \tag{2.19}$$

The solution of (2.18) for this input (with time dependency suppressed for notational reasons) is:

$$q(x) = q_1 \cdot e^{-\zeta x} + q_2 \cdot e^{\zeta x} \tag{2.20}$$

where: $$\zeta = \sqrt{\frac{\omega}{2 \cdot \alpha}} \cdot (1+i) \tag{2.21}$$

This solution can be rewritten in the equivalent format:

$$q(x) = A \cdot cosh(\zeta \cdot x) + B \cdot sinh(\zeta \cdot x) \tag{2.22}$$

For a wall of thickness ℓ the flow into the wall at $x = 0$ and at $x = \ell$ is:

$$q(0) = A = q_1 \tag{2.23}$$

$$q(\ell) = q_1 \cdot cosh(\zeta \cdot \ell) + B \cdot sinh(\zeta \cdot \ell) = q_2 \tag{2.24}$$

In a similar way one also obtains for the temperature in the wall, which is subject to the same diffusion equation:

$$T(0) = T_1 \tag{2.25}$$

$$T(\ell) = T_1 \cdot cosh(\zeta \cdot \ell) + D \cdot sinh(\zeta \cdot \ell) \tag{2.26}$$

At the surfaces of the wall we define the following matrix description of the flows and temperatures:

$$\begin{bmatrix} T(\ell) \\ q(\ell) \end{bmatrix} = \begin{bmatrix} \mathscr{A} & \mathscr{B} \\ \mathscr{C} & \mathscr{D} \end{bmatrix} \cdot \begin{bmatrix} T(0) \\ q(0) \end{bmatrix} \tag{2.27}$$

Or in vector/matrix notation:

$$\boldsymbol{W}(\ell) = \boldsymbol{T} \cdot \boldsymbol{W}(0) \tag{2.28}$$

where: $\boldsymbol{W}(x) = \begin{bmatrix} T(x) \\ q(x) \end{bmatrix}$ and $\boldsymbol{T} = \begin{bmatrix} \mathscr{A} & \mathscr{B} \\ \mathscr{C} & \mathscr{D} \end{bmatrix}$

The $[\mathscr{A}\ \mathscr{B}\ /\ \mathscr{C}\ \mathscr{D}]$ or $\boldsymbol{T}$ matrix is known as the transmission or cascade matrix which gives the values of the heat flow and temperature at $x = \ell$ from the specified values at $x = 0$. The cascade matrix is symmetrical for symmetric structures. It is a very convenient two port representation of the solution of the diffusion equation. Note, we define the flow at surface $x = \ell$ into the wall and at surface $x = 0$ out of the wall as in figure 2.12, this convention is often used but may differ from others in the literature. The cascade matrix is one of a family of two–port descriptions of the sinusoidal heat flow through the wall. A general theory for complicated systems of coupled two ports exists. For a thorough discussion of these methods see [8 and 35].

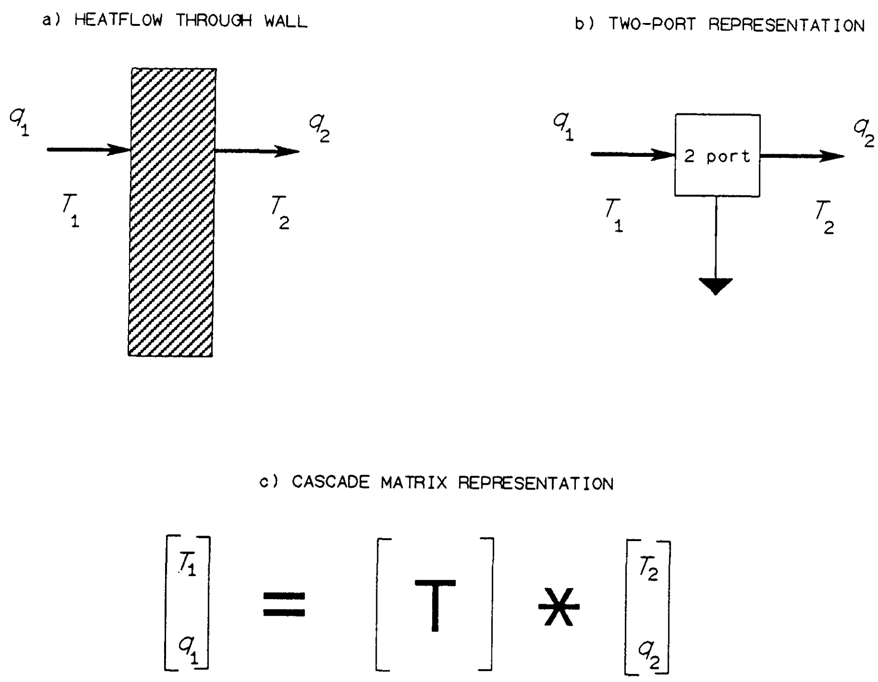

FIGURE 2.12 The cascade matrix or transmission matrix. A two port representation of the solution of the heat conduction equation.

The values of the matrix elements are calculated from (2.22) to (2.26) together with the heat flux equation (Fourier's law of conduction):

$$q(x) = k \cdot \frac{\partial T(x)}{\partial x} \tag{2.29}$$

Differentiating (2.26) with respect to ℓ:

$$\begin{aligned} k \cdot \frac{\partial T(\ell)}{\partial \ell} &= q(\ell) \\ &= k \cdot \zeta \cdot [T_1 \cdot sinh(\zeta \cdot \ell) + D \cdot cosh(\zeta \cdot \ell)] \end{aligned} \tag{2.30}$$

Comparison of this equation with (2.16) gives:

$$B = k \cdot \zeta \cdot T_1 \quad and \quad D = q_1/(k \cdot \zeta) \tag{2.31}$$

Therefore the values of the matrix elements are:

$$\begin{aligned} \mathscr{A} &= cosh(\zeta \cdot \ell) & \mathscr{B} &= Z_0 \cdot sinh(\zeta \cdot \ell) \\ \mathscr{C} &= 1/Z_0 \cdot sinh(\zeta \cdot \ell) & \mathscr{D} &= cosh(\zeta \cdot \ell) \end{aligned} \tag{2.32}$$

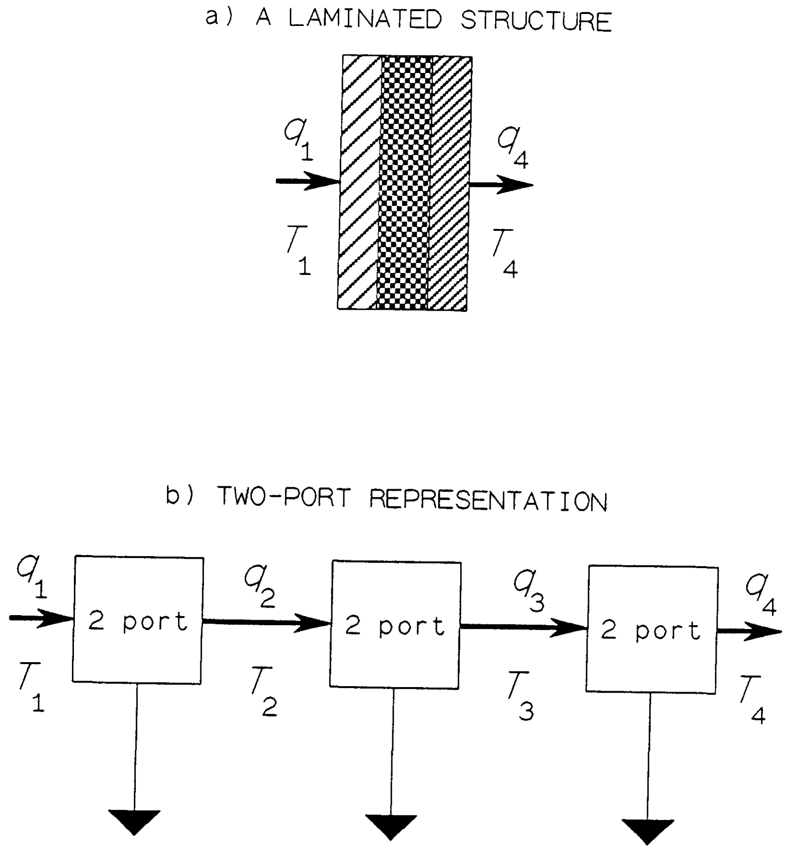

FIGURE 2.13 Cascade matrix for layered structure. The heat–flow is continuous through the structure and the temperatures at the interfaces are equal. Therefore the cascade matrix for the combined structure is the product of the matrices of the layers.

with Z_0 the *characteristic thermal impedance* of the structure defined by:

$$Z_0 = \frac{1}{k \cdot \zeta} = \frac{1}{\sqrt{i \cdot \omega \cdot k \cdot c_p \cdot \rho}} = \frac{1}{\sqrt{2 \cdot \omega \cdot k \cdot c_p \cdot \rho}} \cdot (1 - i) \qquad (2.33)$$

Z_0 is an important property of the material and gives the ratio of temperature over heat flow anywhere on a semi–infinite slab.

The above equations give the exact solution for the 1 dimensional sinusoidal heat flow problem. The advantage of the cascade matrix representation is now evident:– when the wall consists of various layers laminated together, the heat flow into layer *j* equals the heat flow out of layer *i* and the temperatures at the interfaces must be the same, consequently

$$q_i = q_j \quad \text{and} \quad T_i = T_j. \tag{2.34}$$

The solution for the layered structure of figure 2.13 must then be:

$$\boldsymbol{W}_1 = \boldsymbol{T}_1 \cdot (\boldsymbol{T}_2 \cdot (\boldsymbol{T}_3 \cdot \boldsymbol{W}_4)) = \boldsymbol{T}_1 \cdot \boldsymbol{T}_2 \cdot \boldsymbol{T}_3 \cdot \boldsymbol{W}_4. \tag{2.35}$$

Therefore the $\boldsymbol{T}$ matrix of the composite structure is:

$$\boldsymbol{T}_c = \boldsymbol{T}_1 \cdot \boldsymbol{T}_2 \cdot \boldsymbol{T}_3 \tag{2.36}$$

and for a general composite consisting of *n* layers:

$$\boldsymbol{T}_c = \prod_{i=1}^{n} \boldsymbol{T}_i. \tag{2.37}$$

c) <u>Theoretical Values for the Lumped Elements</u>

As indicated before various lumped circuit representations of the wall are possible. Davies [21] discusses the optimum values for lumped models using a minimum mean square error criterion for the elements of the transmission matrix. We derive simpler approximations which turn out to be valid for <u>thin</u> structures.

For the T section of figure 2.14 with resistances *R* in the branches and capacitance *C* in the trunk the cascade matrix is:

$$\boldsymbol{T}_{rc} = \begin{bmatrix} 1+i\cdot\omega\cdot R\cdot C & 2\cdot R + i\cdot R^2\cdot\omega\cdot C \\ i\cdot\omega\cdot C & 1+i\cdot\omega\cdot R\cdot C \end{bmatrix} \tag{2.38}$$

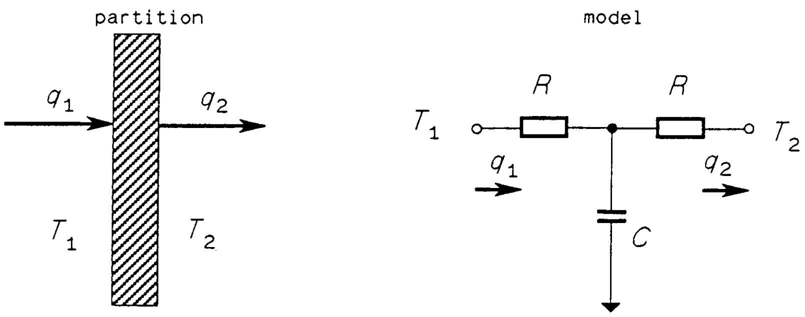

FIGURE 2.14 Lumped RCR T section.

We shall shortly show that this network will adequately represent the distributed parameter system, when the frequency of oscillation ω is small, or equivalently, when the wavelength of the thermal wave is very long. In practice this condition reduces to the statement that the thickness of the wall must be small compared to the wavelength of the temperature wave propagating through the wall. Intuitively, the condition is easily understood by reasoning that if the frequency is small, the wavelength is very long and consequently the temperature across the wall will be approximately uniform if the wall is thin. It is a very satisfactory method of lumping since the two elements R and C of the lumped model are uniquely identified with the two intrinsic properties of the material, k and c_p, exactly as in the case above for small Biot number.

The values of the circuit elements R and C are found from the polynomial expansions of the hyperbolic functions. For the $\mathscr{A}$ and $\mathscr{D}$ elements of the matrix we need to have for a valid approximation

$$\cosh(\zeta\cdot\ell) \approx 1 + i\cdot\omega\cdot R\cdot C. \tag{2.39}$$

$$= 1 + \frac{(\zeta\cdot\ell)^2}{2!} + \frac{(\zeta\cdot\ell)^4}{4!} + \cdots$$

For small values of $\zeta \cdot \ell$ the first term in the series expansion of the hyperbolic function suffice. That is when

$$\frac{(\zeta \cdot \ell)^4}{4!} \ll \frac{(\zeta \cdot \ell)^2}{2!} \text{ or } |\zeta \cdot \ell| \ll 12 \tag{2.40}$$

we can put

$$\frac{(\zeta \cdot \ell)^2}{2!} = \frac{i \cdot \omega \cdot \sigma \cdot \rho \cdot \ell^2}{2 \cdot K} = i \cdot \omega \cdot R \cdot C. \tag{2.41}$$

For the $\mathscr{B}$ element we want

$$\begin{aligned} Z_0 \cdot sinh(\zeta \cdot \ell) &\approx 2 \cdot R + i \cdot R^2 \cdot \omega \cdot C \\ &= Z_0 \cdot \left[\zeta \cdot \ell + \frac{(\zeta \cdot \ell)^3}{3!} + \cdots \right]. \end{aligned} \tag{2.42}$$

For

$$\frac{(\zeta \cdot \ell)^3}{3!} \ll \zeta \cdot \ell \text{ or } |\zeta \cdot \ell| \ll 6 \tag{2.43}$$

we find

$$Z_0 \cdot \zeta \cdot \ell = \ell / k = 2 \cdot R + i \cdot R^2 \cdot \omega \cdot C. \tag{2.44}$$

Setting

$$\ell / k = 2 \cdot R \tag{2.45}$$

and with the further condition that

$$R \cdot C \cdot \omega \ll 2 \tag{2.46}$$

so that the imaginary part of (2.44) is negligible, we have the approximate value of the $\mathscr{B}$ element. For the $\mathscr{C}$ element it is required that

$$\begin{aligned} \frac{sinh(\zeta \cdot \ell)}{Z_0} &\approx i \cdot \omega \cdot C \\ &= \frac{1}{Z_0} \cdot \left[\zeta \cdot \ell + \frac{(\zeta \cdot \ell)^3}{3!} + \cdots \right]. \end{aligned} \tag{2.47}$$

Again, for $|\zeta \cdot \ell| \ll 6$ we have

$$\frac{\zeta \cdot \ell}{Z_0} = k \cdot \zeta^2 \cdot \ell = i \cdot \omega \cdot \sigma \cdot \rho \cdot \ell = i \cdot \omega \cdot C. \tag{2.48}$$

These results and the conditions are summarized in table 2.3.

Element	Distributed	Lumped RCR	Equivalent	Conditions
$\mathcal{A}$, $\mathcal{D}$	$cosh(\zeta\ell)$	$1+i\omega RC$	$1+\frac{i\omega c\rho\ell^2}{2K}$	$\lvert\zeta\ell\rvert \ll 12$
$\mathcal{B}$	$Z_0 sinh(\zeta\ell)$	$R(2+i\omega RC)$	ℓ/K	$\begin{cases}\zeta\ell\omega \ll 6\\ RC\ \omega \ll 2\end{cases}$
$\mathcal{C}$	$\frac{sinh(\zeta\ell)}{Z_0}$	$i\omega C$	$i\omega c\rho\ell$	$\lvert\zeta\cdot\ell\rvert \ll 6$

TABLE 2.3 Conditions and lumped RCR representation.

Note that the equations are consistent if we set:

$$C = c_P\cdot\rho\cdot\ell \tag{2.49}$$

and

$$R = \ell/(2\cdot k). \tag{2.50}$$

The most stringent condition for the above relations to be valid is:

$$R\cdot C\cdot\omega = \frac{c_P\cdot\rho\cdot\ell^2}{2\cdot k}\cdot\omega \ll 2 \tag{2.51}$$

In practice, the frequency is fixed at 1/24·h (diurnal frequency) so that this is a condition on the thickness of the structure. In figure 2.15 we show a graph of this condition for various values of the thermal time constant of the structure defined by:

$$\tau = R\cdot C = \frac{c_P\cdot\rho\cdot\ell^2}{2\cdot k} \tag{2.52}$$

with $\omega = 2\cdot\pi/24$ [/h].

Figure 2.15 shows the relation (2.51) in the equivalent format:

$$\ell \ll \sqrt{48/\pi \cdot \alpha}.$$

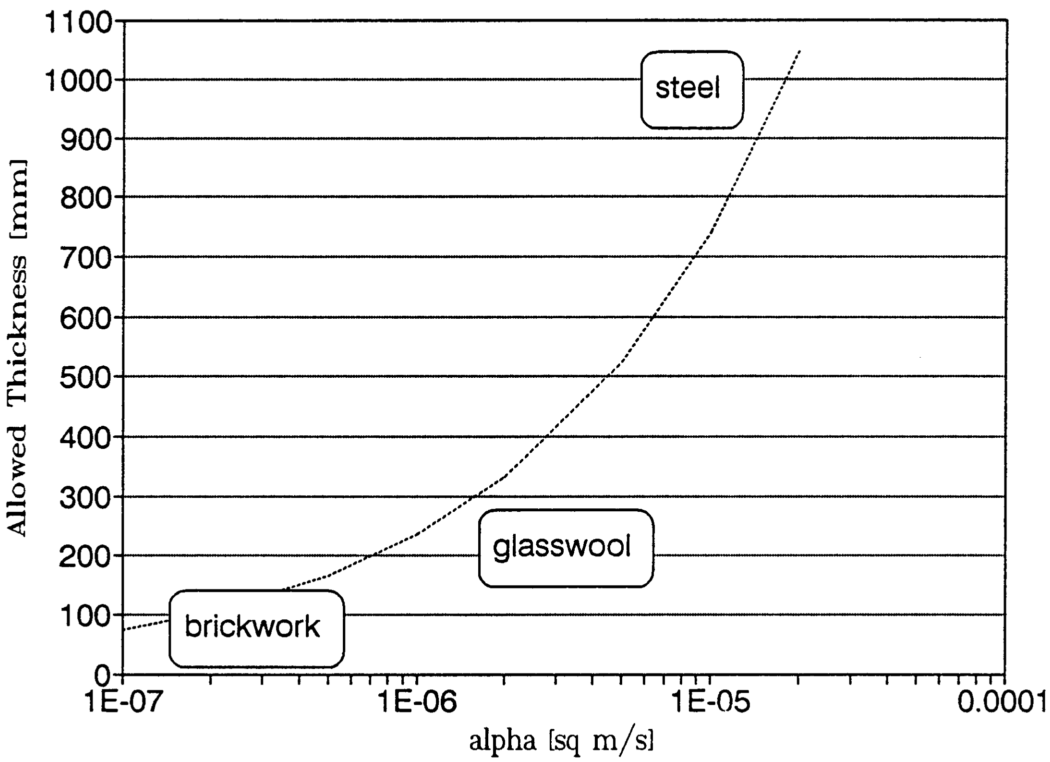

FIGURE 2.15 The lumping condition $\tau \cdot \omega = 2$ for various values of α and $\omega = 2 \cdot \pi/24$ h.

The condition can also be expressed in terms of the wavelength λ of the sinusoidal temperature wave propagating through the structure:

$$\ell/\lambda < 1/\pi \qquad (2.53)$$

or in terms of the Fourier modulus with respect to the period T, defined by [27] $Fo = \alpha \cdot T/\ell^2$:

$$Fo > \pi/2 \qquad (2.54).$$

The Fourier modulus is a characteristic of a specific material at a specific thickness and a specific frequency. For a laminated structure there is no unique definition and one must treat the layers separately. In order to evaluate the above condition for real buildings, the Fourier moduli for over 200 laminae of existing buildings were calculated. The results are given in figure 2.16, with numerical details in appendix 2B.

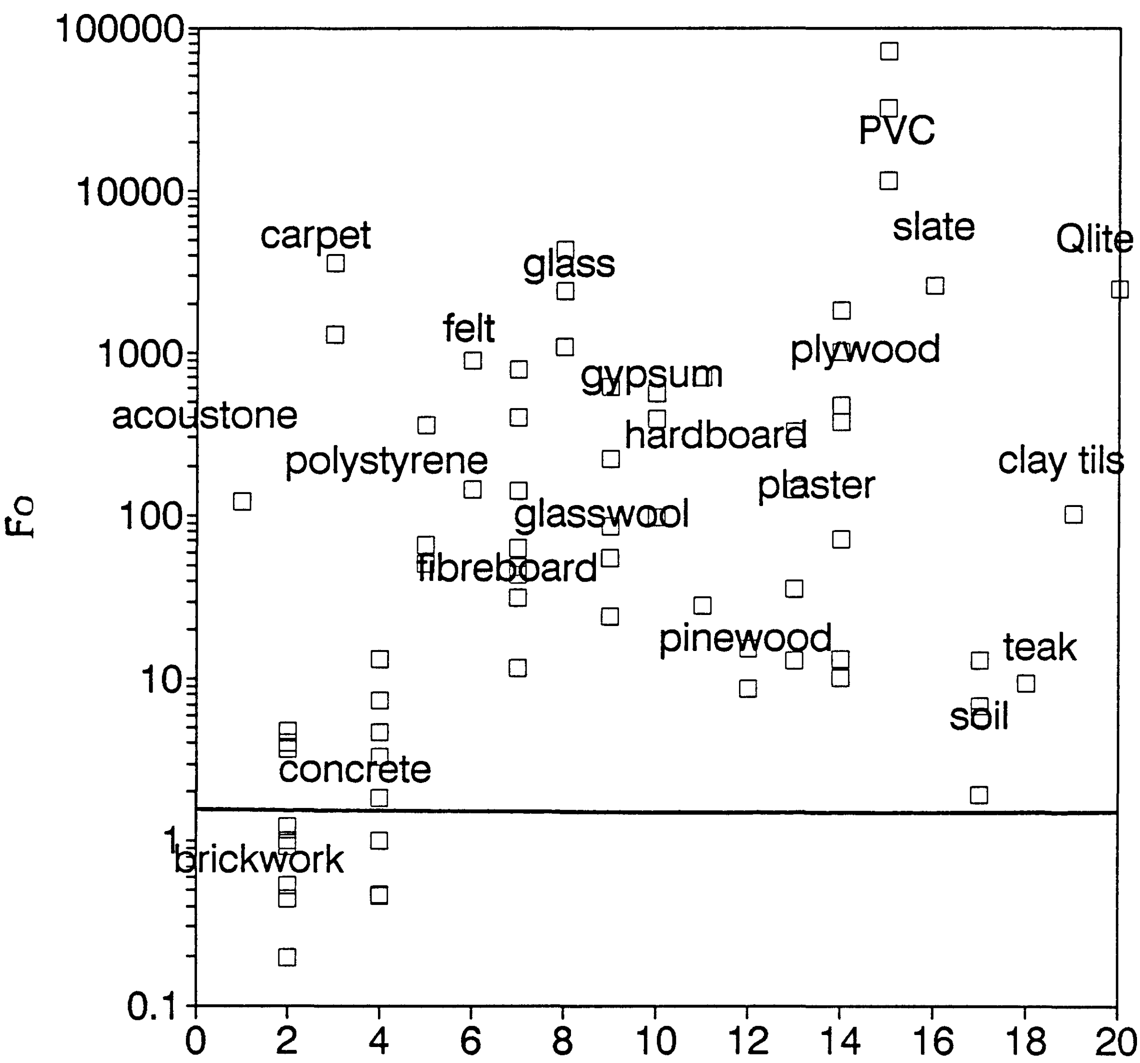

FIGURE 2.16 Fourier moduli for materials of the laminae of real buildings.

Figure 2.16 shows that for most building elements (note that the Fo number is strongly dependent on the thickness of the layer) the Fourier modulus exceeds 10. The only exceptions are brick–work and concrete layers. It appears that condition (2.54) is well satisfied by most layers. In figure 2.17 we give the Fourier modulus of concrete and brick layers as a function of wall thickness. The condition (2.54) is satisfied for layers of brick and concrete up to a thickness of 110 mm.

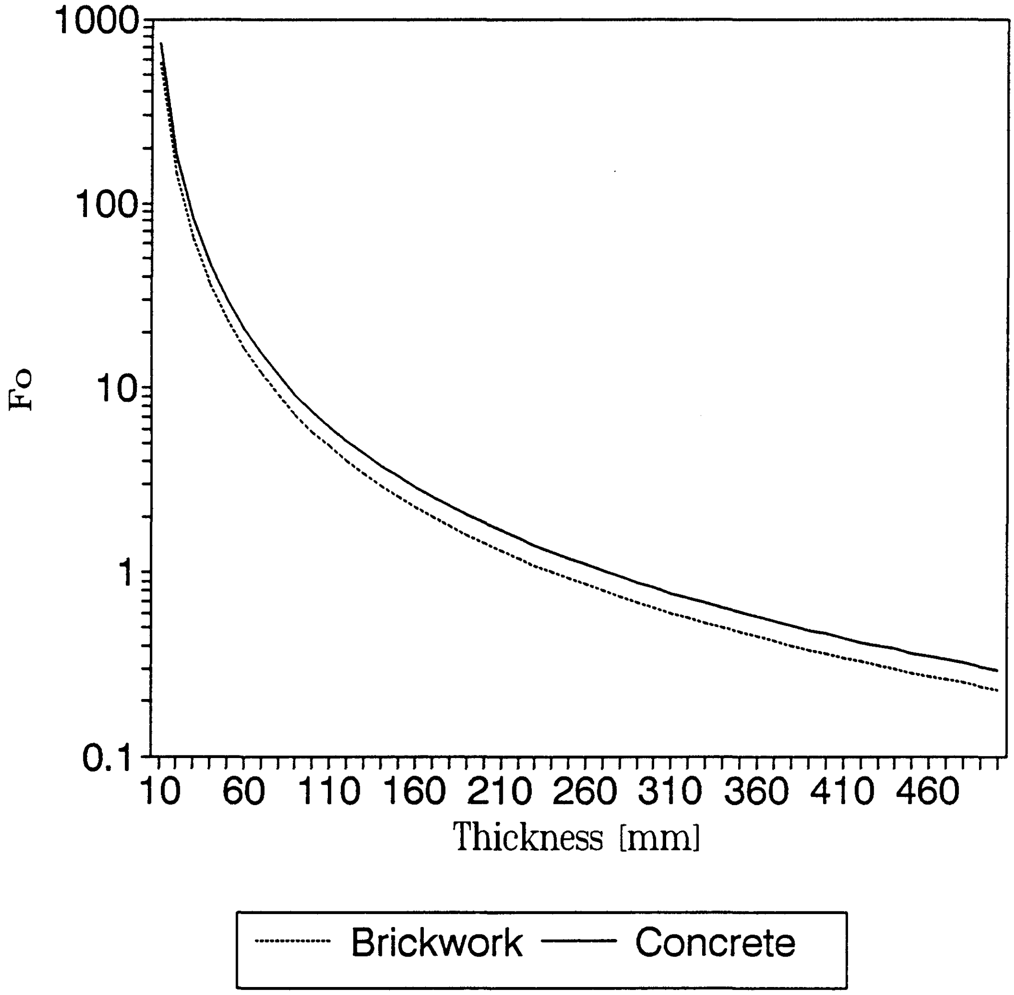

FIGURE 2.17 Fourier modulus of brick–work and concrete layers as a function of layer thickness.

It seems that for most *thin walled* building structures the approximation is reasonably accurate. The definitions of R and C (2.49) and (2.50) are intuitively satisfactory. They indicate that the total heat storage capacitance of the structure is represented by C and the total heat conductance by the two resistances in the branches of the T network. This must indeed be the case if the wall is thin and the temperature difference across the wall is small. Using a similar approach Davies [21] shows that a thick wall is well approximated by taking two, three or more of the T networks in cascade. Thick walls could thus be specified as consisting of two or more layers of the same material. In the exact solution, that is, in the cascade matrix with hyperbolic–trigonometric functions, it makes no difference if a layer is specified as a single layer of thickness ℓ or n sublayers of thickness ℓ/n. However, in the approximate RCR representation it does make a difference, and the accuracy of the RCR approximation increases with the number of sublayers. Of course the number of capacitors and hence the order of the circuit increases with each layer. Since we desire a single C representation, the high order network this procedure yields, consisting of an RCR T section for each layer, must be simplified to a single RCR T section, which represents the complete wall. It will be indicated later that this procedure, for reducing the high order network to a single capacitor network, has the effect that it makes no difference if the thick uniform layer is represented by one or more layers. This single C representation will necessarily represent the active capacitance for non–uniform walls and not the physical capacitance. The procedure for reducing the multiple T section network to a single T section is described next.

d) Laminated Structures

According to (2.37) the transmission matrix of a composite is given by the product of the transmission matrices of the laminae. If each laminate is approximated by a T section as in figure 2.18, *viz.* $\boldsymbol{T}_1$, $\boldsymbol{T}_2$, the resultant transmission matrix for a wall consisting of two layers is:

$$T_1 \cdot T_2 = \begin{bmatrix} \mathscr{A}_r & \mathscr{B}_r \\ \mathscr{C}_r & \mathscr{D}_r \end{bmatrix} \tag{2.56}$$

where:

$$\mathscr{A}_r = 1 + i\omega \cdot (R_1C_1 + [R_2 + 2R_1] \cdot C_2) - \omega^2 \cdot (R_1R_2 + R_1^2) \cdot C_1C_2 \tag{2.57}$$

$$\mathscr{B}_r = 2 \cdot (R_1 + R_2) + i\omega \cdot (2R_1R_2 \cdot [C_1 + C_2] + C_2R_2^2 + C_1R_1^2) - \omega^2 \cdot R_1R_2C_1C_2 \cdot (R_1 + R_2) \tag{2.58}$$

$$\mathscr{C}_r = i\omega \cdot (C_1 + C_2) - \omega^2 C_1C_2 \cdot (R_1 + R_2) \tag{2.59}$$

$$\mathscr{D}_r = 1 + i\omega \cdot (R_1C_1 + [R_2 + 2R_1] \cdot C_2) - \omega^2 \cdot (R_1R_2 + R_2^2) \cdot C_1C_2 \tag{2.60}$$

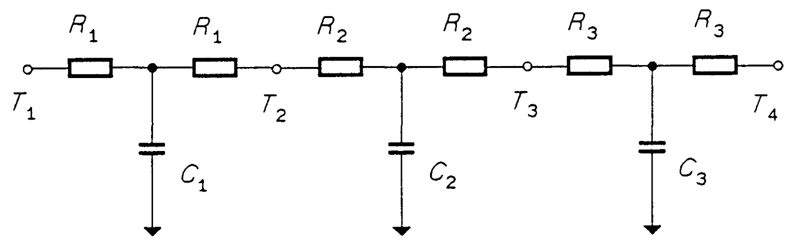

FIGURE 2.18 T sections in cascade.

We wish to approximate the composite structure with a single T network. Therefore, the matrix elements must be reduced to the form of (2.38). Clearly, this is not generally possible. The $\mathscr{C}$ element, for instance, is purely imaginary in (2.38) but contains a non–vanishing real part in (2.59). But, if we neglect all terms in ω^2 we see that the $\mathscr{A}$ and $\mathscr{D}$ elements do reduce to the required $1 + i \cdot \omega \cdot \tau$ form. The effective time constant of the composite is then given by:

$$\tau = R_1 \cdot C_1 + [2 \cdot R_1 + R_2] \cdot C_2. \tag{2.61}$$

Comparison of this equation with figure 2.18 shows a trend:– the time constant is given by the sum of the products of the capacitances with the total resistance to the left of the capacitor. For a rough approximation we may use for the composite structure the single T structure with branch resistances given by half the total resistance, so that the exact steady state response is obtained:

$$R_c = \sum_{i=1}^{n} R_i = \sum_{i=1}^{n} \frac{\ell_i}{2 \cdot k_i}. \tag{2.62}$$

The trunk capacitance is given by a generalized (2.61) divided by this definition of R_c so that the time–constant is preserved and given by $\tau = R_c \cdot C_c$:

$$C_c = \left[R_1 \cdot C_1 + \sum_{j=2}^{n} [R_j + 2 \cdot \sum_{i=1}^{j-1} R_i] \cdot C_j\right] / R_c. \tag{2.63}$$

We note from (2.61) that the T matrix for a uniform thick layer, as obtained from a cascade of two layers of half the thickness, would give $\tau = 4 \cdot R \cdot C$ identical to what would result from a single thick layer.

That the formula for the capacitance (2.63) provides an active capacitance and not the physical capacitance can be seen by taking two layers with the same thickness and capacitance, but with the resistance of the first layer very large i.i. $R_1 > R_2$. From (2.62) we obtain $R_c = (R_1 + R_2) \approx R_1$ for the resistance, and similarly for the capacitance $C_c = [R_1 \cdot C + (R_2 + 2R_1) \cdot C] / R_1 \approx 3 \cdot C$ from (2.63). The physical capacitance is only $2 \cdot C$ so that the active capacitance exceeds the physical capacitance. This somewhat baffling result is easily explained by noting that the definition of the active capacitance (2.63) attempts to preserve the effective time–constant τ in (2.61). The capacitance C_c is therefore fictitious and the result indicates that since R_1 isolates the mass from the external surface, the stored heat will have a larger influence on the interior surface temperature. The converse happens if $R_1 < R_2$. In this case we find $C_c \approx C$ which is only half the physical capacitance; indicating that it is only the capacitance of the second layer which is active since the first layer is isolated from the inner surface. These physical interpretations of the active capacitance should not be taken too seriously. The definitions in (2.61) and (2.62) are fairly arbitrary and designed to obtain a satisfactory approximation to the distributed two–port. The only reason why some sort of physical interpretation is possible at all, is because the resistance R_c were chosen to correspond with the steady state physical resistance.

It was indicated that two related conditions for accurate lumping are:

A Small Biot number for the wall, or

B Large Fourier modulus for each lamination.

The first condition will ensure that both the mean and the swing components of the temperatures and heat flows are accurately represented by the lumped model. The second condition applies only to the swing component. However, the heat capacitance plays no part in calculating the mean component and the definition of the resistances are such that the steady state response is obtained exactly. Therefore, the second condition which applies to non–steady swings is the more important. Fortunately, condition B is also more readily satisfied in buildings than condition A, as can be deduced from figures 2.11 and 2.16.

Equations (2.62) and (2.63) will be accurate when h_o is small and h_i is large. In these circumstances the matrix element $\mathscr{A}$ is the most important and the elements $\mathscr{A}$ and $\mathscr{D}$ are more accurately approximated by the above equations, than elements $\mathscr{C}$ and $\mathscr{B}$ [13]. In buildings, it is rather the converse which is true and the element $\mathscr{D}$ is the most important. To evaluate the accuracy of (2.62) and (2.63) we have computed the exact matrix description and the single RCR description for the walls of more than 20 existing buildings.

To evaluate the accuracy of the cascade matrices, where 4 complex components must be compared, which differ in significance according to

[13]The influence of the various elements of the cascade matrix can be inferred from the transfer function G defined by equation (2.64). E.g. if h_i is very large only $\mathscr{A}$ and $\mathscr{B}$ are important.

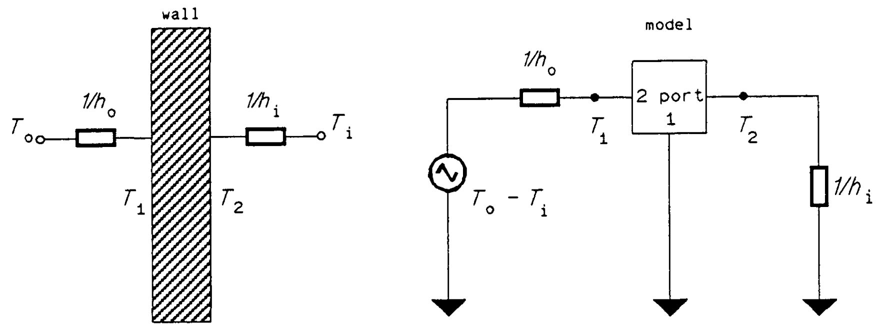

FIGURE 2.19 The transfer factor of a wall, G, is the ratio of the interior surface temperature to the external surface temperature.

the boundary conditions. Davies [21] "minimizes the sums of the squares of the differences between the corresponding elements in the real and model wall matrices". This criterion is not acceptable since it is unclear what its physical interpretation may be. It is better to calculate the effect of the matrices on the surface temperatures, rather than to compare the components themselves. This entails terminating the matrices in the correct boundary conditions and comparing the resultant temperatures on the boundaries. The calculation assumes the boundary conditions at the surfaces are: $h_o = 20$ W/m²·K and $h_i = 3.5$ W/m²·K. In this case, if the two port is driven via h_o and terminated in h_i as in figure 2.19, the ratios $T_i/T_f = G$ for the exact solution and the RCR approximation can be used to compare the accuracy of the lumping. This ratio, which we call the transfer factor, is a complex number which gives the attenuation and phase shift of the sinusoidal temperature wave through the wall. The circuit of figure 2.19 is approximately realized in buildings if T_f is identified with the external sol–air forcing function and T_i with the interior air temperature, provided the contribution of the particular wall to the total heat flow to the interior of the zone is not dominant; T_i must be largely independent of the particular wall under consideration. In this case, we find from figure 2.19:

$$G = \left[\mathscr{A} + h_o \cdot \mathscr{B} + \mathscr{C}/h_i + \mathscr{D} \cdot h_o/h_i\right]^{-1}. \qquad (2.64)$$

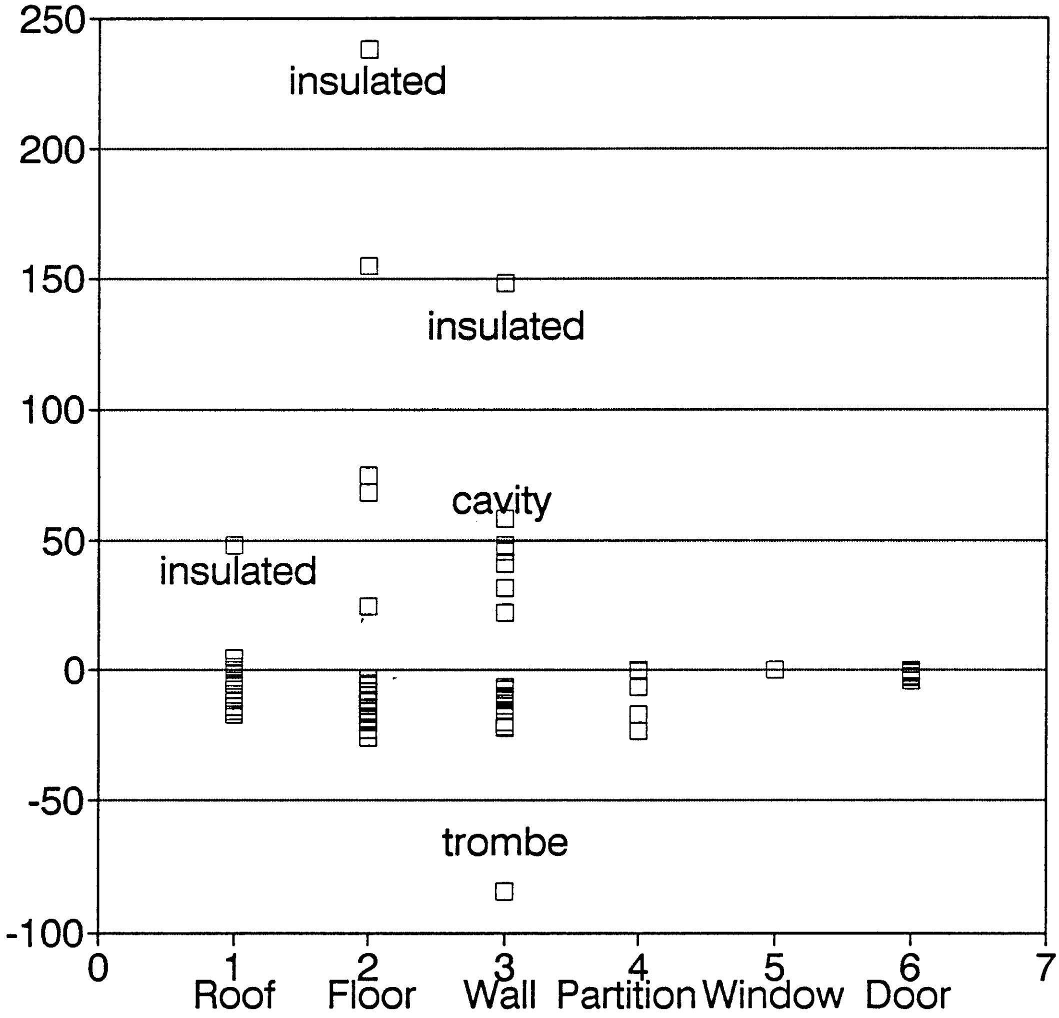

FIGURE 2.20 a Percentage error of the magnitude of the lumped transfer factor.

In figures 2.20 a and b we show the magnitude and phase errors of the lumped transfer factor for 106 existing walls. These results are also tabulated in appendix 2A. Results for the some walls are tabulated in table 2.4. The magnitude error is below 10% for all lightweight constructions and below 20% for a large number of massive constructions. Scrutiny of table 2.4 reveals that the magnitude error for brick and concrete walls are below 15% for thicknesses up to 330 mm. For cavity constructions the error is in the region of 22% and for very thick walls and insulated walls the error is in the order of 50%. The same tendency is visible for the phase error. For 110 mm solid brick walls the phase error is 0.3 h, increasing rapidly to 3 h for 220 mm thicknesses. Cavity and insulated walls have phase errors from 2 to 15 h. These results indicate that the attenuation of the thermal wave as obtained from the lumped model is fairly accurate for most solid and uninsulated walls. The phase error unfortunately grows rapidly if the thickness exceeds 110 mm. For cavity walls the magnitude error of 20% is already significant and the phase error of 3 h is not acceptable.

These results may be interpreted in the following way:

- Since the lumping is accurate for the thin elements such as windows, doors, 110 mm brick and concrete walls etc. the lumped representation will be adequate if these elements determine the heat flow to the interior of the zone.
- If however, the solid, thick elements contribute significantly to the heat flow, a phase error can be expected.
- If insulated and cavity walls also contribute to the heat flow, the magnitude as well as phase will be significantly in error.

If we assume that the thermo–flow in actual buildings is largely determined by the weakest part of the shell, i.e. by the windows and doors and not by the thick insulated elements, we come to the conclusion that the lumped representation is adequate with a magnitude error below 15 % and a phase error below 3 h. However, if the building is entirely constructed from thick, well insulated walls, with insulated windows and doors, large errors can be expected.

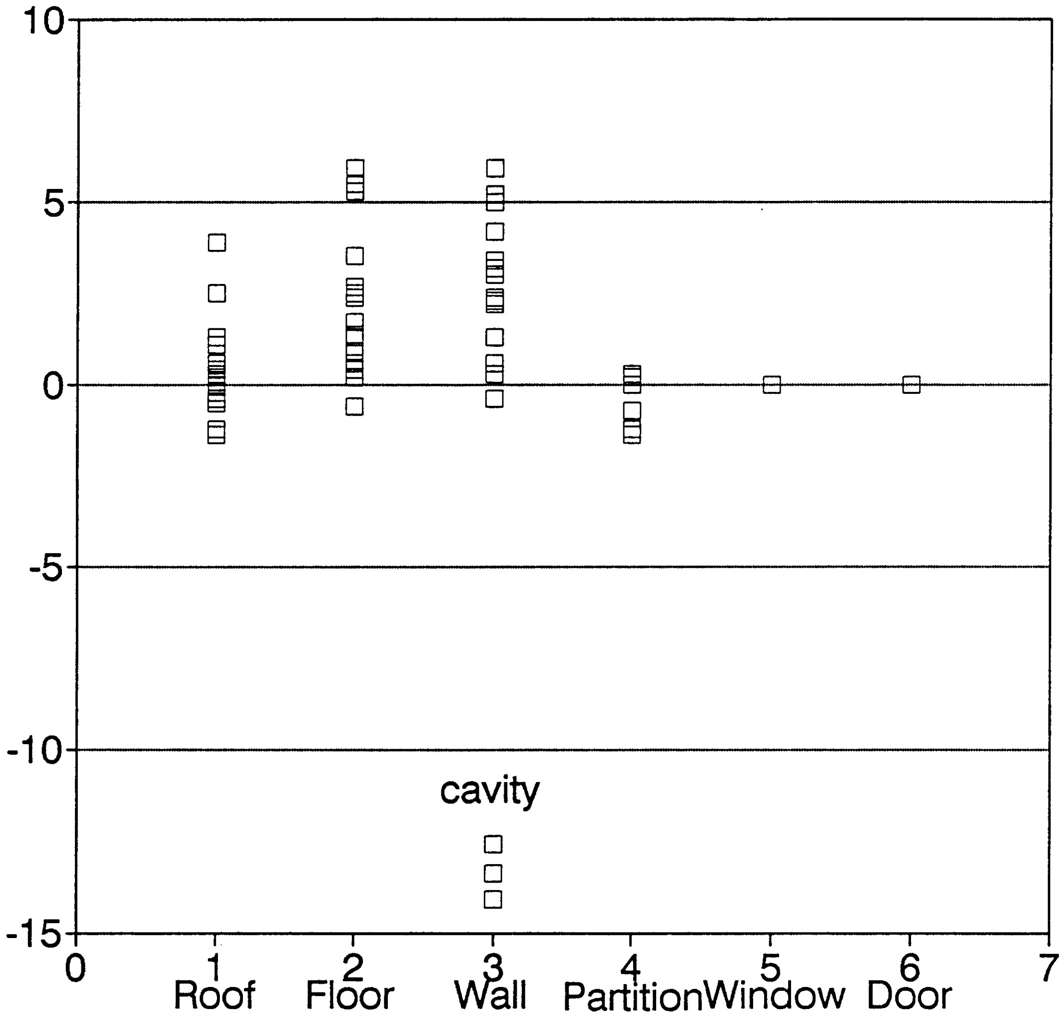

FIGURE 2.20 b Phase error, in hours, of the lumped transfer factor.

Wall Description	Gain (%)	Lag (h)	Gain Error (%)	Lag Error (h)
110 mm brick	7.4	-3.4	-10.5	0.3
220 mm brick	2.1	-8.1	-9.8	3.2
330 mm brick	1.2	-10.4	-14.9	5
150 mm concrete	6.5	-4.4	-11.9	0.6
200 mm concrete	4.6	-5.7	-15.8	1.3
cavity wall	0.3	7.7	45.7	-13.4
9 mm asbestos	12.5	-0.2	~0	~0

TABLE 2.4 Transfer factor accuracy for some typical walls.

In conclusion of this section we note that the value of the total time constant given by (2.61) agrees with the definition of the *Thermal Time–Constant* (*TTC*) of Bruckmayer in [5] if the external surface resistance is also included in the summation of (2.63).

e) Combining the Surfaces

Besides laminated walls, a zone will consist of typically six or more surfaces forming the shell of the enclosure. These walls will also consist of different sections such as brick–work, windows, doors etc.

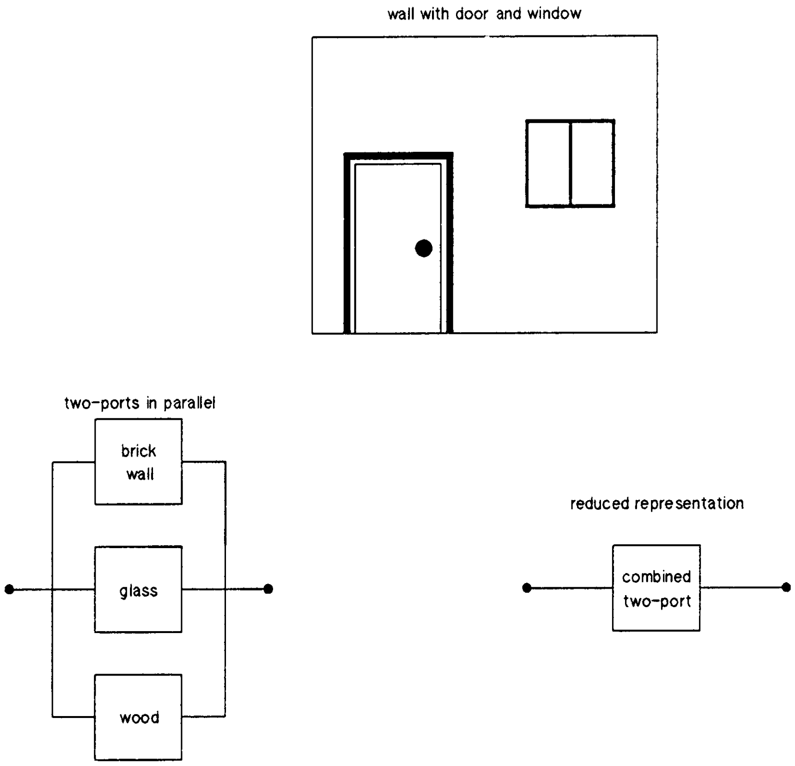

FIGURE 2.21 A typical shell consist of areas of different physical construction, e.g. brick, wood, glass.

E.g. in figure 2.21 the partition consists of several sections differing in area, construction and thermal properties. These sections are effectively connected in parallel if it is assumed that the temperatures on the surfaces are equal. In general, as discussed in §2.5.2, the temperatures on the external surfaces will differ; some surfaces will be in the shade and others will receive direct sun–light. The reduction of the various elements and walls to a single two–port was also discussed in §2.5.2 and it was pointed out, that, depending on the assumptions, various possibilities exist. (See figures 2.8 and 2.9.) The simplest procedure is obtained when the assumption of isothermal surfaces on both sides are used. If this is the case, we see that the above condition for parallel walls are assumed to exist, and that simple two port theory can be used to combine the walls. In this section we discuss only this simple method. A more accurate method is discussed in the next section, in connection with the technique for reducing the external forcing functions to one effective forcing function. In the most general case, the procedures outlined in §2.5.2 must be followed. The objective is still to derive a single RCR T section description, but this time for the total shell.

A rule for combining the various surfaces is given in [5], where Hoffman describes the *Total Thermal Time–Constant* (*TTTCB*) method and gives for the total time constant of an enclosure:

$$TTTCB = \frac{\Sigma_k \cdot A_k \cdot TTC_k}{\Sigma_k \cdot A_k} + \textit{Interior mass terms}$$

where the summation is carried out over all surfaces, k, with areas A_k, of the enclosure and TTC_k is Bruckmayer's thermal time constant for the wall (see discussion above). This method simply takes the area weighted averages of the time constants of the walls. We shall soon see that this method cannot be justified on theoretical grounds.

In previous paragraphs of this section we have derived a solution for the one dimensional heat flow problem in the form of a cascade matrix T, which gives the output temperature and heat flow for a specified input temperature and flow

$$\begin{bmatrix} T_o \\ q_o \end{bmatrix} = \begin{bmatrix} \mathscr{A} & \mathscr{B} \\ \mathscr{C} & \mathscr{D} \end{bmatrix} \cdot \begin{bmatrix} T_i \\ q_i \end{bmatrix}. \tag{2.65}$$

To combine circuits in parallel it is expedient to use a different set of equations for the heat flow through the wall, namely those giving the flows q in terms of the temperatures T.

$$\begin{bmatrix} q_i \\ q_o \end{bmatrix} = \begin{bmatrix} y_{11} & y_{12} \\ y_{21} & y_{22} \end{bmatrix} \cdot \begin{bmatrix} T_i \\ T_o \end{bmatrix} \tag{2.66}$$

The matrix $\boldsymbol{Y} = [y_{11}\ y_{12}\ /\ y_{21}\ y_{22}]$ is also a two port descriptor and is known as the admittance matrix. When elements are connected in parallel, as in figure 2.21, the temperatures at the ports are equal and the flows add. The admittance matrix of the parallel circuits is therefore the sum of the admittance matrices of the individual elements

$$\boldsymbol{Y}_p = \boldsymbol{Y}_1 + \boldsymbol{Y}_2. \tag{2.67}$$

The admittance matrix and transmission matrix representation is transformed from one to the other by the following rules:

$$y_{11} = \mathscr{D}/\mathscr{B}, \quad y_{12} = \mathscr{C} - \mathscr{D}\cdot\mathscr{A}/\mathscr{B}$$
$$y_{21} = 1/\mathscr{B}, \quad y_{22} = -\mathscr{A}/\mathscr{B} \tag{2.68}$$
$$\mathscr{A} = -y_{22}/y_{21}, \quad \mathscr{B} = 1/y_{21}$$
$$\mathscr{C} = y_{21} - y_{11}\cdot y_{22}/y_{21}, \quad \mathscr{D} = y_{11}/y_{21} \tag{2.69}$$

With these rules it is straight–forward to convert between the admittance and the cascade matrices. The procedure for finding the cascade representation of parallel elements is now:

- convert T matrices to Y matrices with (2.68).
- add the components of the Y matrices to find the total Y matrix.
- convert the Y matrix back to a T matrix with (2.69).

This procedure is very general and applicable to any type of T matrix; lumped or distributed elements.

In our application, we are interested in walls which typically consists of two or more areas or sections of different construction. To calculate the parameters of the T section of the combined wall directly from the physical parameters of the sections, we may use the approximations [11]:

$$R_t = \frac{1}{2}\left[\frac{A_1 \cdot k_1}{\ell_1} + \frac{A_2 \cdot k_2}{\ell_2} + \cdots\right]^{-1} \cdot A_t \qquad (2.70)$$

$$C_t = [A_1 \cdot \ell_1 \cdot \rho_1 \cdot \sigma_1 + A_2 \cdot \ell_2 \cdot \rho_2 \cdot \sigma_2 + \cdots]/A_t \qquad (2.71)$$

where A_t is the total area of the shell.

In (2.70) and (2.71) the numerical subscripts refer to the different sections and areas. If the sections are laminated structures the laminae must first be combined with the aid of (2.62) and (2.63).

These equations are rather rough approximations. They are derived on the assumption that the capacitances and conductances of the two areas can be thrown together. For more accurate calculation, it is essential to carry out the matrix procedure outlined before. The nature of this approximation can be demonstrated for the y_{11} parameter of the wall consisting of 2 sections in parallel. For the T section[14] the first of (2.68) gives:

$$y_{11} = \frac{1 + i \cdot \omega \cdot R \cdot C}{R \cdot (2 + i \cdot \omega \cdot R \cdot C)} \qquad (2.72)$$

For 2 similar partitions in parallel; respectively identified by subscripts 1 and 2:

$$y_{11} = \frac{1 + i \cdot \omega \cdot R_1 \cdot C_1}{R_1(2 + i \cdot \omega \cdot R_1 \cdot C_1)} + \frac{1 + i \cdot \omega \cdot R_2 \cdot C_2}{R_2(2 + i \cdot \omega \cdot R_2 \cdot C_2)} \qquad (2.73)$$

This equation must be compared with one obtained directly from the

[14]For full accuracy the distributed two port description of the sections must be used.

physical properties via (2.70) and (2.71):

$$y_{11}' = \frac{1 + i\cdot\omega\left[\frac{R_1 \cdot R_2}{R_1 + R_2}\cdot(C_1 + C_2)\right]}{\frac{R_1 \cdot R_2}{R_1 + R_2}\cdot\left[2 + i\cdot\omega\cdot\left[\frac{R_1 \cdot R_2}{R_1 + R_2}\right]\cdot(C_1 + C_2)\right]} \tag{2.74}$$

Equations (2.73) and (2.74) are obviously not compatible; (2.73) is an equation with terms in ω^2 (if placed over a common denominator) and in (2.74) ω appears only to the first power. It can be shown though, that these equations are similar in many respects if the swing frequency is small, so that the ω^2 terms vanish. Despite the incompatibility, (2.74) is may be used for convenience.

If (2.74) is compared with the procedure of Hoffman above, it is seen that the average time constant is only obtained if the resistance R_1 equals R_2 in (2.74). It follows that Hoffman's procedure is subject to this condition of equal wall resistances and is therefore a very rough approximation of (2.74), which is again only an approximation of (2.73).

Equations (2.74) and (2.73) can be more easily compared if further simplifications are assumed. If, for instance, we assume $R_1 = R_2 = R$ and $C_1 = C_2 = C$ i.e. similar sections, both (2.73) and (2.74) furnish the correct value:

$$y_{11} = \frac{2\cdot(1 + i\cdot\omega\cdot R\cdot C)}{R\cdot(1 + i\cdot\omega\cdot R\cdot C)} = y_{11}' \tag{2.75}$$

In the general case, where the areas and properties are dissimilar, both the magnitude and the phase of the approximate equation (2.74) is somewhat in error because of the ω^2 terms.

Similar equations can be derived for the other elements of the Y matrix. The same observation apply; terms in ω^2 are neglected. In practice, we expect that equations (2.70) and (2.71) will be sufficiently accurate for calculating diurnal swings, where $\omega = 2\pi/24$ h which is quite small.

The main cause of error, in this procedure for combining the elements, is then the assumption that the external and internal surfaces of all the sections are respectively isothermal. Since Mathews and Richards [10] employ (2.70) and (2.71) to combine the various elements of the shell, the assumption of isothermal mass is inherent in their model. Mathews and Richards in fact state that they assume isothermal interior surfaces, and further, obtain a mean sol–air temperature, which affect all external surfaces. Obviously, the simple model of figure 2.1 represents the temperature of the massive parts of the shell with a single node, and therefore requires one representative temperature for all the massive structures. The definition of this mean sol–air temperature is further discussed in the §2.5.4.

Numerical evaluation of the accuracy of equations (2.70) and (2.71) requires a complete implementation of the exact solution. The areas of the various sections are important and the only acceptable calculation should use the actual areas as they occur in practice. Since a full implementation of the exact matrix method is outside the scope of this thesis, we have to content with the admittedly somewhat vague, qualitative discussion above.

We conclude, that from the results obtained here, a simple one capacitor circuit representation of the two port, such as in figure 2.14, can be justified if the frequency of the temperature and load swing is small. This condition is satisfied by the diurnal variations of temperature in buildings.

f) <u>Lumping of Interior Mass</u>

In the network of figure 2.6 we have included a one port model of interior mass, by which we mean all massive objects which are in contact with the interior air, and which have significant heat capacitance, so that heat will be absorbed and released from the mass in sympathy with temperature changes of the internal air. This includes furnishings, partitions etc. and also the capacitance of the internal air itself, although the latter is often negligible compared to the others.

The one–port description of the interior massive elements is obtained from the solution of the conduction equation with all the boundary conditions set to the interior air temperature[15]. The internal objects are only of interest in the modelling of the interior temperature swing so that we may seek solutions for sinusoidally varying temperatures only. The one–port description of the object, $D_{\rm p}$, at a specified frequency, models the heat flow across the surfaces of the object $q_{\rm m}$ in terms of the temperature of the surfaces $T_{\rm m}$:

$$q_{\rm m} = D_{\rm p} \cdot T_{\rm m}. \tag{2.76}$$

$D_{\rm p}$ is also known as a driving point function in electrical terminology and must have the units of an admittance. It is a function of the specific characteristics of the object as well as the geometry. From (2.76) can be seen that the determination of $D_{\rm p}$ requires the full solution of the three dimensional heat conduction equation with sinusoidal temperature variations, which is often an arduous task. However, when the Biot number of the object is small it is again possible to use a simple lumped model consisting of a resistance $R_{\rm m} = 1/h \cdot A$ which models the surface resistance, and a single capacitor $C_{\rm m} = \rho \cdot c_{\rm p} \cdot V$ which models the heat storage. If the Biot number is small the interior conduction resistance of the object is not important.

A similar, simple solution is obtained for small structures, where the size of the object is small compared to the wavelength of the temperature wave in the structure. In this case we can again find a single R, single C description of the object when the Fourier modulus of

[15] We are assuming all surfaces of the object are in contact with the internal air, and radiation heat exchange between internal surfaces and the object can be ignored.

the object is large. The Fourier modulus is now defined with respect to one period of the variation of the surface temperature and a characteristic body dimension. The method is completely analogous to that described above for determining a lumped representation of the walls. It follows that lumping is possible under the same conditions as before, and that the lumped model for the internal object is a single capacitor, driven through a single resistor connected to the interior air temperature.

We shall therefore assume that it is possible to model the effect of interior mass with a single capacitor C_m, connected to the interior air node via resistance R_m, where, C_m includes only the active storage of the object for diurnal sinusoidal variations, and R_m includes the convective surface resistance. The cómpletely reduced model for thermo–flow in buildings is thus as given in figure 2.22. The model of figure 2.22 contains two capacitances, one for the massive elements forming part of the shell, and another for the internal masses. It is not permitted to combine these two capacitances in a single capacitance, unless it is assumed that the bulk temperature of the internal mass is always equal to that of the walls. This assumption can not be justified; the interior mass is driven by the interior air temperature, and the massive parts of the shell are driven by the difference between internal and external temperatures. In figure 2.22, combination of the two capacitors in a single capacitor is clearly tantamount to the assumption $R_2 + R_m > R_1$., However, this can not be true unless the shell contains a layer of insulation on the external surface. For most buildings we will have $R_1 \approx R_2 \approx R_m$ and the condition is violated. We have not attempted to calculate the error which will result from the breakdown of this assumption; for the same reasons given at the end of the previous section. The errors are probably not too severe since most zones contain only relatively light internal structures.

The circuit of figure 2.22, although very close to, still differs significantly from the model of Mathews and Richards of figure 2.1. These differences are discussed in §2.6 and §2.7.

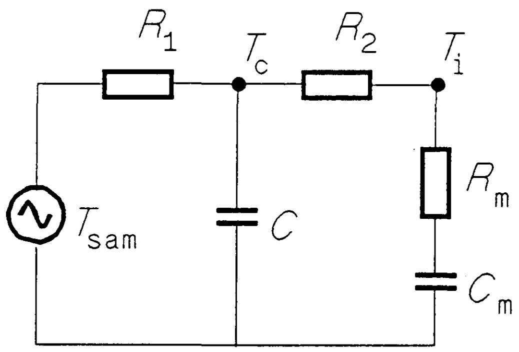

FIGURE 2.22 The completely reduced model. Lumped circuits model the massive elements. The interior heat exchange is modelled with a combined surface coefficient h_i, and the exterior forcing functions are combined in a single effective forcing function T_{sa}.

2.5.4 The Definition of the Mean Sol–Air Temperature

The mean sol–air temperature of Mathews and Richards is based on the assumption that the interior surfaces are isothermal, but takes into account only the conductances of the walls and the external surface coefficients [11]. The capacitance of the walls are ignored. The exact procedure, as discussed in §2.5.2, yields a two port description of the combined shell elements as well as a more complicated definition of the mean sol air temperature, in which all the elements of the circuit, including the capacitance and the interior surface coefficients play a part.

In fact, if the simple T section lumped model for the walls are retained, it is possible to obtain a simple exact definition of the mean sol–air temperature in the way indicated in §2.5.2. In figure 2.23 we have combined the surface coefficients of figure 2.9b in the T section description of the wall. If the Thevenin equivalent representation of all the wall elements and forcing functions are found, the exceedingly simple circuit of figure 2.24 results. This figure is very similar to the model of Mathews and Richards.

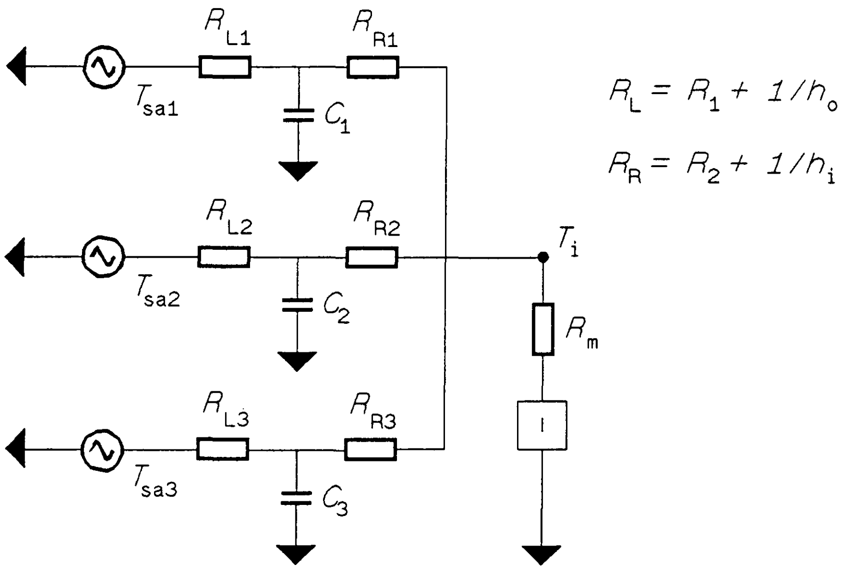

FIGURE 2.23 The lumped representation with surface coefficients absorbed in the branch resistances of the T section.

The mean sol–air temperature, Tsa_m, in figure 2.24 is given exactly by:

$$Tsa_m = \sum_i Tsa_i \;/\; (1 + i \cdot \omega \cdot \tau_i). \tag{2.77}$$

Where Tsa_i is the forcing function for section i and τ_i the time constant for surface element *i* given by:

$$\tau_i = (Rt_i + A_i/ho_i) \cdot Ct_i \tag{2.78}$$

with Rt_i and Ct_i the parameters of the T section, and ho_i is the surface coefficient for the external area, A_i, of element *i*.

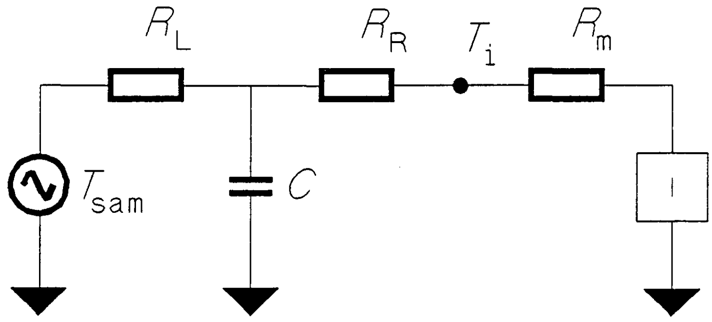

FIGURE 2.24 The Thevenin equivalent circuit of the forcing functions of figure 2.23 represents the mean sol–air temperature.

In figure 2.25 the magnitude and delay of the sol–air contribution is shown as a function of the total time constant of the wall. For single layer brick walls of thickness 110 mm (τ = *6* h) the attenuation is 0.54 and the delay is 3.8 h. For a double layer brick wall of thickness 220 mm (τ = *24* h) the corresponding values are 0.16 and 5.4 h. It is clear that these delays are of the same order as the delay correction which Mathews and Richards have to apply as an *ad hoc* correction [10]. The attenuation and delay of the contribution to the mean sol–air is related to the transfer factor discussed before. It is different though, since in the definition of the mean sol–air, the two–port of the wall is terminated in $h_i = 0$ (see figure 2.19), i.e. it is assumed no heat flows across the inner surface. The mean sol–air is just a convenient mathematical artifact for calculating the solution. It allows the sol–air forcing temperatures to be combined in a single forcing function so that the combined response can be calculated at once. In principle, it is completely equivalent to obtaining the responses to the various sol–air temperatures one by one, and then afterwards combine them to find the total response.

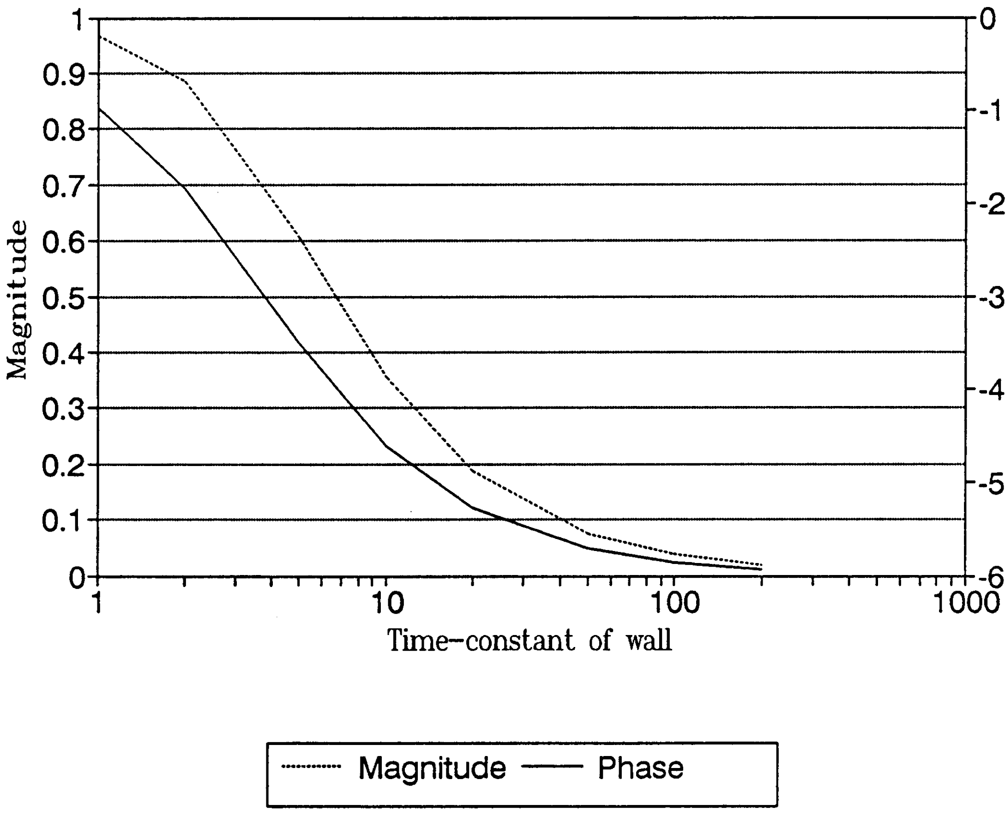

FIGURE 2.25 Attenuation and delay of the sol–air contributions of walls as a function of the thermal time constant of the wall, with resistance from sol–air node to interior air node.

The values of R_1, R_2 and C in figure 2.21 are not so easily obtainable. Each element in figure 2.22 will contribute a capacitor so that the exact representation is a high order network. Methods for obtaining approximate values for the circuit parameters were discussed in §2.5.3. It was shown that reasonable approximations are possible when the frequency of variation is small. Alternatively, if it is assumed that the massive elements are at approximately equal temperatures, C represents the total capacitance of the structure and $R_1 + R_2$ the total thermal resistance of the shell.

The definition of the mean sol air temperature as given in (2.77) is exact for the T section description of the walls. Mathews and Richards [11] ignores the capacitance of the walls when computing the mean sol–air temperature. Equation (2.77) indicates that the individual forcing functions of each external suffers a phase shift according to the time constant of the wall. This effect in all probability explains the empirical phase shift Mathews and Richards [10] requires. Their empirical correction, which is based on the total time constant of the zone, is thus justified if all the walls are of similar construction but will fail when the time constants of the walls differ manifestly.

2.5.5 Interior Heat Transfer

Since the assumption of Mathews and Richards – and others notably [24] – that the interior surfaces are at the same temperature, is not substantiated by measurements [8], it deserves some further attention. According to [8] the surfaces of windows are approximately 10 K below the average wall surface temperature in winter. Nevertheless, Mathews and Richards [10] have found that adequate temperature predictions are possible with this assumption. Similarly Mitalas [30] concludes: "... for (the) emissivities $\epsilon = 0.9$ and $\epsilon = 0.0$ (results) indicate that the heat interchange by radiation between the inside room envelope surfaces is not a major factor affecting the cooling load." We have in previous paragraphs indicated that it is possible to obtain a simple structure without the assumption of isothermal surfaces, by way of network synthesis, although it is not clear at all that in this case the simple one capacitor network will be adequate. However, it was indicated that the assumption of isothermal interior surfaces directly leads to a simple thermo–flow network.

To investigate quantitatively the magnitude of the temperature differences between internal surfaces, the difference in the internal temperatures of two opposing walls can be evaluated. A computer program was written which calculates the temperature difference between the internal surfaces of two walls, when the external surfaces are subjected to a temperature difference[16]. The calculation is done both for a steady (mean) temperature difference and for a sinusoidal temperature swing with period 24 h. The program is based on the thermo–flow network of figure 2.6. The mean temperature difference between the walls are easily found since the heat storage in the massive elements plays no part. If the temperature difference across the external surfaces of the walls is T_0 one finds that the steady temperature difference, ΔT, between the interior surfaces are given by (assuming the convective coefficient, h_c, is the same for both surfaces):

$$\Delta T/T_0 = \frac{1}{\frac{(Bi_1+Bi_2)}{2}\cdot\left(\frac{2\cdot h_r}{h_c}+1\right)+1} \qquad (2.79)$$

where Bi_i is the Biot number of wall i with respect to the internal convection coefficient h_c.

It is seen that the temperature difference is determined solely by the mean Biot number of the walls in relation to the convective and radiative coefficients. In figure 2.26 the fractional mean temperature

[16]It is available on the floppy disk in the back–cover.

difference, $\Delta T/T_0$, is shown as a function of the mean Biot number, with h_r/h_c as a parameter. In table 2.5 the fractional mean temperature difference is given for the walls of a typical office, details are given in appendix 2c. Similar results for 20 other buildings are available on the floppy disk in the back-cover in the file named 'results.txt'.

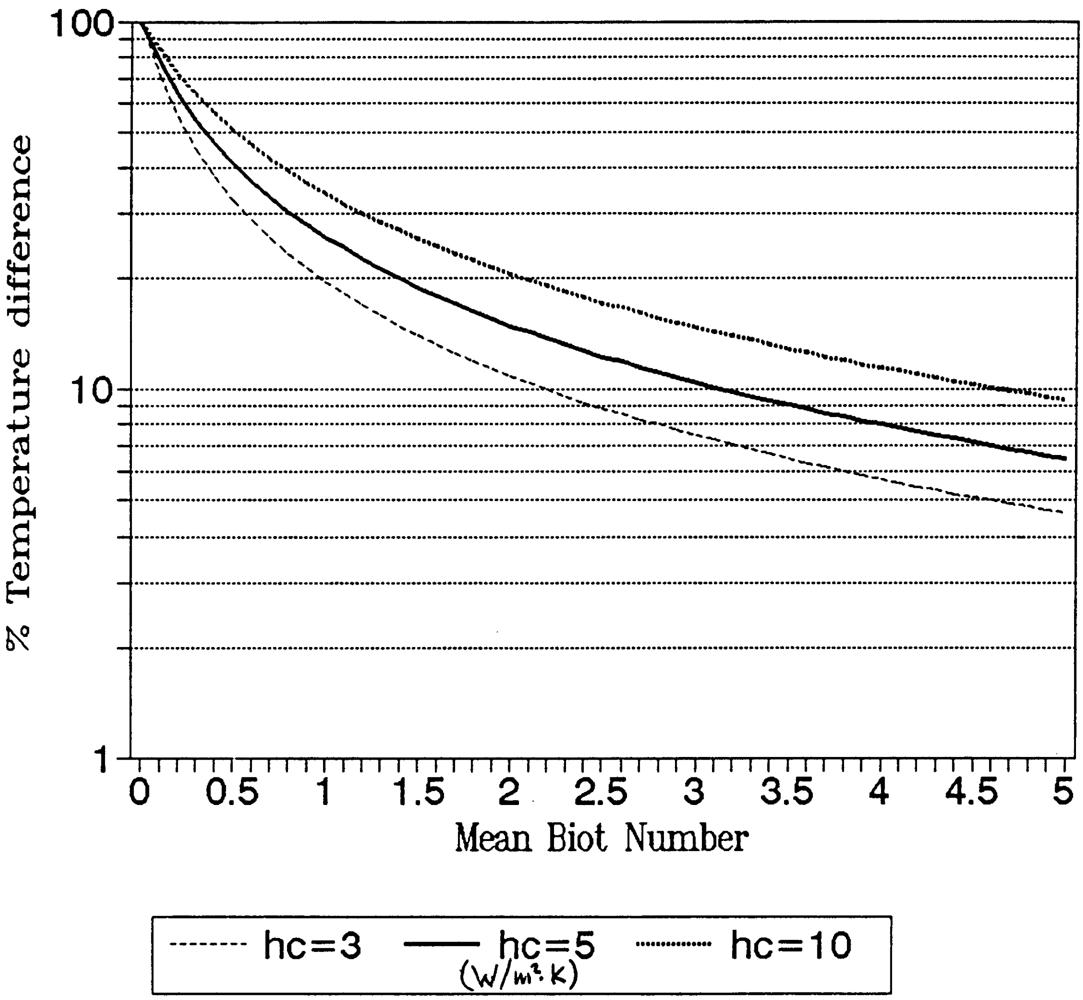

FIGURE 2.26 Fractional mean interior surface temperature difference, as a function of the mean of the Biot numbers of the walls.

	Roof	Floor	Brick (C)	Window	Brick	Door
Roof	26.064					
Floor	25.551	25.057				
Brick (cavity)	22.465	22.083	19.74			
Window	36.346	35.355	29.709	60.023		
Brick (114 mm)	27.901	27.314	23.817	40.021	30.018	
Door	25.252	24.77	21.86	34.786	26.973	24.489

TABLE 2.5 Mean temperature difference between interior wall surfaces as a percentage of the external temperature difference. These results were calculated from data describing an actually existing office. For more details see appendix 2C. The rows and columns indicate the temperature differences for opposing walls taken in pairs.

Figure 2.11 shows Biot numbers for more than 100 elements of existing buildings. These elements have been sorted into 6 groups namely, roof, floor, wall (massive), partition (light), window and door. The Biot numbers were computed from the total resistance of the various laminae which form the elements. It is evident from the figure that the Biot numbers for buildings surfaces fall mostly in the range 0 to 2. Consequently, from figure 2.23 it follows that we must expect quite high mean temperature differences between the surfaces. The results in table 2.5 show that the mean temperature difference between the internal surfaces of two opposing windows may be above 60% of the temperature difference between external surfaces. Examination of the complete set of results indicate that, if one surface is a window and the other a brick wall, the mean interior temperature difference is typically about 20 to

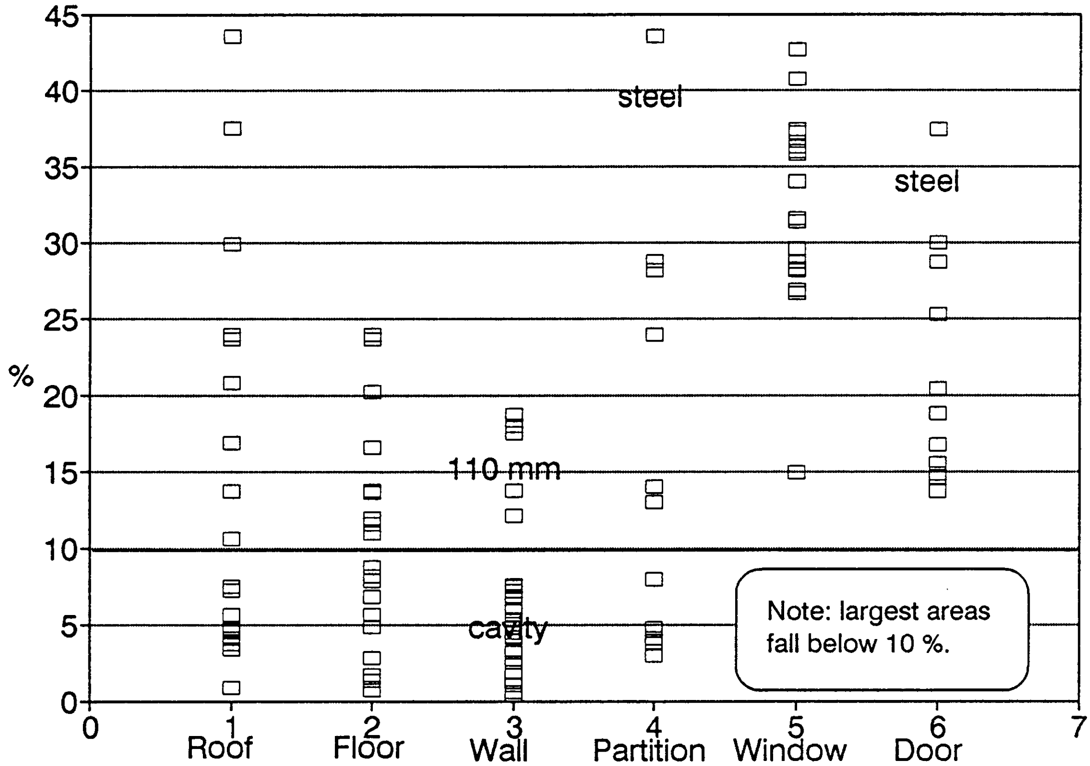

FIGURE 2.27 Averaged temperature swing differences between interior surfaces as a percentage of external temperature swing.

30 % of the external difference. These results indicate that steady state heat transfer between interior surfaces can not be negligible.

To determine the temperature difference between the walls when the external temperature difference is sinusoidal, the heat storage capacity of the walls must be taken into account. We use the two port representation (see §2.5.3) and two port theory to obtain the solution. The detailed results for a typical office are given in appendix 2c. Figure 2.27 shows the average temperature swing difference between interior surfaces when one surface (the one on the side of the forcing temperature) is of the indicated type. The 'average' indicating that the results for opposing surfaces of all other types existing in the building, have been averaged. The results indicate that also for the swing component, a large fraction of the exterior temperature difference appears across the interior surfaces for roofs, windows and doors. For walls the difference is below 20% with most walls actually in the range 0 to 10%.

In figure 2.28 the averaged swing temperature difference is also shown against the time–constant of the wall. There is a definite dependency for the swing temperature difference to decrease for massive, insulated walls.

These results were obtained by calculating the temperature difference which would exist on the interior surfaces of two infinitely large walls of the given construction, when a temperature difference exists between the exterior surfaces. Both convection and radiative heat transfer were taken into account. In actual buildings, surfaces are also at right angles to each other, in which case the convective heat transfer will probably be the same but radiative transfer will be reduced.

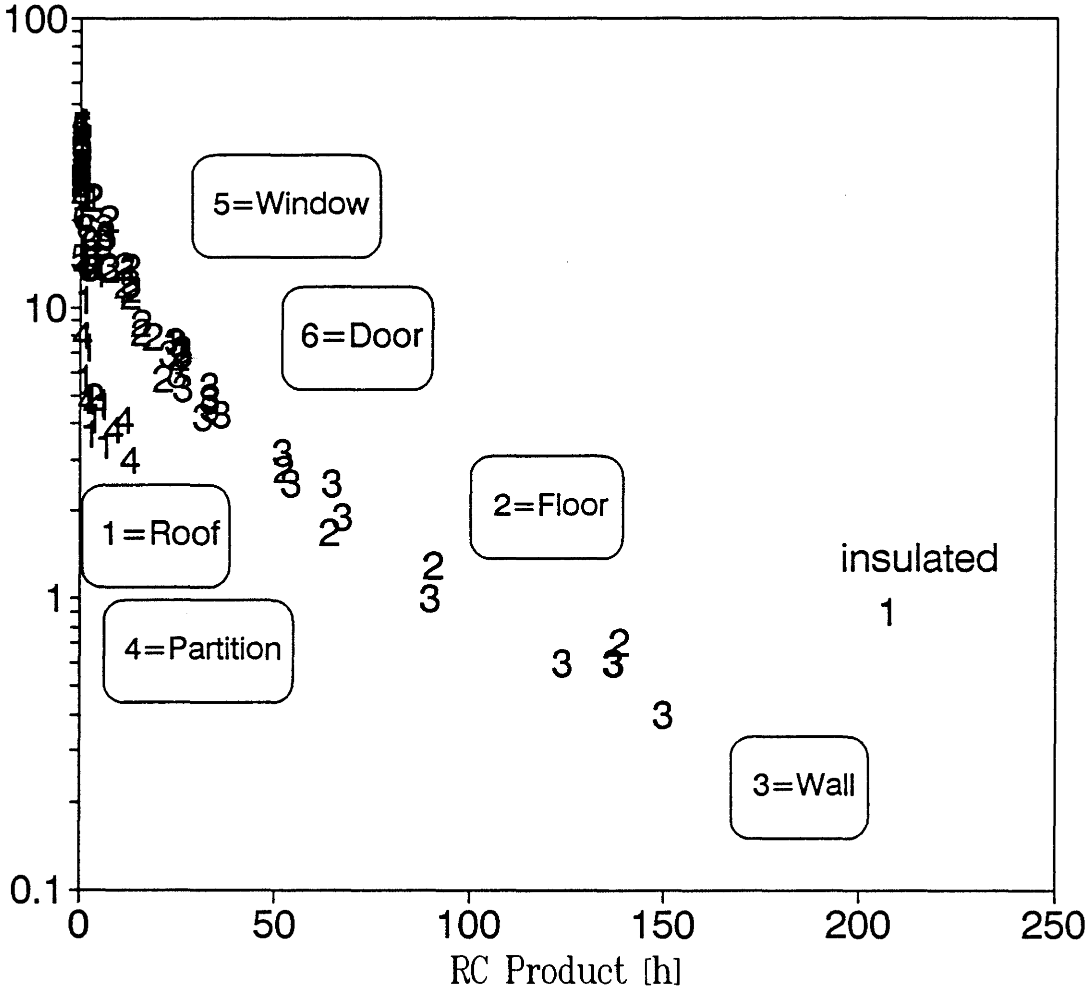

FIGURE 2.28 Averaged temperature swing differences against thermal time constant of the wall.

We can summarize these results by noting that:

- The temperature difference between interior surfaces are above 20% of the exterior temperature difference if one of the surfaces is a door or a window.
- The temperature differences are larger for the steady state component than for the diurnal swing component.
- Massive insulated walls exhibit very small temperature differences across their interior surfaces.

In deriving these results, we have not taken into account the areas and relative prevalence of the various surfaces since these differ much from one design to another.

The correct interpretation of these results is that they indicate that it cannot be assumed *a priori* that heat transfer between interior surfaces are negligible. This basic assumption of Mathews and Richards is therefore not tenable and, theoretically, better accuracy could be obtained with a network which treats the interior surfaces individually. However, with the difficulties experienced in practice in specifying many thermo–flow details, this theoretical improvement will be very difficult to realize. Essentially all the advantages of the simple thermo–flow network will be sacrificed, for marginal improvement, if the assumption is dropped.

It is important to realize that, in actual buildings, temperature differences between interior surfaces are not only due to the temperature differences between the external surfaces but is also the result of solar energy penetrating through the windows and selectively heating some surfaces. This latter factor, although very important, is difficult to calculate in practice because of the hourly variation of the sun angle during the day, the presence of blinds and curtains, shading devices, trees etc. Mitalas [32] investigated the effect of penetrating radiation on the cooling load. He modelled a floor slab, as a single slab at uniform temperature and as two slabs, one adjacent to the window, which received all the solar energy, and another part which received no solar energy. The difference on the calculated cooling load with these two models was very small, less than half of one percent. From this result is appears that energy is quickly distributed to other surfaces from a surface of higher temperature. This would be the case if the inter–surface heat exchange coefficients are much larger than the conductances to the external surfaces. The Biot numbers of figure 2.11, defined as the ratio between the combined coefficient h_i and the conductance of the wall, indicates that this assumption is in general not true since the Biot numbers are of the order of 1 for many building elements.

We are forced to conclude that the internal heat transfer between wall surfaces can not be neglected. It would thus be more appropriate to attempt to derive the simplified network from the second alternative discussed in §2.5.2, i.e assumption iii), which do not require the assumption of equal interior surface temperatures. This task was not attempted since it can not lead to a simplified network with a well defined physical interpretation of the parameters.

2.6 A Refined Simple Model

In the previous sections of this chapter we have simplified the comprehensive thermo–flow network of figure 2.2 to the simple network of figure 2.22. This network can not be further simplified to the network of Mathews and Richards in figure 2.1 without a rather arbitrary assumption that the two resistors in figure 2.1, which represent the shell resistance, can be combined in the single resistor R_0 of figure 2.1. This would have no influence on the calculation of the steady state response but it will definitely affect the swing component of the response. It is also not possible to combine the interior massive structures in a single capacitor with the massive parts of the shell since these masses are subjected to different boundary conditions..

Although the circuit of figure 2.22 is a second order network (two capacitors) and thus more complicated than the first order network of Mathews and Richards it displays some significant advantages.

- The representation of the distributed elements with an RCR T section instead of an RC section is more satisfactory since the capacitance is not directly available through the interior surface coefficient. The capacitance but will be isolated from the surface if an insulating material covers the interior surface. In the model of Mathews and Richards the active capacitance would be reduced if the interior surface is insulated but it is still directly available to the interior air.
- The more balanced representation of the shell and the separate model of internal masses leads to a clearer physical interpretation of the model.
- The circuit contains a node, T_2, which clearly represent the interior surface of the shell. The temperature of the interior surface is required for a better definition of comfort temperature which must take into account radiation from the walls.
- The modelling of internal mass in a separate capacitor, C_m, will increase the accuracy of the prediction if significant interior mass is present.
- It is also a more satisfactory model to extend to multi–zones because the mass of interior partitions are treated separately. It is shown in chapter 4 that a very natural extension to multi–zone thermal response is possible.
- It is easier to extend the model of figure 2.22 because it is a better approximation of reality.

The only drawback is that it is more complicated with 9 elements (including the ventilation resistance) instead of only 4 as in figure 2.1. Because it is a second order network, it is governed by a second order differential equation and it's solution will be only half as efficient. Nevertheless, we are convinced that the benefits of the model of figure 2.22 outweigh it's disadvantages and that it would be prudent to investigate this network further.

2.7 Conclusion, Chapter 2

We set out in this chapter to determine the theoretical foundation of the thermo–flow model of Mathews and Richards as in figure 2.1. We have been able to derive the model of figure 2.22 – which is very similar to the network of figure 2.1 – from a more comprehensive model with the following assumptions:

I The building can be regarded as a single zone for purposes of thermal–analysis. This is justified if the building is air conditioned, the zones are similar and subject to similar conditions, or the zones are isolated from each other.

II The walls are thin so that the heat flow is effectively one–dimensional. This is a very good approximation for most building structures, except for floors with ground contact.

III The massive parts of the structure are thin enough so that the single RCR T section, lumped model can be used instead of the thermal wave solutions of the conduction equation. An alternative statement of this condition is that the frequency of the variation of the forcing functions must be small. This assumption is justified for diurnal variations, and walls not thicker than 220 mm.

IV The interior surfaces can be regarded as approximately isothermal so that the network of interior heat transfer between the surfaces can be simplified. We have shown that this assumption is not tenable but it is required in order to arrive at a simplified model with a clear physical interpretation.

V The bulk temperatures of the massive structures, which form part of the shell, are sufficiently similar that a simplified combination rule can be used. In effect this assumption implies the external surfaces must be isothermal. It is not tenable on empirical grounds.

The practical effect of the breakdown of the last two assumptions is that they set a theoretical limit to the accuracy of the simplified model. This theoretical limit is probably within the practical limit set by unknown details of the physical construction, the weather, internal loads etc.[17] If we compare the model of figure 2.22 with the model of Mathews and Richards in figure 2.1, we see that they differ in the following aspects:

A Mathews and Richards use a single capacitor to describe heat storage in both the internal masses as well as walls forming part of the shell. This representation is only possible if it is assumed the bulk temperature of all the massive parts – the shell as well as internal masses – of the building are equal. According to [11] only a part of the internal mass is active in storing heat and is included in the capacitance of figure 2.1. This procedure ignores the fact that the internal mass is forced by the interior air and not by the external surface temperatures. It can be shown that this simplification will cause a magnitude and a phase error in the solution of the temperature swing.

B In figure 2.22 the conductance of the shell is split in two parts on either side of the capacitance. This ensures that the surface temperatures of the walls are well defined and also the bulk structure temperature. In the model of figure 2.1 it is difficult to ascribe a specific temperature to the interior wall surfaces.

C The definition of the mean sol–air forcing function as given in §2.5.3 includes the delaying effect of the massive walls.

We may conclude this section by noting that the method of Mathews and Richards is, to a large extent, theoretically justified. The accuracy of this method is not determined, in the first place, by the lumping of the distributed elements, but rather, by the assumptions which are made

[17]This is a personal opinion of the author.

to obtain simple definitions of the parameters of the network in terms of the physical properties of the materials, or, which are required for simple combination rules of the various elements. We have further obtained a better founded simplified network for the description of thermo–flow in buildings, which appears to be a refinement of the model of Mathews and Richards, and which may well be worthy of further investigations, implementation and verification.

REFERENCES Chapter 2

[1] **ASHRAE HANDBOOK, FUNDAMENTALS**, *American Society of Heating, Refrigerating and Air–Conditioning Engineers, Inc,* 1989.

[2] **CIBS, A5**, Thermal Response of Buildings, *Chartered Institution of Building Services*, 1979.

[3] **R. W. R. Muncey**, Heat Transfer Calculations in Buildings, *Applied Science Publishers*, 1979.

[4] **P. J. Walsh, A. E. Delsante**, Calculation of the Thermal Behaviour of Multi–Zone Buildings, *Energy and Buildings*, 5(1983) 231 – 242.

[5] **B. Givoni**, Man, Climate and Architecture, 2nd edition, *Applied Science Publishers*, 1976.

[6] **J. D. Wentzel, R. J. Page–Shipp, J. A. Venter**, The Prediction of the Thermal Performance of Buildings by the CR–Method, *NBRI Research Report BRR 396*, CSIR, Pretoria, 1981.

[7] **D. Tuddenham**, *Computers in Air–Conditioning Load Estimation, Air–Conditioning System Design for Buildings*, Editor A.F.C. Sherrat, McGraw–Hill, pp. 96 –111.

[8] **A. K. Athienitis**, Application of Network Methods to Thermal Analysis of Passive Solar Buildings in the Frequency Domain, *PhD Thesis, Department of Mechanical Engineering, Waterloo*, Ontario, 1985.

[9] **A. K. Athienitis, H.F. Sullivan, K.G.T. Hollands**, Discrete Fourier Series Models for Building Auxiliary Energy Loads Based on Network Formulation Techniques, *Solar Energy*, Vol. 39, No. 3, pp. 203 – 210, 1987.

[10] **E. H. Mathews, P. G. Richards**, A Tool for Predicting Hourly Air Temperatures and Sensible Energy Loads in Buildings ate Sketch Design Stage, *Energy and Buildings*, 14(1989) 61 – 80.

[11] **E. H. Mathews, P. G, Rousseau, P. G. Richards, C. Lombard**, A Procedure to Estimate the Effective Heat Storage Capability of a Building, *Energy and Buildings*, accepted for publication, 1990.

[12] **QUICK**, User's and reference Manual, Release 3.0 of 1990, *Centre for Experimental and Numerical Thermoflow*, Department of Mechanical Engineering, University of Pretoria.

[13] **N. O. Milbank, J. Harrington Lynn**, Thermal response and the admittance procedure, *B·S·E, May 1974*, VOLUME 42.

[14] **G. P. Mitalas, D. G. Stephenson**, Room Thermal Response Factors, *ASHRAE Semiannual Meeting, Detroit, Mich., January 30 – February 2, 1967*, No. 2019, III.2.1 – III.2.10.

[15] **K.–I. Kimura**, Scientific Basis of Air Conditioning, *Applied SCience Publishers*, 1977.

[16] **R. K. Otnes, L. Enochsen**, Applied Time Series Analysis, Volume 1, Basic Techniques, *John Wiley and Sons.*

[17] **D. G. Stephenson, G. P. Mitalas**, Cooling Load Calculations by Thermal Response Factors, *ASHRAE Semiannual meeting, Detroit, Mich., January 30 – February 2, 1967*, No. 2018, III.1.1 – III.1.7.

[18] **L. A. Pipes, L. R. Harvill**, Applied Mathematics for Engineers and Physicists, Third Edition, *McGraw–Hill Book Company*, 1970.

[19] **L. O. Chua, P.–M. Lin**, Computer Computer–Aided Analysis of Electronic Circuits, *Prentice–Hall, INC.*

[20] **L. A. Pipes**, Matrix analysis of heat transfer problems, *J. Franklin Institute*, Marc., 1957.

[21] **M. G. Davies**, Optimum Design of Resistance and Capacitance Elements in Modelling a Sinusoidally Excited Building Wall, *Building and Environment*, Vol. 18, No. 1 2, pp. 19 – 37, 1983.

[22] **B. C. Raychaudhuri**, Transient Thermal Response of Enclosures: the Integrates Thermal Time–Constant, *Int. J. Heat Mass Transfer*, Vol. 8, pp. 1439 – 1449.

[23] **M. H. De Wit, H. H. Driessen**, ELAN–A Computer Model for Building Energy Design, *Building and Environment*, Vol. 23, No.4, pp. 285 – 289, 1988.

[24] **G. N. Walton**, Thermal Analysis Research Program Reference Manual, *National Bureau of Standards, U.S. Department of Commerce*, March 1983, NBSIR 83–2655.

[25] **L. Laret**, Use of General Models with a Small Number of Parameters, *CLIMA 2000: 7th Int. Cong. of Heating and Air Conditioning*, Budapest, 1980.

[26] **J. A. Crabb, N. Murdoch, J. M. Penman**, A simplified thermal response model, *Building Serv. Eng. Res. Technol.* 8 (1987) 13–19.

[27] **M. E. Hoffman**, [5] *Chapter 19,* §*19.8*, pp. 434 – 450.

[28] **ASHRAE**, Procedures for Determining Heating and Cooling Loads for Computerizing Energy Calculations, *American Society of Heating, Refrigerating and Air–Conditioning Engineers, Inc*, 1975.

[29] **J. P. Holman**, Heat Transfer, SI Metric Edition, *McGraw–Hill Book Company*, 1989.

[30] **A. E. Delsante**, Steady–State Heat Losses from the Core and Perimeter Regions of a Slab–on–Ground Floor, *Building and Environment*, Vol. 24, No. 3, pp. 253 – 257, 1989.

[31] **J. F. van Straaten**, Thermal Performance of Buildings, *Elsevier Publishing Company*, 1967.

[32] **G. P. Mitalas**, An Assessment of Common Assumptions in Estimating Cooling Loads and Space Temperatures, *ASHRAE 72nd Annual Meeting, July 5–7*, 1965, Portland, Ore., No. 1949, pp. 72 – 80.

[33] **C. O. Mackey and L. T. Wright**, The sol–air thermometer–a new instrument, *Heat. Pip. Air Condit.*, May 1940.

[34] **E. A. Guillemin**, The Mathematics of Circuit Analysis, *John Wiley & Sons, Inc.*, 1959.

[35] **J. M. Penman**, Second Order System Identification in the Thermal Response of a Working School, *Building and Environment*, Vol. 25, No. 2, pp. 105–110, 1990.

[36] **M. G. Davies**, Transmission and Storage Characteristics of Walls Experiencing Sinusoidal Excitation, *Applied Energy* 12(1982) 269–316.

SYMBOLS Chapter 2

A	Area [m²].
$\mathscr{A}$	Upper left element of transmission matrix.
ach	Air changes per hour [/h].
$\mathscr{B}$	Upper right element of transmission matrix.
Bi	Biot number.
C	Heat storage capacitance per unit shell area [kJ/m²·K].
C_c	Capacitance of composite structure [kJ/m²·K].
C_t	Trunk capacitance of T section [kJ/K].
$\mathscr{C}$	Lower left element of transmission matrix.
c_p	Specific heat capacity at constant pressure [kJ/kg·K].
D_p	Driving–point function, 1 port description of interior mass [kW/K].
$\mathscr{D}$	Lower right element of transmission matrix.
Fo	Fourier modulus.
F_{12}	Radiation shape factor between surfaces 1 and 2.
G	Complex ratio between interior– and exterior surface temperatures.
h_c	Wall surface convection coefficient [W/m²·K].
h_{ce}	Exterior wall surface convection coefficient [W/m²·K].
h_i	Wall interior surface effective film coefficient [W/m²·K], convection combined with radiation. Different version are identified with superscripts.
h_m	Fictitious coefficient arising from simplification of interior heat transfer [W/m²·K].
h_o	External wall surface effective film coefficient [W/m²·K].
h_r	Surface radiation coefficient [W/m²·K]
I_s	Irradiance [W/m²].
i	Imaginary number.
k	Thermal conductivity [W/m·K].
ℓ	Wall thickness [m].

Q_c	Convective interior load per unit shell area [kW/m^2].
Q_r	Radiative interior load per unit shell area [kW/m^2].
q	Usually heat–flow [W], sometimes heat–flux [W/m^2].
q_1	Heat flow at node 1 [W/m^2].
q_c	Convective heat loss to to outside air [W/m^2].
q_l	Longwave radiation [W/m^2].
q_m	Heat flow through surfaces of interior mass [W].
q_s	Shortwave radiation from the sun [W/m^2].
R_a	Film heat resistance from interior surface of shell to interior air [K·m^2/kW].
R_c	Surface convection resistance [K·m^2/kW], Resistance of composite structure [K·m^2/kW].
R_o	Shell partial heat resistance [K·m^2/kW], sometimes divided by shell area [K/kW].
R_r	Radiative resistance [K·m^2/kW].
R_t	Branch resistance of RCR T section [K/kW].
R_v	Ventilation equivalent resistance [K·m^2/kW].
S	Conduction shape factor, subscripts w,e, and c denote wall, edge and corner.
$\boldsymbol{T}$	Transmission matrix (bold).
$\boldsymbol{T}_{rc}$	Transmission matrix of RCR T – section.
T	Usually denotes temperature if not bold [°C].
T_1	Temperature at node 1 [°C].
T_c	Mean bulk temperature of the massive parts of the structure [°C].
T_f	Forcing temperature
T_i	Bulk interior air temperature [°C].
T_m	Mean radiant\environment temperature [°C], surface temperature of interior mass [°C].
T_o	Outdoor air temperature [°C].
T_{sa}	Effective Sol–Air temperature [°C], combined contribution from all external surfaces.
TTC	Bruckmayer's thermal time–constant [h].

TTCB	Total thermal time–constant of Hoffman [h].
T_w	Wall surface temperature [°C].
T_∞	Free stream fluid temperature [°C].
t	Independent variable – time [s].
V	Volume of element [m^3].
Vol	Zone volume [m^3].
$\boldsymbol{W}$	2 Dimensional vector of temperature and heat flow.
x	Independent variable – space [m].
$\boldsymbol{Y}$	Admittance matrix or Y matrix (2–port description).
y_{11}..	Elements of admittance (Y) matrix [W/K].
Z_0	Characteristic thermal impedance $1/k \cdot \zeta$ [K/kW].
α	Surface absorptivity (radiation), thermal diffusivity [m^2/h].
ϵ	Surface emisivity.
λ	Wavelength of thermal wave [m].
ω	Independent variable – radian frequency [rad/h].
ρ	Specific density [kg/m^3].
σ	Boltzman's constant = $5.669 \cdot 10^{-8}$ W/$m^2 \cdot$K.
τ	Time–constant of network [h].
ζ	Thermal wave phase factor $\sqrt{\omega / i \cdot \alpha}$.

APPENDIX 2A

ACCURACY OF LUMPING

Wall Types
1 – Roof
2 – Floor
3 – Wall
4 – Partition
5 – Window
6 – Door

This table list for various walls from existing buildings the following:

a) Magnitude and phase of attenuation of sinusoidal temperature wave propagating through the wall.
b) Magnitude and phase error of the lumped representation.
c) The Biot number of the wall.

Wall description	Type	Biot	Attenuation Magnitude	Attenuation Phase[h]	Error Mag. [%]	Error Phase [h]
ROOF 270 concrete	1	0.54	0.029	-7.5	-16.9	2.5
ROOF 200 concrete	1	0.4	0.046	-5.7	-15.8	1.3
ROOF insulated steel	1	5.924	0.021	-0.7	-13.8	-1.4
ROOF 150 concrete	1	0.3	0.065	-4.4	-11.9	0.6
ROOF fibreglass	1	3.914	0.03	-0.2	-7.4	-1.2
ROOF 100 concrete	1	0.2	0.089	-2.9	-5.9	0.2
ROOF 100 concrete	1	0.2	0.089	-2.9	-5.9	0.2
ROOF insulated slate	1	3.942	0.029	-1.1	-3.8	-0.2
ROOF insulated steel	1	4.361	0.027	-0.6	-2.9	-0.4
ROOF insulated steel	1	2.332	0.043	-0.4	-2.8	-0.5
ROOF insulated steel	1	1.455	0.057	-0.3	-0.9	-0.2
ROOF steel	1	0	0.13	0	0	0
ROOF steel	1	0	0.13	0	0	0
ROOF insulated steel	1	0.407	0.096	-0.2	0	0.1
ROOF insulated steel	1	3	0.036	-0.4	0.3	0.3
ROOF insulated steel	1	3.75	0.03	-0.4	0.3	0.3

ROOF clay insulated	1	0.162	0.112	-0.8	1.3	0.4
ROOF 9 asbestos insulated	1	3.68	0.03	-1.3	4.7	1.1
ROOF insulated 200 concrete	1	5.4	0.003	-9.3	48.1	3.9
FLOOR 125 concrete on soil	2	0.515	0.037	-6.5	-26	1.7
FLOOR concrete on soil	2	0.415	0.052	-5.2	-22.9	0.9
FLOOR concrete on soil	2	0.415	0.052	-5.2	-22.9	0.9
FLOOR 100 concrete on soil	2	0.487	0.042	-6	-20	1.4
FLOOR concrete on soil	2	0.326	0.067	-4.2	-18.5	0.4
FLOOR 200 concrete	2	0.4	0.046	-5.7	-15.8	1.3
FLOOR 200 concrete	2	0.4	0.046	-5.7	-15.8	1.3
FLOOR 200 concrete	2	0.4	0.046	-5.7	-15.8	1.3
FLOOR 150 concrete on soil	2	0.3	0.065	-4.4	-11.9	0.6
FLOOR 270 concrete	2	0.578	0.026	-7.6	-7.9	2.7
FLOOR 100 concrete	2	0.2	0.089	-2.9	-5.9	0.2
FLOOR 100 concrete	2	0.2	0.089	-2.9	-5.9	0.2
FLOOR 100 concrete	2	0.2	0.089	-2.9	-5.9	0.2
FLOOR fibreglass	2	2.763	0.038	-0.8	-5.4	-0.6
FLOOR 398 concrete	2	0.811	0.012	-10.7	-3.2	5.3
FLOOR concrete on soil	2	1.106	0.008	-11.3	24.7	5.9
FLOOR 75 concrete on soil	2	0.794	0.026	-6.2	68	2.5
FLOOR 150 concrete	2	0.633	0.033	-5.5	75	2.4
FLOOR 150 concrete on soil	2	1.759	0.005	-10.6	154.3	5.5
FLOOR 9 asbestos insulated	2	4.08	0.004	-7.8	238.2	3.5
TROMBE insulated 100 brick	3	6.255	0.011	-5.3	-84.6	-0.4
WALL 110 brick cavity	3	0.829	0.029	-7.1	-21.9	2.3
WALL 110 brick cavity	3	0.834	0.029	-7.1	-21.9	2.3
WALL 114 brick cavity	3	0.837	0.028	-7.3	-21.6	2.4
WALL 114 brick cavity	3	0.839	0.028	-7.3	-21.6	2.4
WALL 220 brick	3	0.805	0.03	-7	-21.5	2.2
WALL 230 brick	3	0.841	0.028	-7.3	-21.5	2.4
WALL 220 brick	3	0.992	0.022	-8	-20	3
WALL 220 brick	3	0.992	0.022	-8	-20	3
WALL 220 brick	3	0.992	0.022	-8	-20	3
WALL 200 concrete	3	0.4	0.046	-5.7	-15.8	1.3
WALL 115 brick cavity	3	0.946	0.023	-7.9	-15.3	3
WALL 330 brick	3	1.207	0.012	-10.4	-14.9	5
WALL 150 concrete	3	0.3	0.065	-4.4	-11.9	0.6

WALL 114 brick	3	0.417	0.072	-3.5	-11.2	0.3
WALL 114 brick	3	0.417	0.072	-3.5	-11.2	0.3
WALL 110 brick	3	0.402	0.074	-3.4	-10.5	0.3
WALL 220 brick	3	0.992	0.021	-8.1	-9.8	3.2
WALL 330 brick	3	1.395	0.009	-11.4	-7.8	5.9
WALL 400 concrete	3	0.8	0.012	-10.7	-6.5	5.2
WALL 220 brick insulated	3	1.162	0.017	-8.1	22.5	3.4
WALL 500 brick	3	1.829	0.003	8.4	32.1	-14.1
WALL 500 brick	3	1.94	0.003	7.7	41	-13.4
WALL 200 brick cavity	3	1.959	0.003	7.7	45.7	-13.4
WALL 110 brick cavity	3	1.163	0.025	-6.1	48.2	2.4
WALL 550 brick	3	2.012	0.002	6.9	58	-12.6
WALL 220 brick insulated	3	2.169	0.007	-8.6	148	4.2
WALL 9 asbestos insulated	4	3.723	0.029	-1.5	-23.4	-1.4
WALL asbestos	4	4.035	0.026	-2.3	-23.2	-0.7
WALL asbestos	4	3.259	0.033	-1.3	-16.9	-1.2
WALL hardboard	4	0.745	0.074	-1.9	-6.3	0
WALL fibreboard	4	1.049	0.068	-0.3	-0.2	0
WALL steel	4	0	0.13	0	0	0
WALL steel	4	0	0.13	0	0	0
WALL 9 asbestos	4	0.044	0.125	-0.2	0	0
WALL hardboard	4	0.168	0.114	-0.2	0	0
WALL insulated steel	4	1.875	0.049	-0.3	0.2	0.2
WALL insulated steel	4	3.75	0.03	-0.4	0.3	0.3
WINDOW 3	5	0.012	0.129	0	0	0
WINDOW 3	5	0.012	0.129	0	0	0
WINDOW 3	5	0.012	0.129	0	0	0
WINDOW 3	5	0.012	0.129	0	0	0
WINDOW 3	5	0.012	0.129	0	0	0
WINDOW 4	5	0.016	0.129	0	0	0
WINDOW 6	5	0.024	0.128	-0.1	0	0
WINDOW 6	5	0.024	0.128	-0.1	0	0
WINDOW 6	5	0.024	0.128	-0.1	0	0
WINDOW 6	5	0.024	0.128	-0.1	0	0
WINDOW 6	5	0.024	0.128	-0.1	0	0
WINDOW 6	5	0.024	0.128	-0.1	0	0
WINDOW 6	5	0.024	0.128	-0.1	0	0

WINDOW 6	5	0.024	0.128	−0.1	0	0
WINDOW qlite	5	0.027	0.127	0	0	0
WINDOW 4 double	5	0.032	0.127	−0.2	0	0
WINDOW 4 double	'5	0.076	0.122	−0.2	0	0
DOOR	6	0.794	0.074	−1.5	−3.8	0
DOOR	6	0.8	0.075	−1.2	−2.8	0
DOOR	6	0.706	0.078	−1.2	−2.6	0
DOOR	6	0.706	0.078	−1.2	−2.6	0
DOOR	6	0.857	0.073	−1	−2.1	0
DOOR	6	0.75	0.078	−0.8	−1.3	0
DOOR	6	0.6	0.085	−0.8	−1.1	0
DOOR	6	0.4	0.096	−0.4	−0.3	0
DOOR steel	6	0	0.13	0	0	0
DOOR steel	6	0	0.13	0	0	0
DOOR	6	0.148	0.116	0	0	0
DOOR	6	0.187	0.112	−0.1	0	0

APPENDIX 2B

FOURIER MODULI

Non-Air, Non-Metallic layers.

Description	[mm]	Biot	Fo
ACOUSTONE	15	0.563	121.9
BRICKWORK	100	0.366	4.85
BRICKWORK	110	0.402	4.008
BRICKWORK	114	0.417	3.732
BRICKWORK	115	0.421	3.667
BRICKWORK	200	0.732	1.212
BRICKWORK	220	0.805	1.002
BRICKWORK	230	0.841	0.917
BRICKWORK	300	1.098	0.539
BRICKWORK	330	1.207	0.445
BRICKWORK	500	1.829	0.194
CARPET	3	0.2	3600
CARPET	5	0.333	1296
CONCRETE POURED	75	0.15	13.18
CONCRETE POURED	100	0.2	7.416
CONCRETE POURED	125	0.25	4.746
CONCRETE POURED	150	0.3	3.296
CONCRETE POURED	200	0.4	1.854
CONCRETE POURED	270	0.54	1.017
CONCRETE POURED	398	0.796	0.468
CONCRETE POURED	400	0.8	0.463
EXPANDED POLYSTYRENE	15	1.364	362.1
EXPANDED POLYSTYRENE	35	3.182	66.5
EXPANDED POLYSTYRENE	40	3.636	50.91
FELT UNDERCARPET	6	0.4	900
FELT UNDERCARPET	15	1	144
FIBREBOARD	6	0.31	397.3
FIBREBOARD	10	0.517	143
FIBREBOARD	15	0.776	63.56
FIBREBOARD	18	0.931	44.14
FIBREBOARD	35	1.81	11.67
FIBREGLASS	10	0.937	789.9
FIBREGLASS	40	3.75	49.37
FIBREGLASS	50	4.687	31.6
GLASS	3	0.012	4328
GLASS	4	0.016	2434

GLASS	6	0.024	1082
GLASS WOOL	15	1.125	614.4
GLASS WOOL	25	1.875	221.2
GLASS WOOL	40	3	86.4
GLASS WOOL	50	3.75	55.3
GLASS WOOL	75	5.625	24.58
GYPSUM PLASTER BOARD	5	0.088	563.5
GYPSUM PLASTER BOARD	6	0.106	391.3
GYPSUM PLASTER BOARD	12	0.212	97.83
HARDBOARD	4	0.06	708.4
HARDBOARD	20	0.3	28.34
PINE WOOD	30	0.6	15.58
PINE WOOD	40	0.8	8.766
PLASTER	10	0.063	326.8
PLASTER	15	0.094	145.3
PLASTER	30	0.188	36.31
PLASTER	50	0.313	13.07
PLYWOOD	3	0.064	1811
PLYWOOD	4	0.086	1019
PLYWOOD	15	0.321	72.45
PLYWOOD	35	0.75	13.31
PLYWOOD	40	0.857	10.19
PRESSED ASBESTOS CEME	8	0.039	480.2
PRESSED ASBESTOS CEME	9	0.044	379.4
PVC FLOOR COVERING	2	0.015	72000
PVC FLOOR COVERING	3	0.022	32000
PVC FLOOR COVERING	5	0.037	11520
SLATE	5	0.011	2580
SOIL	50	0.176	13.06
SOIL	69	0.244	6.856
SOIL	75	0.265	5.803
SOIL	130	0.459	1.931
TEAK WOOD	40	0.706	9.367
TILES BURNT CLAY	20	0.071	102.6
TRANSLUCENT Q LITE	2	0.027	2475

APPENDIX 2C

Detailed results for OFFICE building.

```
*****OFFICE*****
Number of Walls: 6

WALL NUMBER 1  -  ROOF 270 concrete  Type = 1
Material                     Thickness [mm]        Bi
CONCRETE POURED                   270.0          0.540
R = 180.000 m²•K/kW      C = 471.874 kJ/m²•K  RC = 84937.256 s
Wall Bi (re hi) = 0.540
T matrix
(-0.554, 2.764)  (0.123, 0.177)
(-33.730, 23.543)  (-0.554, 2.764)

WALL NUMBER 2  -  FLOOR  270 concrete  Type = 2
Material                     Thickness [mm]        Bi
PVC FLOOR COVERING                5.0            0.037
CONCRETE POURED                   270.0          0.540
R = 192.500 m²•K/kW      C = 472.474 kJ/m²•K  RC = 90951.172 s
Wall Bi (re hi) = 0.578
T matrix
(-0.976, 3.058)  (0.117, 0.212)
(-33.857, 23.509)  (-0.562, 2.769)

WALL NUMBER 3  -  WALL 114 brick cavity  Type = 3
Material                     Thickness [mm]        Bi
BRICKWORK                         114.0          0.417
AIRSPACE                          10.0           0.005
BRICKWORK                         114.0          0.417
R = 279.662 m²•K/kW      C = 333.062 kJ/m²•K  RC = 93144.791 s
Wall Bi (re hi) = 0.839
T matrix
(-0.860, 2.959)  (0.175, 0.298)
(-25.934, 15.074)  (-0.860, 2.959)
```

WALL NUMBER 4 – WINDOW 3 Type = 5

Material	Thickness [mm]	Bi
GLASS	3.0	0.012

R = 4.000 m²•K/kW C = 4.991 kJ/m²•K RC = 19.963 s
Wall Bi (re hi) = 0.012
T matrix
(1.000, 0.000) (0.004, 0.000)
(-0.000, 0.363) (1.000, 0.000)

WALL NUMBER 5 – WALL 114 brick Type = 3

Material	Thickness [mm]	Bi
BRICKWORK	114.0	0.417

R = 139.024 m²•K/kW C = 166.531 kJ/m²•K RC = 23151.899 s
Wall Bi (re hi) = 0.417
T matrix
(0.882, 0.835) (0.136, 0.039)
(-3.387, 11.825) (0.882, 0.835)

WALL NUMBER 6 – DOOR Type = 6

Material	Thickness [mm]	Bi
PINE WOOD	30.0	0.600

R = 200.000 m²•K/kW C = 27.720 kJ/m²•K RC = 5544.000 s
Wall Bi (re hi) = 0.600
T matrix
(0.993, 0.201) (0.200, 0.013)
(-0.135, 2.013) (0.993, 0.201)

Film coefficients in W/m²•K

hr = 4.667 hi = 3.000
hr/hi = 1.556 he = 12.334
ho = 20.000

MEAN BIOT NUMBERS

WALL:	1	2	3	4	5	6
1	0.540					
2	0.559	0.578				
3	0.689	0.708	0.839			
4	0.276	0.295	0.425	0.012		
5	0.479	0.497	0.628	0.215	0.417	
6	0.570	0.589	0.719	0.306	0.509	0.600

FRACTIONAL MEAN DIFFERENCE *100

WALL:	1	2	3	4	5	6
1	26.064					
2	25.551	25.057				
3	22.465	22.083	19.740			
4	36.346	35.355	29.709	60.023		
5	27.901	27.314	23.817	40.021	30.018	
6	25.252	24.770	21.860	34.786	26.973	24.489

INTERIOR/FORCING TEMPERATURE * 100

WALL:	1	2	3	4	5	6
1	11.030	11.006	12.597	10.822	13.235	16.294
2	10.014	9.991	11.433	9.823	12.009	14.774
3	10.006	9.981	11.645	9.826	12.356	15.921
4	54.361	54.226	62.135	49.991	64.383	75.113
5	25.090	25.023	29.489	24.300	31.356	40.873
6	26.538	26.446	32.643	24.355	35.113	48.464

FRACTIONAL TEMPERATURE SWING DIFFERENCE * 100

WALL:	1	2	3	4	5	6
1	8.537	8.556	7.335	9.283	6.831	4.675
2	7.750	7.767	6.658	8.425	6.199	4.238
3	7.744	7.759	6.781	8.428	6.377	4.567
4	42.071	42.155	36.183	42.880	33.230	21.548
5	19.418	19.453	17.172	20.843	16.184	11.726
6	20.538	20.559	19.008	20.890	18.123	13.903

WALL	Type	Bi	R	C	RC	dT
ROOF 270 concrete	1	0.540	180.0	471.9	23.6	7.5
FLOOR 270 concrete	2	0.578	192.5	472.5	25.3	6.8
WALL 114 brick cavity	3	0.839	279.7	333.1	25.9	6.9
WINDOW 3	5	0.012	4.0	5.0	0.0	36.3
WALL 114 brick	3	0.417	139.0	166.5	6.4	17.5
DOOR	6	0.600	200.0	27.7	1.5	18.8